Modeling Air Traffic Management Technologies With a Queuing Network Model of the National Airspace System

Dou Long, David Lee, Jesse Johnson, Eric Gaier, and Peter Kostiuk
Logistics Management Institute, McLean, Virginia

Contents

FIGURES

TABLES

Chapter 1
Overview

This report describes an integrated model of air traffic management (ATM) tools under development in two National Aeronautics and Space Administration (NASA) programs—Terminal Area Productivity (TAP) and Advanced Air Transport Technologies (AATT). The model is made by adjusting parameters of LMINET, a queuing network model of the National Airspace System (NAS), which the Logistics Management Institute (LMI) developed for NASA. Operating LMINET with models of various combinations of TAP and AATT will give quantitative information about the effects of the tools on operations of the NAS.

An extension of economic models developed by the Institute for NASA maps the technologies' impacts on NAS operations into cross-comparable benefits estimates for technologies and sets of technologies. An application of the Aviation Systems Analysis Capability (ASAC) Air Carrier Investment Model (ACIM), developed for NASA by the Institute, gives estimates of the ways in which the NASA tools impact NAS throughput, as measured by revenue passenger miles (RPMs), enplanements, and operations.

Following this overview chapter, Chapter 2 describes LMINET and its constituent models in some detail. This information will help readers unfamiliar with LMINET to understand ATM models made with LMINET parameters. For completeness, we have included in this report material from three other reports and an LMI white paper, all of which were prepared for NASA by the Institute. [1,2,3,4]

Those familiar with LMINET's components need only consider the material in the sections "Input-Stream Effects" and "Taxi-Delay Queues" in Chapter 2. The first describes a new LMINET parameter, developed to account for the fact that terminal radar approach control (TRACON) controllers may present airport controllers with arrival streams that are difficult to manage efficiently. The second explains the model of taxiway delays that we have developed for this project.

Chapters 3 and 4 and describe, respectively, our models of two reference cases of the NAS and of the TAP and AATT technologies. Chapter 5 summarizes our modeling work. Chapter 6 summarizes the technologies' impacts on some aspects of NAS operation. Chapter 7 summarizes the technologies' economic impacts.

Chapter 8 describes our means of estimating the impacts of delay on system throughput and gives the throughput results. The report concludes with a summary of principal results, given in Chapter 9.

Chapter 2
LMINET

Our principal tool for this study is LMINET, a queueing network model of the NAS, developed by LMI for NASA. [1,3] Presently, LMINET is implemented with 64 airports (Figure 2-1).[1] They account for over 80 percent of the air carrier operations for 1997, as reported in Department of Transportation (DOT) Forms T-100. The LMINET airports are a superset of the Federal Aviation Administration's (FAA's) 57 pacing airports.

Figure 2-1. LMINET Airports

In general terms, LMINET models flights among a set of airports by linking queueing network models of airports with sequences of queuing models of TRACON and Air Route Traffic Control Center (ARTCC) sectors. The user may specify the sequences of sectors to represent various operating modes for the

---

[1] The 64 airports (denoted by three-letter codes) are ABQ, ATL, AUS, BDL, BNA, BOS, BUR, BWI, CLE, CLT, CMH, CVG, DAL, DAY, DCA, DEN, DFW, DTW, ELP, EWR, FLL, GSO, HOU, HPN, IAD, IAH, IND, ISP, JFK, LAS, LAX, LGA, LGB, MCI, MCO, MDW, MEM, MIA, MKE, MSP, MSY, OAK, ONT, ORD, PBI, PDX, PHL, PHX, PIT, RDU, RNO, SAN, SAT, SDF, SEA, SFO, SJC, SLC, SMF, SNA, STL, SYR, TEB, and TPA.

NAS. The sequences may, for example, correspond to optimal routes for the winds aloft of a specific day or to trajectories of flights as flown on a specific day as determined from data in the FAA's Enhanced Traffic Management System (ETMS).

Given the sector sequences for the interairport routes, LMINET is driven by two inputs: traffic demand and weather data. Traffic demand is input by a schedule of hour-by-hour departures from the network airports and a schedule of arrivals to network airports from terminals outside the network. The 1997 Official Airline Guide (OAG)—augmented by data on general aviation (GA) operations from the ETMS and the FAA's Terminal Area Forecast (TAF)—is our source for these schedules.

Weather data are provided to LMINET as hour-by-hour values of surface mete-orological conditions (specifically, ceiling, visibility, wind speed and direction, and temperature) at each network airport and as hour-by-hour values of a single weather parameter for each TRACON and en route sector. Our source for surface weather data is the National Climatic Data Center's On-line Access and Service Information System (OASIS). We did not vary the sectors' weather parameters for this report.

The following sections give more details on LMINET's components.

AIRPORT DELAY MODEL

Operations at each LMINET airport are modeled by a queueing network, as shown in Figure 2-2.

Figure 2-2. Queues in the LMINET Airport Model
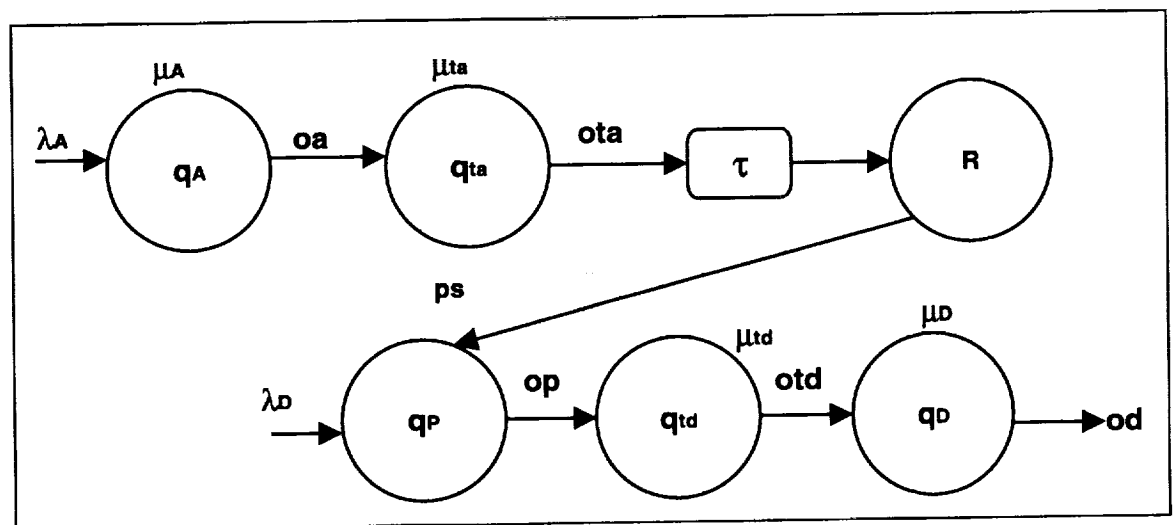
Traffic enters the arrival queue, q_A, according to a Poisson arrival process with parameter $\lambda_A(t)$. Upon service by the arrival server, an arriving aircraft enters the taxi-in queue, q_{TA}. After the turnaround delay, τ, the output of the taxi-in queue, t, enters the ready-to-depart reservoir, R. Each day's operations begin with a certain number of aircraft in this reservoir.

Departures enter the queue for aircraft, q_p, according to a Poisson process with rate λ_D. Departure aircraft are assigned by a process with service rate $\mu_p(t)$. When a departure aircraft is assigned, R is reduced by 1. Having secured a ready-to-depart aircraft, the departure leaves q_p and enters the queue for taxi-out service, q_{td}. Output from the taxi-out queue is input to the queue for service at a departure runway, q_D, where it is served according to the departure service process with rate μ_D. Finally, output from the departure queue, q_D, is output from the airport into the rest of LMINET.

The following subsections describe our models for the several queues in the airport delay model.

Arrival Service Process

The user may choose the arrival service process as either a Poisson process with parameter $\mu_A(t)$ or an Erlang process with mean $\mu_A(t)$ and shape parameter k. Thus, the arrival queue is either an *M/M/*1 queue or an *M/Ek/*1 queue.

Choosing the Erlang family of distributions, several examples of which are shown in Figure 2-3, gives the user a way to specify the concentration of the service time about its mean. For shape parameter 1, the Erlang distribution is the same as the exponential distribution. For increasing values of shape parameter k, the Erlang distribution becomes more and more concentrated. In the limit of very large values of k, the Erlang distribution approaches the discrete distribution $\delta(t-\mu)$.

Figure 2-3. Some Erlang Distributions

Figure 2-3. Some Erlang Distributions
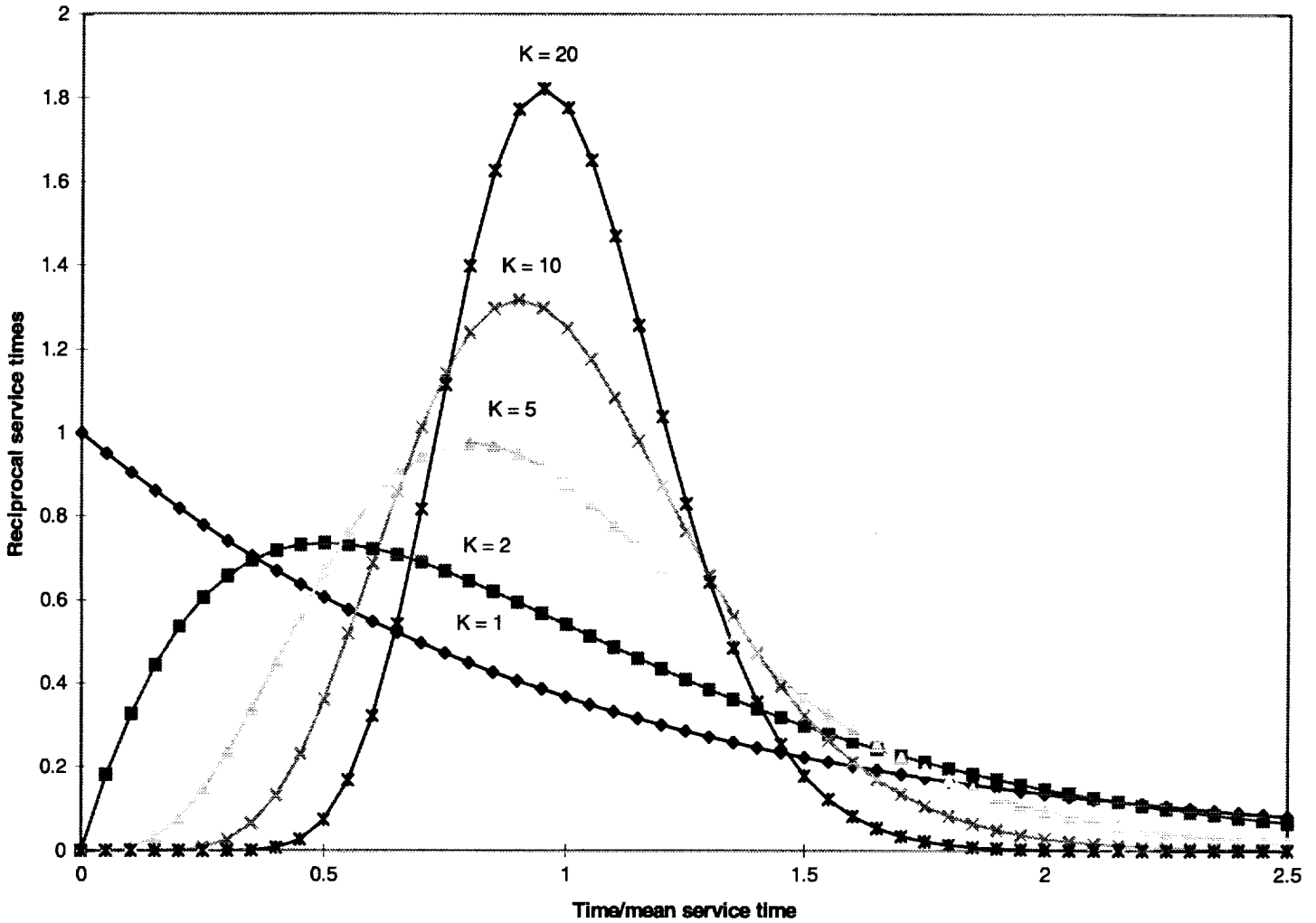
Taxi-Delay Queues

Patterns of surface movement, and related delays, are airport specific. Developing surface-movement models in whose outputs one has high confidence will require studies of individual airports.

Such an effort is beyond the scope of this study. Nevertheless, we are asked to include the effects of surface-movement tools, even if only in a preliminary way.

We discussed causes of surface–movement delays with controllers. Some of the prominent delays mentioned were

♦ taxiways crossing active runways,

♦ aircraft backing out of gates into taxiways,

♦ segments of taxiways too narrow for two-way traffic, and

♦ taxiways intersecting.

The controllers also mentioned that long queues for departure runways impeded both taxi-in and taxi-out operations, and that taxi operations were impeded by poor visibility, like that of Instrument Landing System (ILS) Category II or worse.[2]

Now, while relatively few parts of airport surface movements correspond to single-server queues, those listed previously arguably do. If in fact the chief causes of surface-movement delay correspond to single-server queues, then it may be helpful to model, not the entire taxi process but just the *delays* in the process as single-server queues.

With this idea in mind, we attempted to capture surface-movement delays with two added queues, as shown in Figure 2-2. The queue, q_{ta}, models taxi-in delays, and the queue, q_{td}, models taxi-out delays. We take both these taxi-delay queues to be *M/M/*1 queues.

It is important to keep in mind that with this approach we attempt to model surface-movement *delays*, rather than the complex, actual surface-movement processes on which as yet we have limited information. In this model, we assume that taxi-in and taxi-out operations proceed without delays, except for events whose total delays can be modeled with the two single-server queues.

We incorporate three phenomena in the service rates μ_{ta} and μ_{td} to the taxi-in and taxi-out queues. The first of these phenomena is the airport-specific level of surface-movement demand that causes delays. The second is the effect of congestion caused by large queues for departure runway service, and the third is the impediment of surface movement by poor visibility.

We model these three surface-movement effects by the forms we assume for μ_{ta} and μ_{td}. These are

$$\mu_{tx} = \hat{\mu}_{tx}\left[1-\min\left(\frac{q_D}{r_t},0.25\right)\right]$$

[Eq. 2-1]

---

[2] ILS Category II is an ILS approach procedure that provides for an approach to a height above touchdown of not less than 100 feet with runway visual range of not less than 1,200 feet.

where x is either a or d. The parameter $\hat{\mu}_{tx}$ sets the basic service rate of the queue. It determines the airport-specific level of demand that causes delays. The parameter r_t determines the degree to which long departure queues affect overall taxi capacity. We have arbitrarily imposed the limit of 25 percent as the greatest reduction that departure queues impose on taxi capacity.

To model the effects of poor visibility on taxi operations, we reduce μ_{tx} by 25 percent when visibility is 1 nautical mile or less. We based this threshold, and the 25 percent reduction, on discussions with aircrew members.

Departure Service Processes

The departure processes begin with service at the queue for ready-to-depart aircraft. This service depends on the state of the ready-to-depart reservoir, R. If R is not empty, then the service rate, $\mu_p(t)$, is very large compared to 1 (service time is very short). If R is empty, then departing aircraft are supplied by output of the arrival queue, delayed by the turnaround time, τ. The precise form of the somewhat complicated expression for service to the queue for ready-to-depart aircraft is given in Equation 2-13 in the following subsection. It is discussed in detail there.

Since aircraft are not interchangeable, this assumption on the supply of departing aircraft is tenable only when delays in the arrival process do not significantly alter the sequence of arrivals.

The taxi-out queue has been discussed previously. The departure queue, q_D, like the arrival queue, q_A, may be either $M/M/1$ or $M/Ek/1$. We chose Erlang service-time distributions.

Equations of the Extended Airport Delay Model

The specific equations that we use to treat the queuing network model of Figure 2-2 incorporate several different queuing models, as well as our priorities for eliminating a queue for airplanes, q_p, and restoring a depleted reservoir, R. We wrote the modeling equations to conserve aircraft. For completeness, we give the model equations with a brief discussion.

We chose the Erlang service model for the arrival queue. We treat this queue with a closure hypothesis that permits us to approximate the first moment of the distribution of the number of clients in the queue, i.e., the mean number. In this approximation, we write

$$\dot{q}_a = f_1(\lambda_a, \mu_a, k, q_a) , \qquad \text{[Eq. 2-2]}$$

where

$$f_1(\lambda_a, \mu_a, k, q_a) \equiv k(\lambda - \mu) + k\mu \frac{k(k+1)}{k(k+1) + 2kq_a} .$$ [Eq. 2-3]

Appendix B gives a derivation of this approximate model for the $M/E_k/1$ queue.

Conservation of aircraft in the arrival process requires the condition

$$oa = \lambda_a - \dot{q}_a$$ [Eq. 2-4]

on the process output rate *oa*. Equation 2-4 shows that the rate at which aircraft arrive is equal to the sum of the rate at which aircraft leave the arrival process and the rate-of-change of the arrival queue. That is, arriving aircraft either exit the arrival process or enter the arrival queue.

The output rate, *oa*, is the input to the taxi-in queue, q_{ta}. We model the $M/M/1$ taxi-in queue with the Rothkopf-Oren closure hypothesis, which allows us to approximate first and second moments. [5] The equations are

$$\dot{q}_{ta} = oa - \mu_{ta}\left[1 - P_0(q_{ta}, v_{ta})\right]$$ [Eq. 2-5]

and

$$\dot{v}_{ta} = oa + \mu_{ta}(2q_{ta} + 1)P_0(q_{ta}, v_{ta}),$$ [Eq. 2-6]

where

$$P_0(q, v) \equiv \left(\frac{q}{v}\right)^{\frac{q^2}{v-q}} .$$ [Eq. 2-7]

To conserve aircraft, we impose

$$ota = oa - \dot{q}_{ta} .$$ [Eq. 2-8]

Equation 2-8 implies that the rate of output, *oa*, of the arrival process is equal to the rate at which aircraft leave the taxi-in process plus the rate of change of the taxi-in queue. Adding Equations 2-4 and 2-8 leads to

$$\lambda_a = ota + \dot{q}_a + \dot{q}_{ta},$$ [Eq. 2-9]

which shows that, in our present airport delay model, arrivals either exit the entire arrival-taxi-in process or accumulate in either the arrival queue or the taxi-in queue.

The output rate of the taxi-in process, *ota*, after the turnaround delay, τ, is the input rate to the reservoir, R, of ready-to-depart aircraft. Conservation of aircraft for the reservoir is expressed by

$$\dot{R} = ota(t - \tau) - ps,$$
[Eq. 2-10]

where *ps* is the plane-service rate. We will specify *ps* in connection with the departure process, to which we now turn.

A departing flight first queues for service with a ready-to-depart airplane. Our equations for this queue for airplanes are

$$\dot{q}_p = f_{fluid}(\lambda_D, ps, q_p),$$
[Eq. 2-11]

where

$$f_{fluid}(\lambda, \mu, q) \equiv \begin{cases} \lambda - \mu, & q > 0 \\ (\lambda - \mu)^+, & q = 0 \end{cases}.$$
[Eq. 2-12]

In Equation 2-12, $(x)^+$ is equal to x when $x > 0$, and is zero for nonpositive x. It follows from Equation 2-11 with Equation 2-12 that q_p will remain zero, if *ps* $= \lambda_D$. Accordingly, we choose *ps* $= \lambda_D$ whenever that is possible, i.e., whenever $R > 0$.

If $R = 0$, then *ps* cannot be greater than the input rate to the reservoir, i.e., $ota(t-\tau)$. When $R = 0$, we choose *ps* to have this maximum value whenever $q_p > 0$. When $R = 0$ and $q_p = 0$, we choose *ps* to be the smaller of λ_D and the maximum value. This choice has the effect of first eliminating any queue for airplanes, and then replenishing the reservoir, when the airport is recovering from a depleted reservoir. Our choice for the function *ps* is thus

$$ps = \begin{cases} \lambda_D, R > 0 \\ \begin{cases} ota(t - \tau), q_p > 0 \\ \min\left((\lambda_D, ota(t - \tau))\right), q_p = 0 \end{cases}, R = 0 \end{cases}.$$
[Eq. 2-13]

To conserve aircraft, we determine the output rate, *op*, of the queue for ready-to-depart airplanes by

$$op = \lambda_D - \dot{q}_p.$$
[Eq. 2-14]

The output rate, *op*, is the input to the taxi-out queue, q_{td}. As for the taxi-in delay queue, q_{ta}, we model the taxi-out queue, q_{td}, as an *M/M/*1 queue, using the Rothkopf-Oren closure hypothesis. Our equations for this queue are

$$\dot{q}_{td} = op - \mu_{td}\left[1 - P_0(q_{td}, v_{td})\right]$$ [Eq. 2-15]

and

$$\dot{v}_{td} = op + \mu_{td}(2q_{td} + 1)P_0(q_{td}, v_{td}).$$ [Eq. 2-16]

By conservation, we determine the output rate, *otd*, of the taxi-out queue by

$$otd = op - \dot{q}_{td}.$$ [Eq. 2-17]

The output, *otd*, of the taxi-out queue is then input for the departure queue, q_D. As for the arrival queue, we model departure runway service as an *M/E$_k$/*1 queue with a first-moment closure hypothesis. Its equation is

$$\dot{q}_D = f_1(otd, \mu_D, q_D).$$ [Eq. 2-18]

Finally, for conservation, the output rate of the departure process, *od*, is

$$od = otd - \dot{q}_D.$$ [Eq. 2-19]

At each epoch, we treat the eighth-order system of ordinary differential equations, given by Equations 2-2, 2-5, 2-6, 2-10, 2-11, 2-15, 2-16, and 2-18, numerically, using Equations 2-3, 2-4, 2-7, 2-8, 2-12, 2-13, 2-14, and 2-17. Equation 2-19 gives the departure rate from the airport.

Calibrating the Airport Delay Model

As noted previously in this chapter, we chose the value at which reduced horizontal visibility impacts taxi operations, 1 nautical mile, and the value of that impact, a 25 percent reduction in service rate, from discussions with aircrew. We somewhat arbitrarily set r_t, the length of the queue for departure runway service that interferes with surface movements, at one-fourth of the basic taxi-in rate, $\hat{\mu}_{ta}$. We made this choice on the assumption that a taxi-out queue equal to 15 minutes' taxi traffic was likely to cause trouble. Other calibrated model parameters are described in subsequent chapters.

ERLANG SHAPE PARAMETER, K

We calibrated this value with a representative distribution of interarrival times given by the airport capacity models LMI developed for NASA. These models are discussed in this chapter. Figure 2-4 shows the fit of an Erlang distribution with shape parameter $k = 22$ to the capacity model's distribution of interarrival times.

Figure 2-4. Comparison of Service-Time (Interarrival Time) Distributions
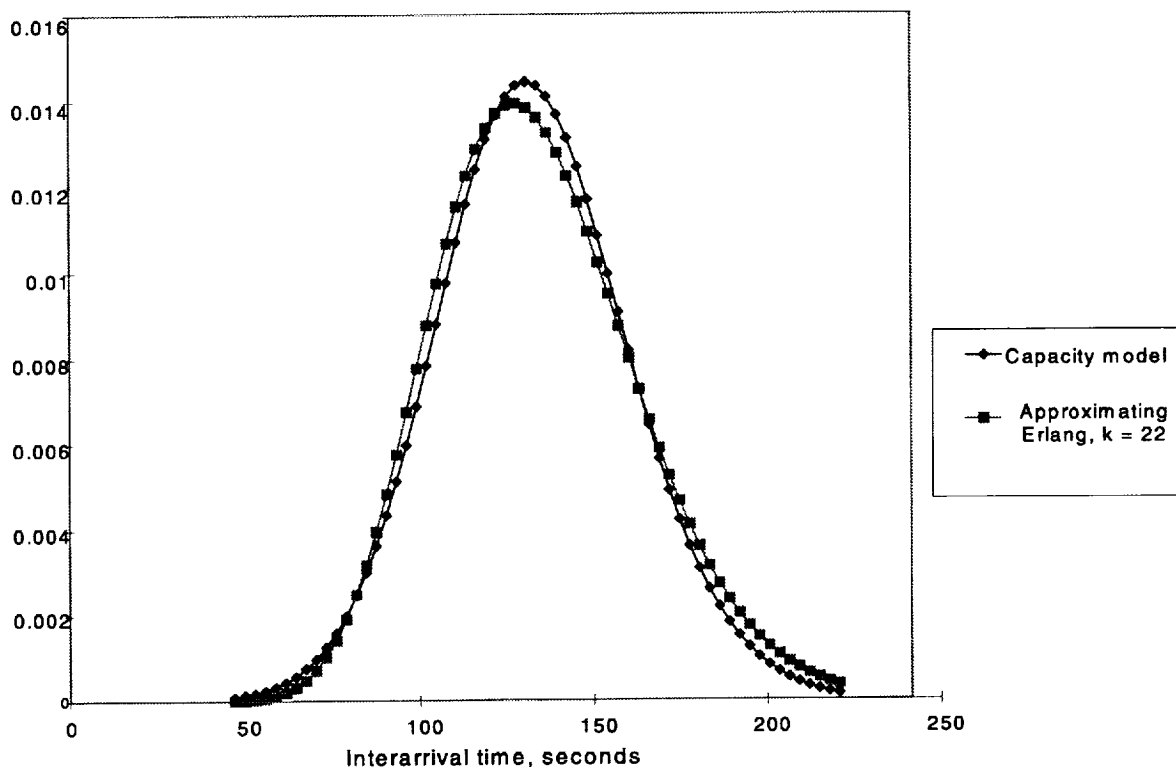
BASIC TAXI-IN SERVICE RATE

We calibrated the basic taxi-in service rate, μ_{ta}, with data from the FAA's Performance Monitoring Analysis Capability (PMAC). From this source, we obtained mean taxi-in delays for each of the 64 LMINET airports for 1995. We then operated LMINET with universal good weather inputs and adjusted the 64 values of μ_{ta} to obtain acceptable agreement between mean taxi-in delays from LMINET and the observed values. The agreement between LMINET outputs and observed delays is shown in Figure 2-5.

PMAC's taxi-out delay data include the effects of queues for departure runways. Those delays are, of course, not part of surface-movement problems. For that reason, we did not calibrate taxi-out service with PMAC's taxi-out delay data. Rather, for this report, we set taxi-out service rates equal to taxi-in service rates. That is reasonable only if aircraft taxiing out encounter similar delays to those taxiing in.

An Example of the LMINET Airport Delay Model

We illustrate the working of the extended LMINET airport delay model with an example. Table 2-1 shows the hour-by-hour model outputs for BOS, for April 8, 1996.

Figure 2-5. Calibration of Surface-Delay Model
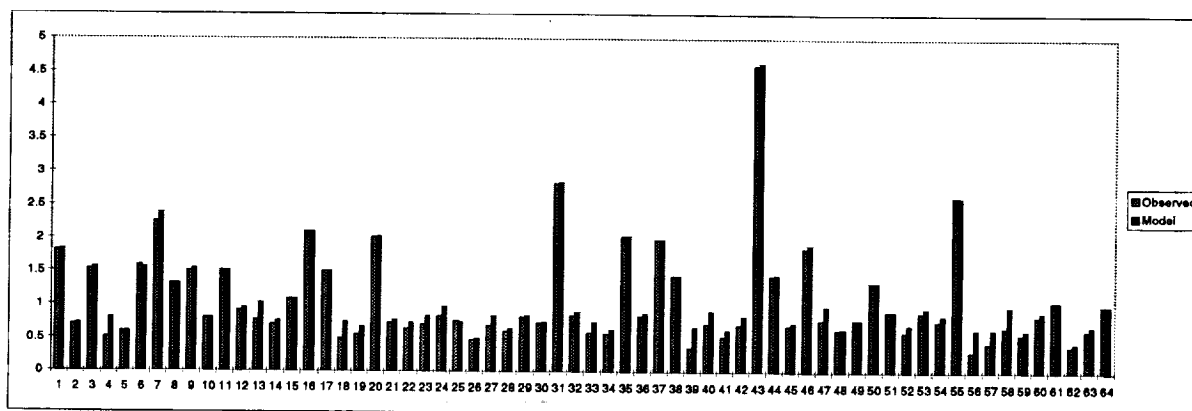
This was a bad day at BOS. Poor visibility kept the field in instrument meteorological conditions (IMC) all morning. This restricted capacity, causing queues to develop for both arrival and departure service. Most of the arrival delays were taken as ground holds at departure airports, as shown in the last column of Table 2-1.

Reduced arrivals, together with the need for aircraft already at BOS to depart, depleted the reservoir by 0900. This caused a queue for planes to develop. All during this time of reduced capacity, taxi-in and taxi-out queues were small because there was actually less taxi traffic than usual.

At 1300, conditions improved to marginal visual meteorological conditions (VMC), and capacities increased sharply. Both arrival and departure queues dropped. Increased taxi demand generated increases in taxi delays. After the 1-hour turnaround delay, increased arrivals caused the queue for airplanes to decrease, but it was not eliminated until 2100. Starting at that hour, the reservoir began to rebuild. With dwindling demand for both arrivals and departures, and continued VMC—there was even one period of VMC-1,[3] in which instrument flight rules (IFR) flight plans could be concluded with visual approaches—the arrival and departure queues fell to negligible levels, and the reservoir recovered. (Indeed, since demand profiles are not necessarily balanced, the BOS reservoir recovered to 30 more than its starting value of 122 airplanes.)

---

[3] VMC-1 at BOS is defined as the minimum visibility of 3 miles and minimum ceiling of 2,500 feet.

Table 2-1. LMINET Output For BOS, April 8, 1996

EDT	λ_A	μ_A	Arrivals	q_A	q_{ta}	Reservoir	q_p	q_{td}	λ_D	μ_D	Departures	q_D	Ground hold
6	6.4	7.6	4.7	1.6	0.1	88.9	0	1	33.1	39.2	29.5	2.6	0
7	31.1	18.7	16.7	15.4	0.7	48.4	0	3.4	45.2	27.8	26.1	19.3	0
8	7.7	11.2	11.2	12.4	0.3	14.4	0	5.5	50.7	35.5	34.8	33	16.3
9	2	7	6.8	7.7	0.2	0	17.4	0.2	43.4	39.9	39.2	25.1	34.2
10	16.2	15.7	14.5	9.2	0.5	0	49.4	0.1	38.8	30.9	29.4	2.6	44
11	13.9	20.5	18.9	4.1	0.5	0	74.7	0.3	39.7	26	16.2	0.7	55.4
12	29.4	22.9	21.1	12.1	0.7	0	91.5	0.4	35.7	23.5	17.6	1.9	62.9
13	63.7	62.4	57.1	15.7	3.8	0	109.9	0.4	39.5	49.7	22.6	0.4	50.1
14	62.8	62.5	54.9	17.9	9.6	0	89.1	7.8	36.3	48.8	41.7	8.5	39.6
15	67.5	62.2	55.5	24.7	14.8	0	72	9.4	37.8	51	48.7	13	27.6
16	57.8	61.3	56.2	22.5	18.6	0	66.2	11.4	49.7	57.2	54.9	11.7	23.9
17	56.5	61.2	56.4	19.4	21.9	0	58.7	13.3	48.7	58.1	55.5	10.5	19.6
18	67.2	61.3	56.6	26.6	25.2	0	55.3	15	53	57.2	54.5	10.7	12.6
19	48.1	60.9	56.7	15.3	27.9	0	46.1	16.6	47.4	60.1	57	8.6	12.2
20	71.4	62.9	56.8	25.4	32.3	0	16.6	18.1	27.2	46.6	44.8	19	0
21	30.3	57.5	56.8	1.6	29.6	11.1	0	10.5	29.1	65.8	63.5	8.8	0
22	34.5	69.6	55.9	0.5	9.3	59.7	0	0.9	8.2	53	26.4	0.1	0
23	16.6	73.6	24.5	0.2	1.7	112.3	0	0	3.3	18.6	4.2	0.1	0
0	6.3	73.6	8.1	0.1	0.1	136.9	0	0	0	1.8	0.1	0	0
1	7.5	67	7.4	0.1	0.1	145	0	0	0	0.1	0	0	0
2	1.8	67	1.9	0	0	152.4	0	0	0	0.2	0	0	0

EDT = Eastern Daylight Time.

It was an expensive day of delays. The delays are priced at the cost of the aircraft plus the fuel used during the delay. Pricing the taxi in delays at $22.07 per minute leads to a cost of almost $420,000 for the roughly 19,000 aircraft-minutes of taxi delays. Departure delays are slightly less expensive at $21.18 per minute, but nevertheless the roughly 11,000 aircraft-minutes of departure delays would cost over $230,000. Airlines see ground holds as very expensive. Without considering the effects of customer displeasure on future business, ground holds are priced at $18.80 per minute (Table 2-1). Priced in this way, the total cost of the roughly 24,000 aircraft-minutes of ground holds due to arrival delays and 45,000 minutes of airplane delays would approach $1.3 million.

Effect of Night-Time Taxi Speeds

According to NASA personnel, aircraft taxi more slowly in the dark, and an effect of the Taxiway Navigation and Situation Awareness (T-NASA) tool is to remove this decrease in taxi speeds.[4] This reduced speed presumably affects all taxi

---

[4] The T-NASA tool will help pilots improve visibility and situation awareness through radar.

operations, so it is not appropriately modeled with our queuing model of delays at surface bottlenecks.

We made a crude preliminary model of the night-time speed reductions in the following way: The time required to taxi a distance, d, at speed, V, is of course d/V. If all typical taxi operations proceeded at "full speed," then taxi time would increase relatively by the same amount as the relative decrease in V.

Only part of a taxi operation will be conducted at full speed, however. Taxiing aircraft slow down in gate areas, for example, and when approaching intersections at which a stop may be required. Only the full speed taxi operation seems likely to be affected by darkness, and we intend to capture the effects of intersections with the queuing model of taxi delays.

We do not have the resources in the present task to develop statistics for either the distances taxied or for taxi times unconstrained by delays. To have a preliminary estimate of the effects of slower night-time taxi speeds, we developed a triangular distribution of the distances aircraft may be expected to taxi at full speed.

Arguably, most taxi paths include at least one-quarter mile of full-speed taxiing. Given that runways are often roughly 2 miles long, a plausible upper extreme for the distance, d, on which aircraft may taxi at full speed is one and one-half runway lengths, or 3 miles. A more common distance, which we take as the mode of the triangular distribution, is likely to be one-half the runway length, or 1 mile.

The mean of the triangular distribution just produced is $(0.25 + 1 + 3)/3$, or about 1.4 miles. NASA personnel inform us that daytime taxi speeds are about 18 knots, and night-time taxi speeds about 15 knots. This implies a daytime taxi time of about 5 minutes and an increase of about 1 minute per taxi operation conducted at night.

AIRPORT CAPACITY MODEL

Individual airport capacity models determine service rates to the arrival and departure runways, $\mu_A(t)$ and $\mu_D(t)$, respectively. These models generate arrival and departure capacities as functions of surface meteorological conditions (ceiling, visibility, wind speed and direction, and temperature) and arrival and departure demand. In this section, we describe our airport capacity model in some detail to show the parameters available for modeling AATT and TAP technologies.

We define runway capacity as a Pareto frontier in the arrival-rate/departure-rate plane, as shown in Figure 2-6.

Figure 2-6. Example Runway Capacity
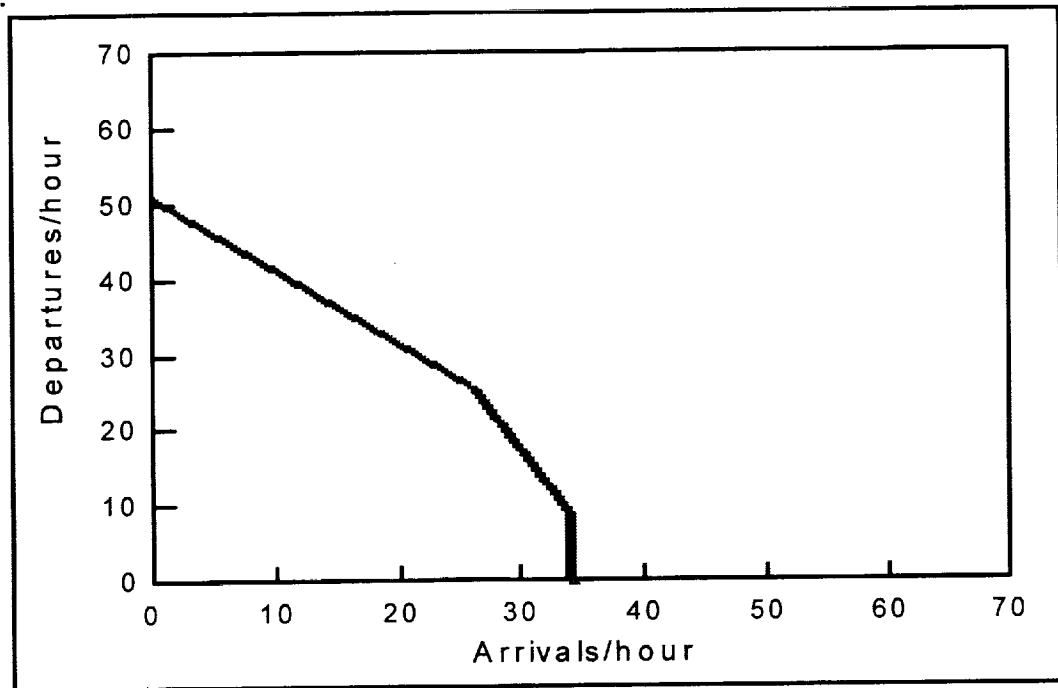
All cases of arrival rate/departure rate inside the region bounded by the capacity curve and the axes are feasible. The capacity curve itself is the set of feasible points at which not both arrival rate and departure rate can be increased.

We develop capacity from a "controller-based view" of runway operations. That is, we assume that a human controller manipulates aircraft, introducing time (or, equivalently, space) increments in traffic streams to meet all applicable rules— e.g., miles-in-trail requirements, single-occupant rule—with specified levels of confidence. The desired confidence may differ from rule to rule. For example, while respecting all rules, controllers may want greater confidence that two aircraft never attempt to occupy a runway simultaneously than that miles-in-trail minima are met.

As an example of this approach, consider the arrival-arrival sequence of Figure 2-7, which shows space-time trajectories of the two arrivals. Zero distance is the beginning of the common approach path, and zero time is the instant at which the lead aircraft enters the common approach path.

In our model, the controller maneuvers the following aircraft so that it enters the common approach path a time, μ, after the lead aircraft enters it. (The controller may actually achieve this by bringing the following aircraft onto the common path when the lead aircraft has advanced a specified distance along the path.) The controller chooses the time interval, μ, through knowledge of typical approach speeds for the two aircraft and of disturbances affecting their relative positions (winds, position uncertainties, variations in pilot technique) to ensure that miles-in-trail

2-14

requirements and runway occupancy rules are met with assigned levels of confidence. As we will see in the following subsections, this action of the controller—together with information on statistics of aircraft operating parameters and the disturbances to arrival operations, such as winds and position uncertainties—leads directly to statistics of operations and runway capacity.

Figure 2-7. Flight Trajectories, Gaining Follower
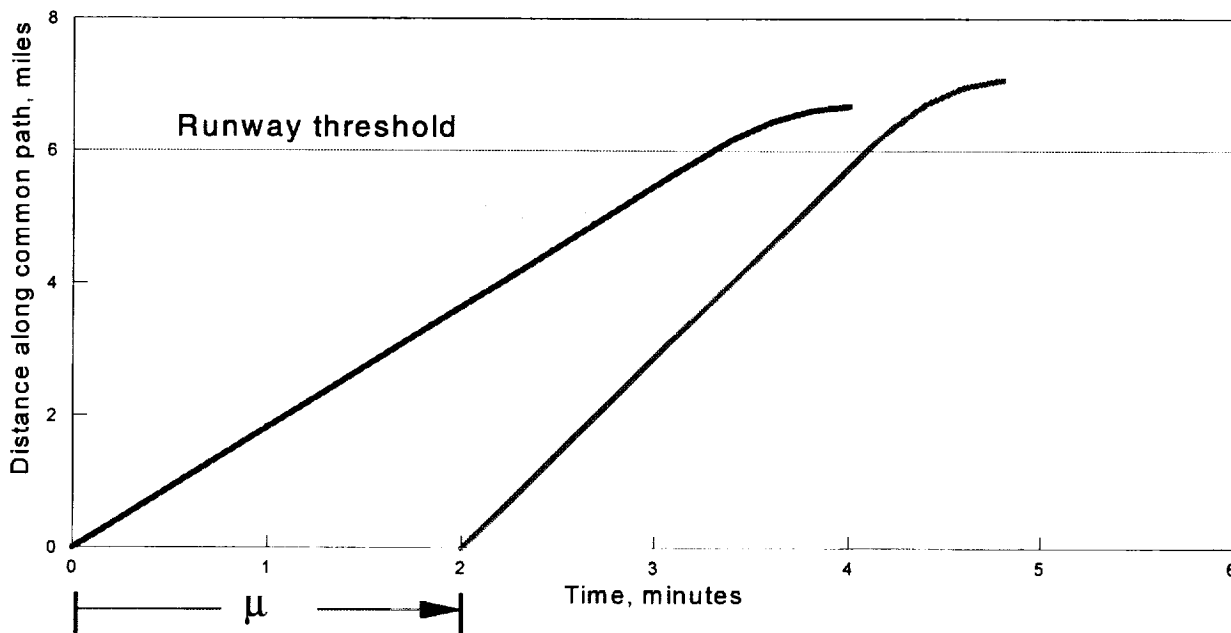
Arrivals Only

We consider first the controller-based paradigm for a runway devoted entirely to arrivals. Two cases are important: when the following aircraft's approach speed is greater than that of the lead aircraft ("gaining follower") and when it is less ("lagging follower"). The gaining-follower case also covers the case of equal approach speeds.

GAINING FOLLOWER

The first of these cases, illustrated by Figure 2-7, occurs when the mean approach speed of the following aircraft exceeds that of the leader.

In this case, the miles-in-trail constraint applies as the leader crosses the runway threshold. At that time, the leader's position is D. We will derive a condition on the controller's interval, μ, to guarantee that the miles-in-trail requirement is met, i.e., that at the time the leader crosses the threshold, the follower is at least distance S away from the threshold, with a specific probability, which we take as 95 percent.

The position of the lead aircraft is given by

$$X_L = \delta X_L + (V_L + \delta V_L + \delta W_L)t \qquad \text{[Eq. 2-20]}$$

and the position of the following aircraft by

$$X_F = \delta X_F + (V_F + \delta F_F + \delta W_F)(t - \mu) \qquad \text{[Eq. 2-21]}$$

The leader crosses the runway threshold at time t_{LO}, given by

$$t_{LO} = \frac{D - \delta X_L}{V_L + \delta V_L + \delta W_L} \qquad \text{[Eq. 2-22]}$$

At time t_{LO}, the follower is at $X_F(t_{LO})$, given by

$$X_F(t_{LO}) = \delta X_F + (V_F + \delta V_F + \delta W_F)\left(\frac{D - \delta X_L}{V_L + \delta V_L + \delta W_L} - \mu\right) \qquad \text{[Eq. 2-23]}$$

We wish to derive a condition on μ, to make $D - X_F(t_{LO}) \geq S$, with a probability of at least 95 percent. To keep the problem tractable, we will assume that all disturbances are of first order, and linearize Equation 2-23. When linearized, Equation 2-23 becomes

$$X_F(t_{LO}) = \delta X_F + \frac{DV_F}{V_L}\left(1 + \frac{\delta V_F + \delta W_F}{V_F} - \frac{\delta X_L}{D} - \frac{\delta V_L + \delta W_L}{V_L}\right) - \mu V_F\left(1 + \frac{\delta V_F + \delta W_F}{V_F}\right) \qquad \text{[Eq. 2-24]}$$

In this linear approximation, $X_F(t_{LO})$ is a normal random variable of mean $\dfrac{DV_F}{V_L} - \mu V_F$ and variance

$$\sigma_1^2 = \frac{D^2 V_F^2}{V_L^2}\left(\frac{\sigma_{VF}^2 + \sigma_{WF}^2}{V_F^2} + \frac{\sigma_{XL}^2}{D^2} + \frac{\sigma_{VL}^2 + \sigma_{WL}^2}{V_L^2}\right) + \mu^2 V_F^2 \frac{\sigma_{VF}^2 + \sigma_{WF}^2}{V_F^2} + \sigma_{XF}^2 \qquad \text{[Eq. 2-25]}$$

The condition that $D - X_F(t_{LO}) \geq S$, with a probability of at least 95 percent, may then be stated as

$$\frac{DV_F}{V_L} - \mu V_F + 1.65\,\sigma_1 \leq D - S$$

or

$$\mu \geq \frac{D}{V_L} - \frac{D - S}{V_F} + \frac{1.65\sigma_1}{V_F} \qquad \text{[Eq. 2-26]}$$

Inequality in Equation 2-26 gives, in essence, the desired condition. However, μ is present on both sides of the inequality. Straightforward manipulations lead to an explicit condition on μ, which, neglecting terms of second order in relative disturbances in comparison with one, may be written

$$\mu \ge A + \sqrt{A^2 B^2 + C^2}$$ [Eq. 2-27]

where

$$A \equiv \frac{D}{V_L} - \frac{D - S}{V_F}$$ [Eq. 2-28]

$$B^2 \equiv 1.65^2 \left\{ \frac{\sigma_{VF}^2 + \sigma_{WF}^2}{V_F^2} \right\}$$ [Eq. 2-29]

and

$$C^2 \equiv \frac{1.65^2}{V_F^2} \left\{ \frac{D^2 V_F^2}{V_L^2} \left(\frac{\sigma_{VF}^2 + \sigma_{WF}^2}{V_F^2} + \frac{\sigma_{XL}^2}{D^2} + \frac{\sigma_{VL}^2 + \sigma_{WL}^2}{V_L^2} \right) + \sigma_{XF}^2 \right\}$$ [Eq. 2-30]

To determine numerical values of the smallest μ that meet 2-26, we find the iterative scheme

$$\mu_{n+1} = \frac{D}{V_L} - \frac{D - S}{V_F} + \frac{1.65 \sigma_1 (\mu_n)}{V_F}$$

more convenient than using Equation 2-27.

Now let us develop a condition on μ that will guarantee that the follower does not cross the runway threshold until the leader has left the runway, with a specified probability, which we choose to be 98.7 percent. The leader will exit the runway at time $t_{LO} + RA_L$, and the follower will cross the threshold at time t_{FO}, given by

$$t_{FO} = \frac{D - \delta X_F}{V_F + \delta V_F + \delta W_F} + \mu$$ [Eq. 2-31]

Linearizing as previously, we find that in the linear approximation $t_{FO} - t_{LX}$ is a normal random variable with mean $\frac{D}{V_F} + \mu - \frac{D}{V_L} - \overline{RA_L}$, where $\overline{RA_L}$ denotes the mean of RA_L, and variance

$$\sigma_2^2 = \frac{D^2}{V_F^2} \left(\frac{\sigma_{XF}^2}{D^2} + \frac{\sigma_{VF}^2 + \sigma_{WF}^2}{V_F^2} \right) + \frac{D^2}{V_L^2} \left(\frac{\sigma_{XL}^2}{D^2} + \frac{\sigma_{VL}^2 + \sigma_{WL}^2}{V_L^2} \right) + \sigma_{RAL}^2$$ [Eq. 2-32]

It follows that the condition on μ for the follower not to cross the threshold until the leader has exited the runway—i.e., that $t_{FO}-t_{LX} > 0$—with a probability of 98.7 percent is

$$\mu \geq \frac{D}{V_L} - \frac{D}{V_F} + \overline{RA_L} + 2.215\sigma_2 \qquad \text{[Eq. 2-33]}$$

The controller will in effect impose that value of time interval μ that is the smallest μ satisfying both Equations 2-26 and 2-32.

Given μ, the time between threshold crossings of successive arrivals is, in our approximation, a normal random variable of mean

$$\frac{D}{V_F} - \frac{D}{V_L} + \mu \qquad \text{[Eq. 2-34]}$$

and variance

$$\sigma_3^2 = \frac{D^2}{V_F^2}\left(\frac{\sigma_{XF}^2}{D^2} + \frac{\sigma_{VF}^2 + \sigma_{WF}^2}{V_F^2}\right) + \frac{D^2}{V_L^2}\left(\frac{\sigma_{XL}^2}{D^2} + \frac{\sigma_{VL}^2 + \sigma_{WL}^2}{V_L^2}\right) \qquad \text{[Eq. 2-35]}$$

LAGGING FOLLOWER

When the follower's approach speed is slower than the leader's in the controller-based view, the controller will bring the follower onto the common path after the leader has advanced a distance S along it, as illustrated in Figure 2-8.

Figure 2-8. Flight Trajectories, Lagging Follower
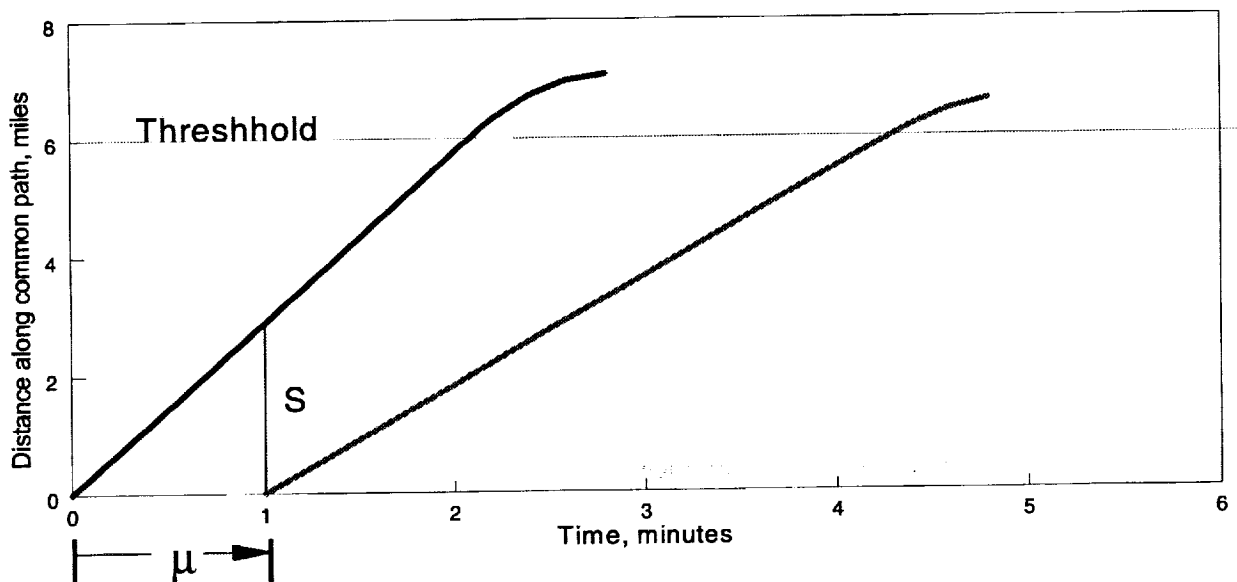
The positions of the two aircraft as functions of time are again given by Equations 2-20 and 2-21. The miles-in-trail requirement is now that $X_L(\mu)-X_F(\mu) \geq S$, with a probability of at least 95 percent. But

$$X_L(\mu) - X_F(\mu) = \delta X_L + (V_L + \delta V_L + \delta W_L)\mu - \delta X_F \qquad \text{[Eq. 2-36]}$$

is a normal random variable of mean $V_L\mu$ and variance

$$\sigma_4^2 = \mu^2(\sigma_{VL}^2 + \sigma_{WL}^2) + \sigma_{XF}^2 + \sigma_{XL}^2 \qquad \text{[Eq. 2-37]}$$

It follows that the condition that the miles-in-trail requirement is met, with 95 percent confidence, is

$$\mu \geq \frac{S}{V_L} + 1.65\frac{\sigma_4}{V_L} \qquad \text{[Eq. 2-38]}$$

Equation 2-38 may be written as a single condition on μ, using Equation 2-27, by replacing Equations 2-28, 2-29, and 2-30 with the new definitions

$$A \equiv \frac{S}{V_L},$$

$$B^2 \equiv 1.65^2 \frac{\sigma_{VL}^2 + \sigma_{WL}^2}{V_L^2}, \text{ and}$$

$$C^2 \equiv 1.65^2 \frac{\sigma_{XL}^2 + \sigma_{XF}^2}{V_L^2}.$$

The condition that the single-occupant rule is met with 98.7 percent confidence is derived exactly as we derived that condition for $V_F \geq V_L$, i.e., condition Equation 2-33. In the present case, too, the result is given by Equation 2-33. Also, in the present case, equations for the mean and standard deviation of interarrival time, given μ, are given by Equations 2-34 and 2-35.

Sequences of Alternating Arrivals and Departures

We can readily translate the preceding results for repeated *A–D* operations, by replacing RA_L with $RA_L + RD_D$, where the subscript, *D*, denotes the intervening departure aircraft. This case is illustrated by Figure 2-9.

Figure 2-9. Flight Trajectories, Mixed Arrival and Departure
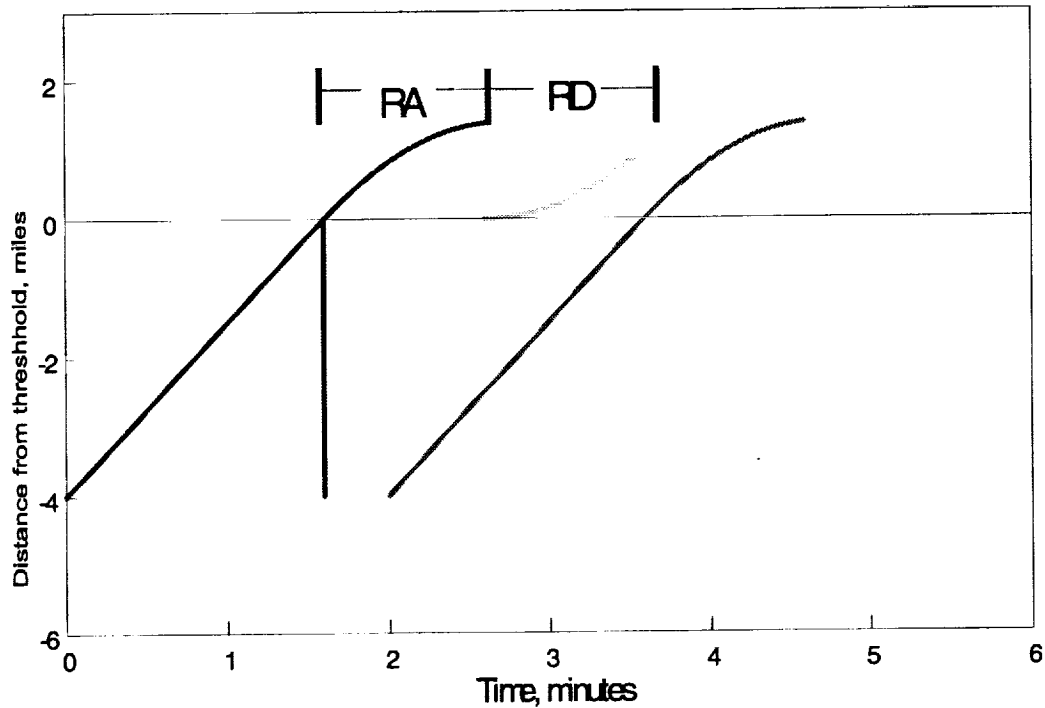
It may be desirable to consider the effect of a communications lag, c, on the departure. If so, then RA_L is replaced by $RA_L + c + RD_D$.

Statistics of Multiple Operations

At this point, we have expressions for the means and variances of normal random variables representing interarrival times for two cases: when the runway is used for arrivals only and when it is used for alternating arrivals and departures. Now we wish to use these to generate statistics of multiple arrivals, or multiple arrivals and departures, to capacity curves for single runways.

First, we consider the statistics of sequences of arrivals only. Statistics of the overall interarrival time will be determined by the mix of aircraft using the runway, with their individual values of the aircraft parameters of Table 2-2. Suppose n aircraft types use the runway, and let the fraction of the aircraft of type i in the mix be p_i. Then the results of the preceding sections give interarrival time for each leader-follower pair as a normal random variable. Let t_{AAij} denote the random variable that is the interarrival time for aircraft of type i following an aircraft of type j. As we have seen, in our model t_{AAij} is a normal random variable; let its mean and standard deviation be μ_{ij} and σ_{ij}, respectively.

2-20

Table 2-2. Runway Capacity Parameters

Symbol	Definition
λ	Reciprocal of mean input-stream delay
c	Mean communication time delay
δc	Standard deviation of communication time delay
D	Length of common approach path
D_D	Distance-to-turn on departure
p_i	Fraction of operating aircraft that are type i
RA_i	Mean arrival runway occupancy time of ith aircraft type
δRA_i	Standard deviation of arrival runway occupancy time of ith aircraft type
RD_i	Mean departure runway occupancy time of ith aircraft type
δRD_i	Standard deviation of departure runway occupancy time of ith aircraft type
S_{ij}	Miles-in-trail separation minimum, aircraft of type i behind aircraft of type j
S_{ij}^D	Departure miles-in-trail separation minimum, aircraft of type i behind aircraft of type j
IMC	Binary variable; 1 means instrument meteorological conditions prevail
V_i	Approach speed of aircraft type i
δV_i	Standard deviation in approach speed of aircraft type i
δW_i	Wind variation experienced by aircraft of type i
δX_i	Standard deviation of controller's information on position of aircraft i

Now, to determine the distribution of the overall interarrival time, t_{AA}, we consider a classical "urn" problem: we have a population of interarrival times, from which we draw one member, and we wish to know the distribution function of the result. The probability of drawing t_{AAij} is $p_j p_i$, and the distribution function of the result is the weighted sum of the distribution functions for the individual t_{AAij}. That is, the distribution function for the overall interarrival time $t_{AA}(1)$ is

$$t_{AA}(1) \sim \sum_i \sum_j p_i p_j N(t; \mu_{ij}, \sigma_{ij})$$

[Eq. 2-39]

where $N(t; \mu, \sigma)$ denotes the normal probability distribution function. Obviously, the distribution of interarrival times is not necessarily normal. An example of an interarrival time distribution of the type Equation 2-39 is shown in Figure 2-10.

Figure 2-10. Example Probability Distribution of Interarrival Time
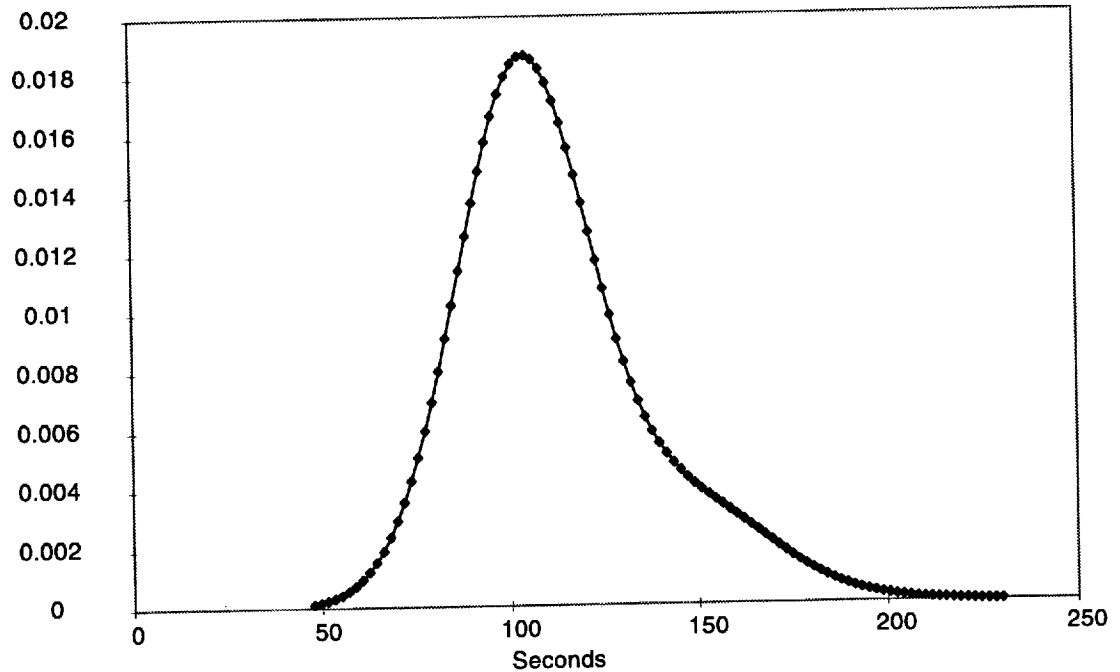
As Figure 2-10 suggests, the interarrival time distribution is not necessarily monomodal.

One can compute the mean and variance of the interarrival time distribution in Equation 2-39 straightforwardly: the results are

$$<t_{AA}(1)>=\sum_i\sum_j p_i p_j \mu_{ij} \qquad \text{[Eq. 2-40]}$$

and

$$\text{var}(t_{AA}(1)) = \sum_i \sum_j p_i p_j (s_{ij}^2 + m_{ij}^2) - <t_{AA}(1)>^2 \qquad \text{[Eq. 2-41]}$$

To find the number of arrivals that the runway can accommodate in a given period of time with a specified confidence, we need the distribution of the time required for a sequence of M arrivals. We determine that distribution as follows.

Consider first the case of two arrivals. With probability $p_i p_j p_k$, the observed total time for a sequence of two arrivals will be $t_{AAij} + t_{AAjk}$. For given i, j, and k that total time is distributed normally, with

$$t_{AAij} + t_{AAjk} \sim N\left(\mu_{ij} + \mu_{jk}, \sqrt{\sigma_{ij}^2 + \sigma_{jk}^2}\right) \qquad \text{[Eq. 2-42]}$$

Thus, the time $t_{AA}(2)$ for a sequence of two arrivals will have the distribution

$$t_{AA}(2) \sim \sum\sum p_i p_j N\left(\mu_{ij} + \mu_{jk}, \sqrt{\sigma_{ij}^2 + \sigma_{jk}^2}\right),$$ [Eq. 2-43]

where the sums range over the number of aircraft in the mix.

Continuing in this way to reckon the distributions of the time required for 3, 4, ..., M arrivals, we conclude that $t_{AA}(M)$ has the distribution

$$\sum\sum \cdots \sum p_i p_j \cdots p_y p_z N\left(\mu_{ij} + \mu_{jk} + ... + \mu_{yz}, \sqrt{\sigma_{ij}^2 + \sigma_{jk}^2 + ... + \sigma_{yz}^2}\right).$$ [Eq. 2-44]

In Equation 2-25, the sums range over the set of aircraft using the runway. There are $M + 1$ summations, and $M + 1$ terms in $p_i p_j \cdots p_y p_z$. There are M terms in both the sums $\mu_{ij} + \mu_{jk} + ... + \mu_{yz}$ and $\sigma_{ij}^2 + \sigma_{jk}^2 + ... + \sigma_{yz}^2$.

Evaluating the expected value $<t_{AA}(M)>$ is straightforward. We find

$$<t_{AA}(M)> = \sum\sum \cdots \sum p_i p_j \cdots p_y p_z \left(\mu_{ij} + \mu_{jk} + ... + \mu_{yz}\right),$$ [Eq. 2-45]

which leads directly to

$$<t_{AA}(M)> = M \sum\sum p_i p_j \mu_{ij},$$ [Eq. 2-46]

since the p_i sum to one.

Evaluating the variance of $t_{AA}(M)$ is more involved. After considerable manipulation, we find

$$\mathrm{var}\left(t_{AA}(M)\right) = M \sum\sum p_i p_j \left(\sigma_{ij}^2 + \mu_{ij}^2\right) + 2(M-1)\sum\sum\sum p_i p_j p_k \mu_{ij}\mu_{jk} - (3M-2)\left(\sum\sum p_i p_j \mu_{ij}\right)^2.$$ [Eq. 2-47]

In Equation 2-47, the sums again range over the set of aircraft types that use the runway.

Evaluating the number of arrivals that a runway can accommodate in 1 hour, with assigned confidence, is conceptually straightforward: one finds the largest M for which the cumulative distribution corresponding to the probability distribution Equation 2-44, evaluated at 3,600 seconds, is not less than the desired confidence. It is tempting to approximate the distribution in Equation 2-44 with a normal distribution for this purpose, since direct evaluation of the cumulative distribution function corresponding to Equation 2-44 involves lengthy sums when M takes values near typical hourly arrival numbers, which are around 30.

If the individual interarrival times in a sequence of arrivals were statistically independent, an appeal to the central limit theorem would justify that approximation.

Of course, they are not independent, because the follower in a given pair is the leader for the next pair of the sequence.

Nevertheless, numerical experiments suggest that members of the family of distributions in Equation 2-44 are well approximated by normal distributions, even for fairly small M, even when the distribution of a single interarrival time departs considerably from a normal distribution. Figures 2-11 and 2-12 illustrate this, with the distribution functions of the time for two and for four arrivals, respectively. The single-arrival distribution is the same as that of Figure 2-10.

In view of results like those of Figures 2-11 and 2-12, we approximate the distribution of the time required for M arrivals as a normal distribution whose parameters are the mean and variance given by Equations 2-46 and 2-47, respectively. Then the largest number of arrivals that the runway can accommodate in 1 hour, with 95 percent confidence, is the largest value of M for which

$$<t_{AA}(M)>+1.65\sqrt{\mathrm{var}(t_{AA}(M))} \leq 3{,}600,$$ [Eq. 2-48]

where $t_{AA}(M)$ and var$[t_{AA}(M)]$ are evaluated by Equations 2-46 and 2-47, respectively. For the case illustrated by Figures 2-10, 2-11, and 2-12, this leads to a capacity of 30 arrivals per hour.

An alternative definition of runway capacity is the largest number of arrivals for which the expected total time is not longer than 3,600 seconds. With this definition, the capacity of the runway for the case illustrated in the figures is 32 arrivals per hour.

Figure 2-11. Distribution Function of the Time for Two Arrivals
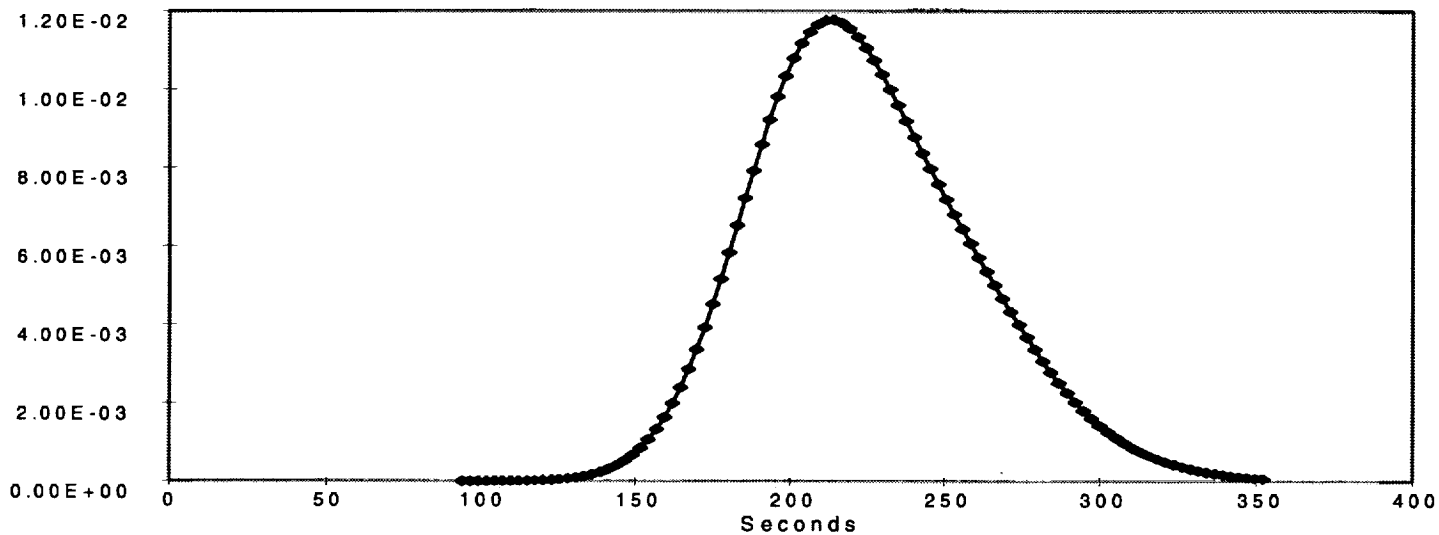
Figure 2-12. Distribution of the Time for Four Arrivals
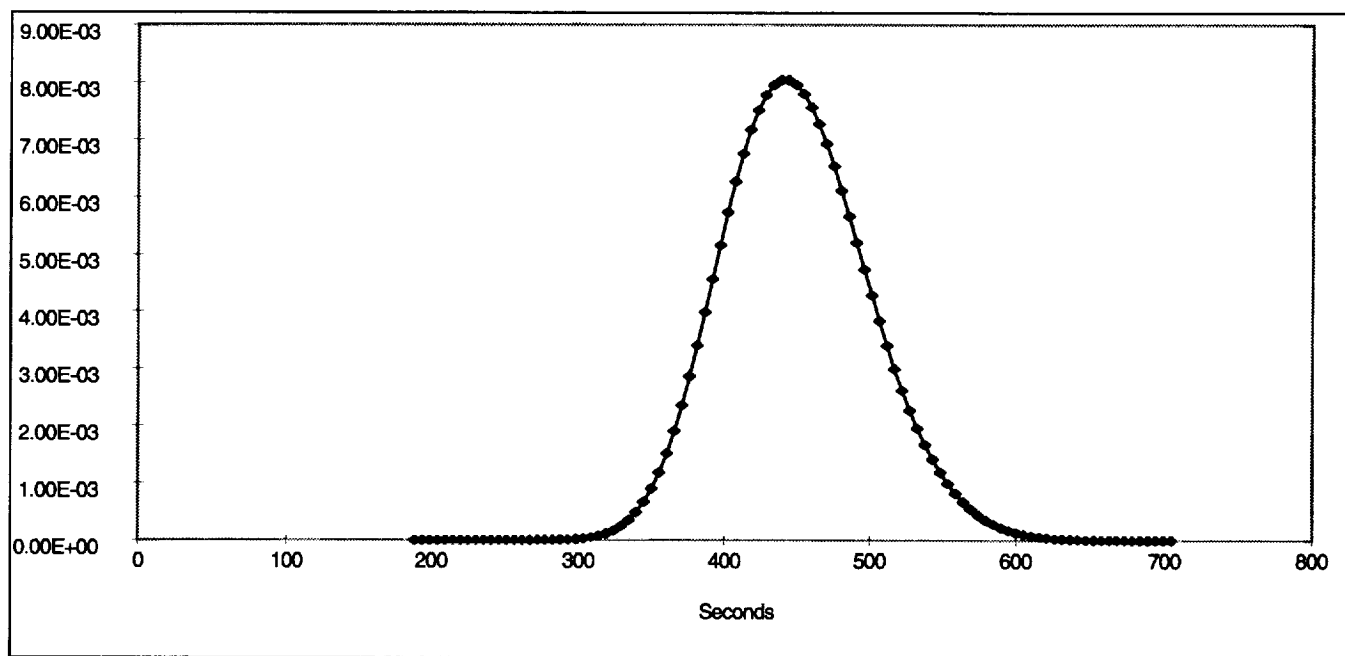
Input-Stream Effects

So far, we have developed our model as though the controller could always impose the desired time separation, μ, whatever the nature of the incoming stream of aircraft. This may not in fact always be the case, and we extend our model to cover input-stream effects in this way:

We suppose that the controller, wishing to impose separation μ, is actually able to impose the separation μ + ν, where ν is a random variable, independent of all others in the analysis, characterizing input-stream effects. We take ν to have the exponential distribution with parameter λ, i.e.,

$$\nu \sim \lambda e^{-\lambda \nu}.$$ [Eq. 2-49]

With the addition of the random variable, ν, the distribution of interarrival times for a fixed leader-follower pair is no longer a normal random variable, but the convolution of a normal random variable and an exponential random variable. Specifically, the distribution is

$$H(t;\mu,\sigma,\lambda) \equiv \frac{\lambda}{\sqrt{2\pi}\sigma} \int_0^\infty e^{-\frac{(t-\tau-\mu)^2}{2\sigma^2}-\lambda\tau} \, d\tau.$$ [Eq. 2-50]

This distribution function may be evaluated conveniently using

$$H(t;\mu,\sigma,\lambda) = \lambda e^{-\lambda(t-\mu)+\frac{\lambda^2\sigma^2}{2}} \left[1 - C(\mu, t - \lambda\sigma^2, \sigma)\right].$$ [Eq. 2-51]

where $C(x,\mu,\sigma)$ denotes the cumulative normal distribution for mean μ and standard deviation σ, evaluated at x.

Figure 2-13 shows an example of this class of distribution, together with the normal distribution that would have been seen absent input-stream effects. The example of Figure 2-13 is somewhat extreme, for the sake of illustration. Typically, input-stream effects would introduce a mean error of 10 seconds or less.

With our model of input-stream effects, the distribution of interarrival times changes from Equation 2-39 to

$$t_{AA}(1) \sim \sum_i \sum_j p_i p_j H(t;\mu_{ij}, \sigma_{ij}, \lambda)$$ [Eq. 2-52]

Figure 2-13. Example Interarrival Distribution with Input-Stream Effects
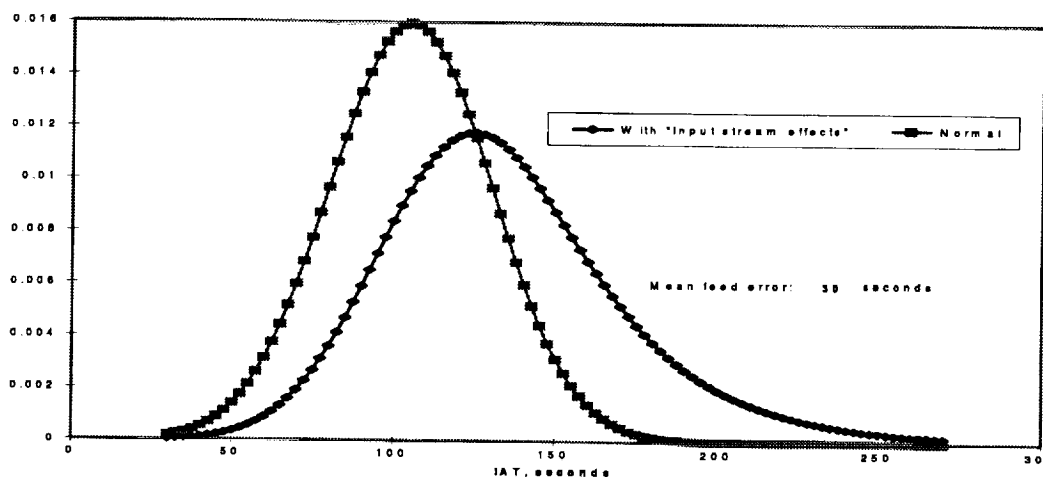
and the distribution function of $t_{AA}(M)$ changes from Equation 2-44 to

$$\sum\sum\sum p_i p_j \cdots p_y p_z H\left(t; \mu_{ij} + \mu_{jk} + \ldots + \mu_{yz}, \sqrt{\sigma_{ij}^2 + \sigma_{jk}^2 + \ldots + \sigma_{yz}^2}, \lambda, M\right) \qquad \text{[Eq. 2-53]}$$

where

$$H(t; \mu, \sigma, \lambda, K) \equiv \frac{\lambda^K}{\sqrt{2\pi}\sigma(K-1)!} \int_0^\infty \tau^{K-1} e^{-\frac{(t-\tau-\mu)^2}{2\sigma^2} - \lambda\tau} \, d\tau \qquad \text{[Eq. 2-54]}$$

It is not difficult to show that the mean and variance of $t_{AA}(M)$ may be obtained from the values in Equations 2-46 and 2-47, simply by adding M/λ to $<t_{AA}(M)>$ and $M/(\lambda^2)$ to $\text{var}(t_{AA}(M))$. With these results, and the assumption that the distribution of $t_{AA}(M)$ may be adequately approximated by a normal distribution for sufficiently large M, we may compute runway capacities with our model of input-stream effects. For example, taking the value $1/\lambda = 6.3$ seconds, which certain data for operations at DFW suggest, reduces the 95-percent-confidence capacity to 28 arrivals/hour, and the "expected-total-arrival-time" capacity to 30.

Completing the Pareto Frontier of Runway Capacity

At this point, we have developed our model for one point on the Pareto frontier that describes runway capacity, the point for all arrivals and no departures. We give this fairly complete discussion of that point because it is often a very important one and to illustrate our modeling work.

We completed our runway capacity models by systematically continuing the approach described previously, to cover three other cases: when the runway is devoted wholly to departures, when the runway operates with alternating departures

and arrivals, and when the runway operates with as many departures as possible, while continuing to accommodate the same number of arrivals as in the arrivals-only case. We thus characterize the Pareto frontier by four points.

When these steps are completed, several parameters characteristic of a specific airport are found to affect runway capacity. The complete list of capacity parameters is shown in Table 2-2.

In addition to the runway capacity parameters, LMINET's airport capacity models respond to information on the configurations in which the airport is usually operated. This information includes the specific runways that make up the configuration, with their individual minimum visibility restrictions. Our airport capacity models systematically select the configuration most capable of meeting demand, in view of meteorological conditions. The airport models report the feasible arrival-rate/departure-rate combination that best meets demand as the airport's instantaneous capacity.

MODELS OF TRACON AND ARTCC SECTORS

Recent work done for NASA at the Institute has produced new models of both ARTCC and TRACON sectors as multiserver queues, specifically as $M/E_k/N/N+q$ queues. That is, as queues with Poisson arrivals, service times with the Erlang distribution with parameter k, and N servers; not more than q clients will wait for service, so the maximum number in the system is $N + q$.

The models were developed with input from FAA people, including controllers at the Denver ARTCC and the Denver TRACON as well as experienced supervisory controllers working at the FAA's National Command Center in Herndon, VA. The development and calibration of the queuing models of sectors is described in [1]. The following section gives some details of the model and of the numerical treatment that we made for operating LMINET.

$M/E_3/N/N+Q$ Sector Model

In our queuing model for the ARTCC and TRACON sectors of the NAS, the times between aircraft arrivals to each sector are assumed to have the Poisson distribution, and the time that an aircraft stays in a sector is assumed to be a random variable distributed according to Erlang-3 distribution. A sector can simultaneously handle no more than N aircraft at a time, where the capacity N is determined by the sector's characteristics and the weather. We also assume that, at most, q aircraft will "wait"—i.e., be delayed by speed changes or vectoring—to be served in a sector.

The arrival demand for a sector is determined by the network flight schedule. The choice of the Erlang-3 distribution for the times-in-sector was made in view of ETMS data and is explained in [1]. We chose 18 as the maximum number of

aircraft that a sector's controllers can handle at one time, to be consistent with [13]. We base our choice of the maximum number of "wait" aircraft on interviews with controllers at the Denver ARTCC.

Solving the model poses a significant challenge. There is no closed form solution, not even for the steady state, for the $M/E_k/N/N+q$ queue. We determine the probabilities of each state of the system numerically.

That is itself a respectable challenge because the number of states is large. For a $M/E_3/N/N+3$ system, there are 1,950 states. [6] The number of states increases rapidly with N. For example, if $q = 3$, the number of states is 27,000 if N is 50, the number of states is 192,000 if N is 100, and the number of states is 620,000 if N is 150. Thus, determining the state probabilities directly from the evolution equations means solving a very large system of ordinary differential equations.

The systems' plant matrices are sparse, and the systems seem reasonably well-conditioned, so that brute-force numerical methods may succeed for some cases. We have, in fact, generated numerical solutions of the full equations for $N=18$ and $q = 3$ in this way, to have means of checking the results of approximate solution methods. This approach takes too much time, however, to be at all appealing for routine use. Fast-executing approximate solutions are greatly to be desired. The trick lies in reducing the number of states.

Our key idea for improving the computer execution involves a new concept called mega state. The Erlang-3 distribution is mathematically equivalent to the distribution that results from service by three servers in tandem, each of which has the same Poisson distribution of service times. Thus, the state of an $M/E_3/N/N+q$ system is determined by four numbers i, j, k, and q, where i denotes the number of aircraft that have not completed one service of the three required, j denotes the number that have completed one but not two services, k is the number that have completed two but not three, and q is the number of aircraft waiting.

The mega state, m, is defined as $m = i + j + k$. If the sector capacity is N, then $m \in [0, N]$. After checking the state transition matrix, we realized that a state interacts only with states of neighboring mega states. This further implies that for mega states $m_1, m_2, m_1 < m_2$, if $Pr(m_1)=0$, then $Pr(m_2)=0$, which can be proved by mathematical induction.

In practice, we can maintain a dynamic upper bound of the mega state such that the probability of any mega state less than this upper bound is nonzero and the probability of any mega state equal or larger than this upper bound is negligibly small. Therefore, we do not need to solve all the state transition equations; we need to solve only the ones whose mega state is equal to or less than the upper bound. This technique alone reduces more than 90 percent of computer execution time. Since the upper bound is dynamic, there is virtually no loss of accuracy of solution, which we have verified by comparison with exact solutions.

For solving those state evolution equations that must be solved, we have tried forward Euler, second- and fourth-order Runge-Kutta integration schemes. Of the three, the second-order Runge-Kutta gives us the best speed, contrary to the conventional wisdom that the fourth-order Runge-Kutta would. The higher the order in the Runge-Kutta integration scheme, the more accuracy we may get; hence, we may afford larger integration steps to speed up the process. However, due to the large number of differential equations with which we have to deal, stiffness is likely to prevent our using large steps. We finally settled on the second-order Runge-Kutta scheme with adaptive step.

The adaptive step control works as follows. In moving the time by one step, we also move the time by two half steps. We then compare their results. If their difference is smaller than a specified number, we will enlarge the step in the next iteration; if their difference is larger than a specified number, we will reduce the step and go back to redo this integration step. Their differences are also used to get better precision. In working out several cases, we find that we gain a small fraction of the total time by using a second-order Runge-Kutta scheme with adaptive step size.

Another important method for keeping the queuing calculations tractable is to introduce subsectors. This is particularly helpful for the rectangular-area sectors of LMINET, which can have large peak demands.

In operating the NAS, the FAA subdivides busy sectors, geographically and/or by altitude. We model this by our subdividing busy sectors into sets of independent sectors, each of which has the N of a single sector. We have been careful not to carry this process beyond the point at which the subdivisions are at least arguably feasible for actual operations.

LMINET's rectangular en route sectors are roughly 120 miles on a side. They represent airspace above Flight Level 230. With present altitude-direction conventions, this affords about 14 levels at which modern turbojet transports may cruise: eastbound traffic at flight levels 230, 250, 270, 290, 330, 370, and 410; westbound traffic at flight levels 240, 260, 280, 310, 350, 390, and 430.

Thus, division into two subsectors can be accomplished feasibly, either by altitude or geographic sectioning: two geographic subsectors would be 60 × 120 nautical miles, and two altitude subsectors would each have 7 available flight levels.

Subsectoring with two geographic subsectors and two altitude subsectors is also feasible, so divisions with four subsectors are feasible.

Subsectoring into three geographic regions could certainly be accomplished feasibly, giving sectors 40 × 120 miles. Division of a rectangular sector into three subsectors by altitude division probably is feasible, as well: each subsector would

have at least two altitudes. But the resulting combination, giving nine subsectors, may be about as far as one should go.

Internally, LMINET assumes that aircraft arriving at a subsectored sector are roughly evenly divided among the subsectors. Queue statistics are generated for just one of these, so, to get overall delay statistics, one scales up the single-sector result by the number of subsectors. The advantage for the queuing calculations is that we never consider a sector capacity N larger than the value, typically 18, that is characteristic of a single controller team.

With megastates and subsectoring, and compiling the C code in which LMINET is written to optimize execution speed, we can generate statistics for one 20-hour "day" of CONUS operations in roughly 15 minutes on LMI's HP D370 with RISC 2.0.

TRACON Models

Each airport's TRACON is modeled with two arrival sectors and one departure sector. All the sectors are modeled as *M/Ek/N/N+q* queues.

LMINET allocates arrivals to an airport so that each arrival TRACON sector sees roughly half of the arrivals in each epoch of operation. For the work reported here, an epoch is 1 hour long.

En Route Sector Models

Like the TRACON sectors, en route sectors are modeled as *M/Ek/N/N+q* queues.

Automatic Traffic Flow Controller

This element of LMINET models the FAA's practice of delaying scheduled aircraft departures to congested airports. The function of this module can be summarized as limiting the arrivals to each airport by the airport's arrival capacity for each time epoch of the day so that large arrival queues never form.

To perform this function, we construct a planning window, composed of the rest of day, to facilitate the planning of ground hold decisions. At each epoch of the day, the module checks each airport's arrivals for the rest of the day. If the scheduled arrivals exceed the arrival capacity, the module will move some arrivals to the next epoch so that arrival demand meets capacity.

This process continues successively to the end of the day for each airport. Once this is done, the departure schedule is permanently changed, based on the delays calculated during the process. The arrival queue and departure queue at the end of the last epoch are counted as additional demands to arrival and departure at the

current epoch in the planning window, and the queue for planes from the last epoch is counted as demand to both arrival and departure at the current epoch.

Even with the traffic flow controller, we cannot totally eliminate the arrival queues due to the fact that (1) we cannot delay an aircraft that is already in departure, (2) we will not delay the arrivals from the out-of-network airport, (3) airport capacities are dynamic and depend upon both arrivals and departures, which means that arrivals may exceed the arrival capacity even if arrivals equal capacity in the planning due to the large departure demand, and (4) delays are always possible in a queuing system.

We implement the automatic flow controller in accordance with the following guidelines:

◆ Only departures *to* the congested airport will be delayed. The amount of delay is equally distributed among all the flights eligible to be delayed. We will not delay the departures *from* the congested airport to reduce congestion.

◆ Only the flights in the network airports may be delayed. The departures from airports outside the 64-airport network will not be delayed.

◆ We assume each airport is independent in its traffic flow control planning, and the decision to delay flights to the congested airport is solely based on the current schedule, current delays and queues, and forecasted airport capacities. Since the air traffic flow control planning is done at each epoch for the rest of the day for each airport, the network effect of the traffic flow control is done through the modified schedule for the rest of the day. TRACON congestion is not a decision criterion.

◆ Local weather information, for the rest of the day, is assumed to be known to the air traffic controller at any time of the day.

◆ A flight can be delayed repeatedly as long as it has not yet departed.

The typical cause of airport and TRACON congestion is inclement weather, which will reduce both capacities. However, as we found out, we do not need to specifically count TRACON congestion as decision criterion because once the arrivals and departures are curtailed, the demand to the associated TRACONs will also be reduced.

Chapter 3
Adjusting LMINET to Model the NAS

Users may adjust several LMINET inputs: demand profiles, airport capacity models, sector capacity models, surface weather and weather aloft, routes between airports, and so on. This chapter explains our choices for the baselines.

DEMAND INPUTS

In general, the demand input to an NAS model must provide all requests for service, at any time and anywhere in the NAS. Since other inputs to LMINET provide the four-dimensional (4-D), or space and time, flight trajectories between every airport pair, and since LMINET has models that handle the queues and delays, the principal demand input to LMINET is the flight departure schedule, s_{ijk}, where $i, j \in I = \{0,1,...,64\}$ and $k \in K=\{0,1,...,20\}$. Here i and j are the indices of the airports in the LMINET, where 0 represents an out-of-network airport, and k is the time index, where 0 represents the beginning of the day (0600 EDT). For this study, we operated LMINET in 1-hour epochs, so that the 21 epochs cover the period from 0600 EDT to 2300 Pacific time.

The remaining demand inputs to LMINET are a_{ik}, arrivals to airport i at epoch k from outside the network, and b_{ik}, extra-network arrivals to sector i at epoch k. For this report, we input extra-network arrivals to an arrival TRACON at each airport and to the airport's arrival queue.

Demand in 1996

We considered both scheduled air transport service and itinerant GA traffic. We based demand for scheduled air transport service on the schedule published by the OAG. We constructed the time variation in GA demands from data recorded in the ETMS. Since the OAG schedule is the planned rather than the observed air traffic schedule, and only the GA filing IFR will be recorded in ETMS, both the OAG and GA schedules are scaled to conform with the corresponding data given in the FAA's TAF.

April 8, June 12, and November 22, 1996, are the days for which we run our model. We chose these in view of the variation in weather throughout a year. The demand schedule we used for each specific day is based on the OAG for that day.

Demand in 2007

The future air traffic demand, expressed in terms of the schedule, s_{ijk}, must be constructed. Our construction method is based on the current schedule, the TAF, and a traffic distribution model. Since the TAF forecasts airport-specific growth rates, one cannot generate future traffic demands by simply multiplying each airport's departure demands by its individual growth rate: to do that would not give the desired new arrival rates at the other airports.

In fact, generating demand schedules for the entire network corresponding to individual overall growth rates at its airports is a challenging task. The following subsections review our methods for determining the individual growth rates and developing future demands.

AIRPORT OPERATIONS GROWTH RATE

The TAF is our data source for the growth rate of airport operations. We used the total of air carrier, air taxi, and itinerant GA in the TAF as the airport operations measure. Air carrier and air taxi are the operations of scheduled air transport service corresponding to the OAG; air taxi is for aircraft with less than 60 seats, which is typical of commuter operations. For the most recent TAF, released in February 1998, the data from 1976 to 1996 are the annual totals reported by the airport control tower, while the data from 1997 through 2010 are the FAA's predicted values. From these predictions, we can derive the operations growth rate from the baseline year 1996 to the target year 2007. Since the forecasts stop at year 2010 in the TAF, we used the last year's growth rate from 2009 to 2010 reported under each category and by each airport and then compounded it to get the forecast beyond 2010

The forecasted operation figures for major airports in the TAF are derived by FAA in the following ways: (1) forecasting the enplanements based on the socioeconomic models; (2) forecasting the load factors to and from each airport based on the demand, fare yield, and airlines cost; (3) forecasting the average number of seats per aircraft for arrivals and departures at the airport; and (4) dividing the forecasted enplanement by the forecasted load factor and by the forecasted average number of seats per aircraft.

Table 3-1 shows the FAA's values for operations and enplanements at the LMINET airports for 1996, 2007, and 2017. Tables 3-2 and 3-3 compare LMINET to the network for operations and enplanements, respectively. Figures 3-1 and 3-2 graphically depict the LMINET airport annual operations and enplanements for 1996 through 2017.

Table 3-1. Annual Operations (thousands) and Enplanements (millions) at LMINET Airports

Airport	Operations			Enplanements		
	1996	2007	2017	1996	2007	2017
BOS	462	509	543	12.3	16.0	18.9
BDL	151	181	214	2.7	4.1	5.9
HPN	153	160	159	0.5	0.9	1.3
ISP	109	117	122	0.6	0.9	1.3
TEB	189	189	189	0.0	0.0	0.0
LGA	342	381	413	10.3	13.8	17.0
JFK	360	397	432	15.0	20.7	26.0
EWR	443	561	661	14.2	20.7	26.7
PHL	401	509	584	9.1	14.8	19.7
BWI	260	338	411	6.6	10.3	13.8
DCA	305	318	330	7.2	8.6	10.1
IAD	323	397	463	6.0	9.7	13.3
GSO	138	170	187	1.4	2.5	3.5
RDU	217	256	285	3.1	4.8	6.9
CLT	454	563	656	10.7	15.6	20.1
ATL	770	916	1050	30.7	41.4	51.3
MCO	337	502	665	11.8	22.6	32.8
PBI	182	196	207	2.8	3.9	4.9
FLL	234	304	365	5.2	9.4	13.2
MIA	540	694	850	16.1	27.4	38.3
TPA	269	331	396	6.2	9.2	12.0
MSY	162	190	215	4.2	5.9	7.5
MEM	358	467	581	4.6	6.2	7.7
BNA	222	260	285	3.4	5.4	7.3
SDF	168	215	243	1.8	2.9	3.9
CVG	392	613	818	8.8	16.9	24.6
DAY	143	160	176	1.0	1.0	1.1
CMH	185	238	268	3.1	5.3	7.3
IND	230	305	375	3.5	5.8	7.9
CLE	287	373	450	5.4	8.6	11.5
DTW	530	708	873	15.0	24.7	33.8
PIT	438	536	628	10.1	14.4	18.5
SYR	122	148	170	1.0	1.3	1.5
MKE	187	239	276	2.7	4.3	6.1
ORD	906	1039	1182	32.2	43.2	53.9
MDW	251	297	335	4.5	6.4	8.4
STL	511	637	752	13.5	20.5	27.0
IAH	391	566	728	11.9	20.0	27.5
HOU	252	287	319	4.0	5.3	6.6
AUS	203	245	299	2.8	4.6	6.2

Table 3-1. Annual Operations (thousands) and Enplanements (millions) at LMINET Airports (Continued)

Airport	Operations			Enplanements		
	1996	2007	2017	1996	2007	2017
SAT	238	293	359	3.3	5.5	7.6
DAL	219	264	305	3.5	5.2	7.0
DFW	869	1234	1571	27.4	43.7	59.0
MSP	478	615	742	13.4	20.8	27.8
MCI	195	244	285	5.0	7.1	9.0
DEN	453	553	644	15.2	20.6	25.5
ABQ	173	217	258	3.2	5.1	6.9
ELP	122	125	128	1.8	2.8	3.8
PHX	531	698	854	14.6	24.2	33.3
SLC	369	491	604	9.8	15.5	20.8
LAS	445	637	815	14.3	26.1	37.3
SAN	238	309	376	6.8	10.4	13.7
SNA	369	483	588	3.6	6.4	9.0
LGB	263	312	356	0.2	0.4	0.6
LAX	761	947	1120	28.2	41.9	55.0
BUR	180	222	262	2.5	4.3	6.1
ONT	149	177	203	3.2	4.6	6.0
RNO	144	189	216	3.0	5.4	7.6
SMF	145	201	241	3.5	5.7	7.8
OAK	400	494	581	4.8	7.8	10.7
SFO	426	562	687	18.3	29.4	38.3
SJC	210	258	302	4.8	8.0	11.0
PDX	290	384	471	6.1	10.2	14.1
SEA	397	503	601	11.7	17.5	22.8

Table 3-2. LMINET Airports Versus the Network (operations)

Location	Operations (millions)					
	Count	1996	2000	2010	Growth rate 1996–2000	Growth rate 2000–2010
Large hubs	29	13.6	14.9	18.3	2.37	2.04
Medium hubs	42	9.2	9.9	11.6	2.04	1.53
Small hubs	67	8.2	8.6	9.3	1.24	0.74
Nonhub towers	305	30.9	31.8	33.5	0.70	0.54
Total	443	61.9	65.3	72.7	1.35	1.08
LMINET airports	64	20.7	22.6	27.3	2.20	1.91

Table 3-3. LMINET Airports Versus the Network (enplanements)

Enplanements (millions)						
Location	Count	1996	2000	2010	Growth rate 1996–2000	Growth rate 2000–2010
Large hubs[a]	29	412.6	490.1	684.3	4.40	3.39
Medium hubs[b]	42	135.7	163.6	237.9	4.79	3.81
Small hubs[c]	67	41.6	48.8	67.5	4.08	3.30
Non hub towers	273	15.5	17.6	22.2	3.18	2.38
Total	411	605.5	720.2	1,012.0	4.43	3.46
LMINET airports	64	514.0	613.0	863.0	4.50	3.50
Share of LMINET airports		85.0	85.1	85.3		

Source: Department of Transportation, *Terminal Area Forecasts, Fiscal Years 1997-2010,* Report No. FAA-APO-97-7, Federal Aviation Administration, Office of Aviation Policy and Plans, Statistics and Forecast Branch, Washington, DC, October 1997.

[a] > 1% of total enplanement

[b] > 0.25% of total enplanement

[c] > 0.05% of total enplanement

Figure 3-1. Total LMINET Airport Annual Operations (millions)
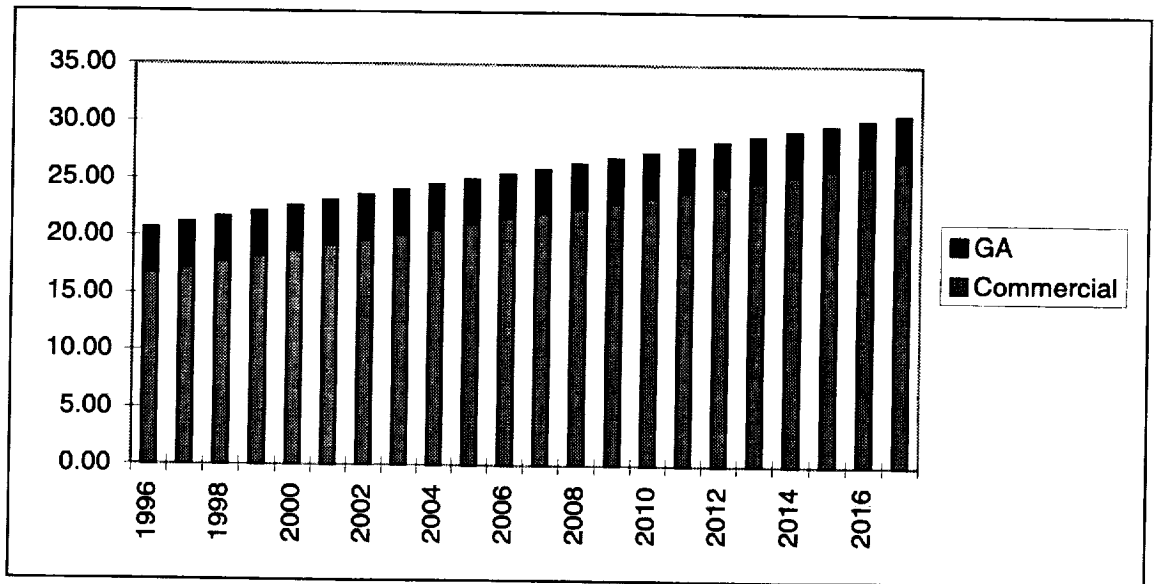
Figure 3-2. Total LMINET Airport Annual Enplanements (millions)
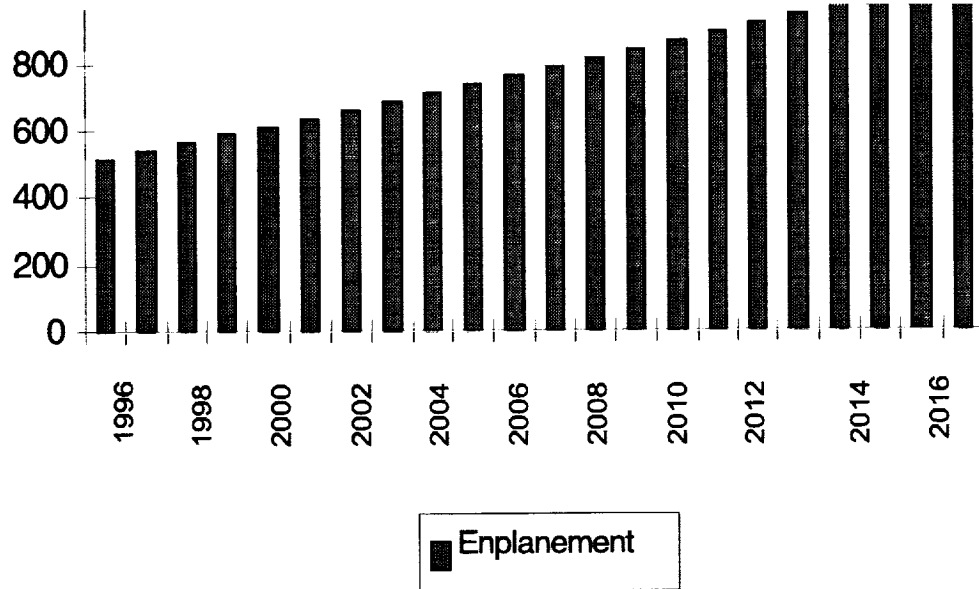
FRATAR ALGORITHM

This algorithm is the most widely used method of generating trip distributions based on the terminal area forecast. It has been used by both DOT and FAA in their transportation planning models, such as the National Air Space Performance Analysis Capability (NASPAC), an event simulation model of NAS. The traffic, t_{ij}, from airport i to airport j, total departures, d_i, from airport i, and total arrivals, a_j, to airport j are related to the schedule, s_{ijk}, as follows:

$$t_{ij} = \sum_k s_{ijk},$$

$$d_i = \sum_j t_{ij},$$

$$a_j = \sum_i t_{ij}.$$

If the schedule is balanced, or the network does not have any sinks, then $d_i = a_i$, $\forall$ $i \in$ I.

Let D_i, $i \in I$ be the total number of departures in the target year taken from the forecast. The Fratar method is an iterative algorithm that takes the following steps:

Step 0: Assign t_{ij}, d_i, a_j, $\forall i, j \in I$, based on the current year schedule.

3-6

Step 1:

$$g_i = \frac{D_i}{d_i}, \forall i \in I,$$

Step 2:

$$T_{ij} = t_{ij} \cdot g_i \cdot g_j \cdot \frac{1}{2}\left[\frac{d_i}{\sum_l t_{il} \cdot g_l} + \frac{a_j}{\sum_l t_{lj} \cdot g_l}\right], \forall i,j \in I,$$

Step 3:

If $\sum_l T_{il} = D_i, \forall i \in I$, then go to Step 4;

else

$$t_{ij} = T_{ij}, \forall i,j \in I,$$

update d_i, a_j, $\forall i,j \in I$ accordingly, go to Step 1.

Step 4: Compute the traffic growth factor r_{ij}, $\forall i,j \in I$, by dividing the traffic T_{ij} in the target year by the one in the current year; compute the schedule S_{ijk} in the target year by multiplying the schedule in the current year by the traffic growth factor r_{ij}. Stop.

The schedule in the target year made by the Fratar algorithm has some interesting properties. First, the schedule will always meet the terminal departure totals predicted in the TAF. Second, $r_{ij} = r_{ji}$, which means the traffic growth is undirectional. Third, the growth factor is uniform across the entire day, which is a desired property if we assume that the underlying time-of-day travel demand pattern in the future is unchanged and the schedules are designed to best serve the demand across the day. Unless there is any drastic change in air transportation technology that will substantially reduce travel time, it is reasonable to assume that the same time-of-day demand pattern will remain the same in the future. Another assumption hinges on the rational behavior and maturity of the air transport industry. The airline industry appears to have reached its maturity two decades after its deregulation. For the past few years, the industry has enjoyed record profits, stable network configuration, steady capacity growth, and rational route development in contrast to the record loss, brutal market share competition, explosive capacity growth, countless startups, and massive industry consolidation typical in the years just after deregulation.

The fact that the growth factor is uniform across the day implies another property of the schedule in the target year: the airport traffic is dynamically balanced, and the bank operations in hub airports are preserved. Let d_{ik}, a_{jk}, $\forall i \in I$, $\forall k \in K$, be the total departures and arrivals in time k.

$$d_{ik} = \sum_j s_{ijk},$$

$$a_{ik} = \sum_j s_{jik}.$$

An airport i is said to be dynamically balanced if $d_{ik} = a_{ik}$, $\forall k \in K$, which means there are no idle aircraft sitting on the ground. In reality, a flight has to spend some time in the terminal before taking off, but we will keep this simple definition, and real operations can be modeled by shifting the time index. Let D_{ik}, A_{ik}, $\forall i \in I$, $\forall k \in K$, be the total departures and arrivals at airport i at time k in the target year. By the Fratar algorithm,

$$D_{ik} = \sum_j S_{ijk} = \sum_j r_{ij} s_{ijk} = G_i \sum_j u_j s_{ijk},$$

$$A_{ik} = \sum_j S_{jik} = \sum_j r_{ji} s_{jik} = \sum_j r_{ij} s_{jik} = G_i \sum_j u_{ij} s_{ijk},$$

where

$$G_i u_j = r_{ij}, \forall i, j \in I,$$

$$\sum_j u_j = 1.$$

Now one can see that the right hand sides of D_{ik} and A_{ik} resemble the expectations of the product of two discrete random variables. If two random variables are independent, then the expectation of their product is equal the product of their expectations. If we assume that the traffic growth rate is independent of the current schedule (which is a reasonable assumption), then

$$D_{ik} \cong G_i \left(\sum_j u_j \right) \left(\sum_j s_{ijk} \right) = G_i d_{ik},$$

similarly,

$$A_{ik} \cong G_i a_{ik}.$$

Since $d_{ik} = a_{ik}$, $\forall i \in I$, $\forall k \in K$, then $D_{ik} \cong A_{ik}$. And, interestingly, G_i must be the growth factor implied by TAF in order to satisfy the binding terminal total departure constraint.

CAPACITY MODELS

This section explains how we adjusted our airport capacity models to make a baseline case for 2007. We treat the airside and surface-delay models separately.

Airport Airside Capacity Models

We derived the 64 airport capacity models in two steps. The initial development was done for NASA as Task 97-10, "AATT Benefits Prioritization," under contract NAS2-14361. This development used two sources. For the 10 airports treated in the TAP studies LMI performed for NASA,[1] we developed models from discussions with controllers at the individual airports. For the remaining airports, we developed models by reviewing airport diagrams in the several volumes of *U. S. Terminal Procedures*, published by the Department of Commerce. (These flight information publications are commonly called "approach plates.")

We validated the models in two ways. First, we operated LMINET with universal good weather inputs and observed that the outputs indicated minimal, but not zero, delays. We also observed that the total number of aircraft required in the airports' initial ready-to-depart reservoirs is roughly 80 percent of the total number of aircraft in the commercial fleet for 1994, as reported in the *FAA Statistical Handbook* for 1994. This is consistent with the fact that the LMINET airports account for roughly 80 percent of CONUS operations.

The second validation was by discussing the results with controllers at the FAA's Command Center. The controllers with whom we spoke agreed with the LMINET outputs in some cases and disagreed in others. When there was disagreement, we modified our airport capacity models in accordance with the controllers' suggestions.

For the present study, we extended the models developed under Task 97-10 to include input-stream effects, as described previously. Our baseline capacity models infer the mean time impact of input-stream effects (i.e., the value of $1/\lambda$) from an equivalent distance. Specifically, we generate the value of $1/\lambda$ as the equivalent distance divided by the average of the approach speeds of the aircraft types using the runway. For the 1996 reference, we take the equivalent distance to be 0.25 nautical mile, which gives $1/\lambda = 6.4$ seconds for a representative case of aircraft types and mix. We obtained a value of 0.25 nautical mile by adjusting our capacity model with input-stream effects to agree generally with results given by Ballin and Erzberger and by Credeur et al. [7,8]

For the baseline capacity models in 2007, we changed the 1996 models to include certain planned FAA upgrades at specific airports. We reviewed the FAA's *1996 Aviation Capacity Enhancement (ACE) Plan* and airport database and *National Airspace System Architecture*, Version 2.0, to determine these. [9,10]

---

[1] These 10 airports are ATL, BOS, DFW, DTW, EWR, JFK, LAX, LGA, ORD, and SFO.

For the 2007 baseline, we included only those few airport construction projects described in the ACE database that would be finished after 1996 but before 2006, would clearly increase capacity, and had *approved* environmental impact statements. These are

- DEN—Runway 16R/34L;

- DTW—Fourth north-south parallel runway, Runway 4/22;

- LAS—Upgrade of Runway 1L/19R to accommodate air carrier traffic;

- MEM—New north-south parallel Runway 18L/36R;

- PHL—Commuter runway, Runway 8/26;

- SDF—Replace Runway 1/19 with two new parallel runways separated by 4,950 feet, Runways 17R/35L and 17L/35R; and

- LAX—Remove 84/hour arrival-rate maximum imposed by groundside capacity limits.

Because we wish to capture benefits of all NASA ATM technologies, our 2007 baseline will *not* include any implementations of the Passive Final Approach Spacing Tool (P-FAST), even though our review of the *National Airspace System Architecture*, Version 2.0, suggests that the FAA plans to implement the Center-TRACON Automation System (CTAS) Builds 1 and 2, which include P-FAST, at eight airports by 2006. The FAA architecture review does not specifically identify the airports.

Airport Surface-Delay Model

One could assume that airport operators and airlines will make no substantial improvements addressing surface-movement bottlenecks before 2007 and leave the capacities of our surface-delay model unchanged. This would be a pessimistic assumption.

We discussed the relative importance of surface-movement delays with FAA personnel at several airports. All said that surface-movement delays were significant at their airports, and all said that, without corrective actions, they would expect surface-movement delays to increase as a fraction of total delay as operations increase.

The discussions also suggested a less pessimistic assumption, however, about the ways that airports are likely to address surface-movement bottlenecks between now and 2007. As we pointed out, long queues ("conga lines") for service at a departure runway interfere with both taxi-in and taxi-out operations. We model this

effect with a reduction in service rate at the taxi-delay queues as departure queues increase.

All the airport representatives with whom we discussed surface-movement delays said that this effect was presently a significant cause of delays at their airports. All but one of the representatives also said that "pads" to accommodate taxi-out queues were either under construction or definitely going to be built. In view of these inputs, we decided to model surface-movement delays in 2007 by keeping the basic service rates μ_{ta} and μ_{td} fixed at the values calibrated for them with delay data for 1995, while removing the factor $1 - \min(\frac{q_d}{r_t}, 0.25)$ with which we modeled taxi delays due to lengthy departure queues.

Chapter 4
Modeling IndividualATM Technologies

This chapter describes how the parameters of LMINET and its components may be adjusted to reflect the effects of individual ATM technologies.

MODELING TAP TECHNOLOGIES

This section describes options for modeling several implementations of the TAP technologies.

Dynamic Runway Occupancy Measurement

Dynamic runway occupancy measurement (DROM) provides real-time data on runway occupancy times. We expect that DROM will confirm runway occupancy times (ROTs) under 50 seconds and allow the use of 2.5-nautical-mile minimum separations for IMC-1 wet runways. The effect will be to change the minimum miles-in-trail requirements, as shown in Table 5-1 under FAA 2.5.

Roll Out and Turn Off

Roll out and turn off (ROTO) technology enables shorter ROTs in poor visibility. We model the effects of significantly reduced visibility on ROTs by increasing ROTs by 20 percent in ILS Category II and Category III conditions. We model ROTO by removing the 20 percent ROT penalty and allowing 2.5-nautical-mile minimum separations in IMC-2 conditions.

Aircraft Vortex Spacing System

We model two versions, or builds, of the Aircraft Vortex Spacing System (AVOSS). AVOSS Build 1 allows prediction of wake vortex transport and demise by aircraft class. AVOSS Build 2 allows predictions of safe separation for specific aircraft pairs. We model AVOSS with reduced separation matrices. For Build 1 we reduce the separations by 0.5 nautical mile. Either 2.5- or 3.0-nautical-mile minimums are used, depending on the meteorological condition and the presence of DROM and ROTO. For Build 2 we further reduce the separations to levels approaching those seen in VMC-1 conditions. Again, the minimums allowed depend on the meteorological condition and the presence of DROM and ROTO.

ATM

The TAP technology called ATM has two versions. We describe our models of the two in the following sections.

ATM-1: A-FAST/3-D FMS DATA LINK

ATM-1 combines the Active Final Approach Spacing Tool (A-FAST) with a data link to the aircraft flight management system (FMS). We model ATM-1 by reducing the wind uncertainty. The standard deviation of the wind uncertainty is reduced from 7.5 knots to 5 knots. This reduction assumes that FMS reports from all aircraft during approach will allow A-FAST to better predict winds along the flight path.

ATM 2: A-FAST/FMS INTEGRATION WITH 4-D DATA LINK

ATM-2 includes integration of A-FAST with the aircraft's 4-D FMS. This integration allows required time of arrival (RTA) operations. We model ATM-2 by further reducing wind and velocity uncertainties. We also reduce the inefficiency buffer, $1/\lambda$, to zero. The standard deviations of the wind and velocity are reduced to 2.0 and 1.2 knots, respectively.

T-NASA

We understand that T-NASA will enable taxi operations to proceed as efficiently during periods of poor visibility as in periods of good visibility. We also understand that T-NASA is expected to eliminate the night-time reduction in taxi speeds discussed in Chapter 2. Accordingly, we modeled this technology by eliminating the 25 percent reductions of taxi-in and taxi-out capacity imposed when visibility is 1 mile or less and by eliminating the delays caused by reduced night-time taxi speeds.

MODELING NASA AATT TECHNOLOGIES

This section describes options for modeling NASA AATT DSTs. The discussion is inclusive; however, describing how specific DSTs can be evaluated—and even when to do so—requires more resources and time than the present study affords.

The following subsections discuss general considerations for modeling DSTs and give some specifics for modeling a set of DSTs.

General Considerations for Modeling DSTs

LMINET may be adjusted at several levels, using any parameter of its constituent models, to reflect DST performance. At the highest level, airport capacities may

be adjusted simply by multiplicative factors applied to arrival and/or departure capacities. At the most detailed level, DST effects may be reflected in changes to the runway capacity model parameters of Table 2-2.

The effects of DSTs on airspace outside airports may enter LMINET by adjustments to the parameters of the queues that model TRACON and en route sectors. A DST that reduces a controller's workload might, for example, be reflected in an increase to the maximum number, N, of aircraft that could be accommodated at one time. A DST, like Expedited Departure Path (EDP), that reduces the amount of time aircraft spend in a sector as well as the controller's workload, could be modeled by an increase in N and a decrease in the mean of the Erlang distribution of service times.

To develop values for the variations in LMINET parameters that model DSTs' effects on sectors, we used the Functional Analysis Model (FAM), a discrete event model—developed for NASA by LMI—designed to analyze alternate concepts of air traffic management and control.

TMA, P-FAST, and A-FAST

We will treat these three related DSTs together.

TRAFFIC MANAGEMENT ADVISOR

The Traffic Management Advisor (TMA) gives the ARTCC Traffic Management Coordinator (TMC) predictions on throughput demand, recommendations for efficient sequencing, and optimally spaced times for crossing feeder gates. This information should make it possible for the ARTCCs to deliver more manageable traffic streams to TRACON controllers. We model its effects by reducing the equivalent distance of the mean input-stream delay by 20 percent, from 0.25 to 0.20 nautical mile. This gives a decrease in $1/\lambda$ from roughly 6.4 to approximately 5.2 seconds. We change no other ARTCC or TRACON parameters. In particular, we do not assign benefits from TMA's potential to improve arrival sequences because arrival sequences to runways are more affected by actions of the TRACON controllers than by actions of the ARTCC, where TMA's information is delivered. As described in the following subsection, we assign sequencing benefits as an important benefit of P-FAST.

PASSIVE FINAL APPROACH SPACING TOOL

P-FAST provides controllers with advisories for landing sequence, and for the selection of landing runway. As described by Davis et al., the test installation of P-FAST at DFW raised the average peak arrival rate by roughly 10 percent for both IFR and visual flight rule (VFR) operations. [11] In the baseline for that comparison, however, about 3 to 5 arrivals per hour were diverted to runways other than those in the normal set of arrival runways. Correcting for this difference in the

capacity of the runways used leads to the conclusion that P-FAST caused an increase of about 13 percent in the capacity of the set of normally used arrival runways. Davis et al. also indicates that a significant part of P-FAST's benefits were due to better balancing of the loads on separate runways.

Effects of Runway Imbalance

This "thought experiment" shows that runway balancing is likely to be important at any airport with multiple runways. Suppose two independent runways are accommodating arrivals, each with a capacity of 35 arrivals per hour. Also suppose that arrival demand is 50 per hour. For simplicity, let us consider steady-state operations.

If the arrival stream is evenly balanced between the two runways, each will receive 25 aircraft per hour and will thus operate at a utilization ratio of 5/7. In steady state, that would cause a mean queue of 2.5 aircraft, which implies a mean delay of approximately 4.3 minutes for each arrival. Thus, with balanced runway use, the airport handles the arrival demand with delays that are significant, but probably tolerable.

Now suppose there is a moderate imbalance, with the arrivals reaching the two runways in a 20-30 split. There is little delay—about 2 minutes—on the less-loaded runway, but arrivals to the more heavily loaded runway will see a mean delay of more than 10 minutes. Delays of that magnitude threaten airlines' schedule integrity.

Even a slightly more serious imbalance, say an 18-32 split, would create an intolerable 18-minute delay on the more heavily loaded runway. It is likely that flights would divert from that runway to bring delays down to at least the 10-minute level. That would imply about two diversions per hour, or a reduction in the runways' effective capacity of 4 percent.

Effects of Optimal Sequencing

To gain an indication of the potential effects of efficient sequencing, we considered operations for two mixes of aircraft types, which we called "domestic" and "international." They characterize airports with mostly domestic traffic and those with significant international traffic, respectively. The domestic mix is 10 percent small, 80 percent large, and 5 percent each for B757 and heavy; the international mix is 10 percent small, 60 percent large, 10 percent B757, and 20 percent heavy.

For the domestic mix, allowing aircraft to arrive at random gave a runway arrival rate of 32.9 per hour. Restricting the runway to just one type of aircraft gave a spread of arrival rates, ranging from 24.65 (all small) to 36.38 (all large). Weighting each of these "one-type" arrival rates by the fraction of that type in the mix gave a weighted average arrival rate of 34.57. We take this weighted average as a

crude indicator of the improvement in arrival rate that could be achieved by efficient sequencing. By this measure, efficient sequencing could increase arrival rates at domestic airports by 5 percent. Repeating the process for international airports gave an arrival-rate improvement of 7 percent.

Specific P-FAST effects

The analyses of the effects of optimal sequencing and runway balancing suggest that sequencing and balancing together might result in around a 10 percent improvement in arrival capacity. This appears consistent with the benefits observed at DFW. Also, the analyses suggest that benefits of about that size might be expected at any airport with multiple runways at which balancing was imperfect with present ATM methods.

At present, our airport capacity models do not include any adjustment for less-than-perfect runway balancing. In effect, they assume perfect balancing. In view of this, we model only two of P-FAST's benefits. We model P-FAST's improvement on the traffic flows reaching the controller, by a 50 percent reduction in the distance equivalent to the mean input-stream delay, from 0.2 nautical mile (the TMA value) to 0.1 nautical mile.

We model P-FAST's improvement in sequencing in the following way: we change the Pareto parameters from those of the assigned mix to the weighted average of the runway capacities when the runway is operated with aircraft of one type only. This leads to increases of about 4 percent in departure capacity, in addition to the arrival capacity increases. Since P-FAST is an aid to arriving traffic, that might appear to give P-FAST an unmerited effect on departures. However, DFW tests reported significant increases in departure capacity during P-FAST operations, so we are content to have our model assign some departure capacity improvements to P-FAST. [11] In work to model effects of tools, like ASMA, that should directly affect departure capacity, this point should be revisited so that appropriate benefits can be associated with each tool.

ACTIVE FINAL APPROACH SPACING TOOL

Now let us consider A-FAST. A-FAST will "augment the capabilities of Passive FAST with an interface that provides speed and heading advisories to the TRACON final approach controller. It will also have improved conflict detection and resolution capabilities." [12] It also should result in "tighter means and smaller standard deviations of in-trail separations on final approach ... and shorter common approach path lengths." [12]

In the context of our models, we see A-FAST, in comparison with P-FAST, as further reducing input-stream errors, giving controllers much more accurate position information for arrivals, and reducing variations in approach speeds.

Specifically, we model A-FAST's improvement over P-FAST by the reduction of the

- ◆ equivalent distance of the input error by 50 percent, from 0.1 to 0.05 nautical mile;

- ◆ position uncertainty from 0.25 nautical mile to 100 feet; and

- ◆ standard deviations of approach speeds from 5 to 2 knots.

The approach speed and position uncertainties are reduced because speed and position data transmitted from the aircraft by the Automated Dependent Surveillance–Broadcast (ADS-B) system will allow A-FAST to make more accurate predictions. The standard deviation of the position uncertainty is reduced from 0.25 nautical mile to 100 feet (≈ 0.2 nautical mile). The wind uncertainty is not reduced because no integration with the aircraft flight management system is assumed in the A-FAST baseline.

The steps in capacity from the current reference through TMA and P-FAST to A-FAST are shown in Figure 4-1, which compares the Pareto frontiers describing runway capacities in ILS Category I conditions, for the four cases.

Figure 4-1. Capacity Comparisons
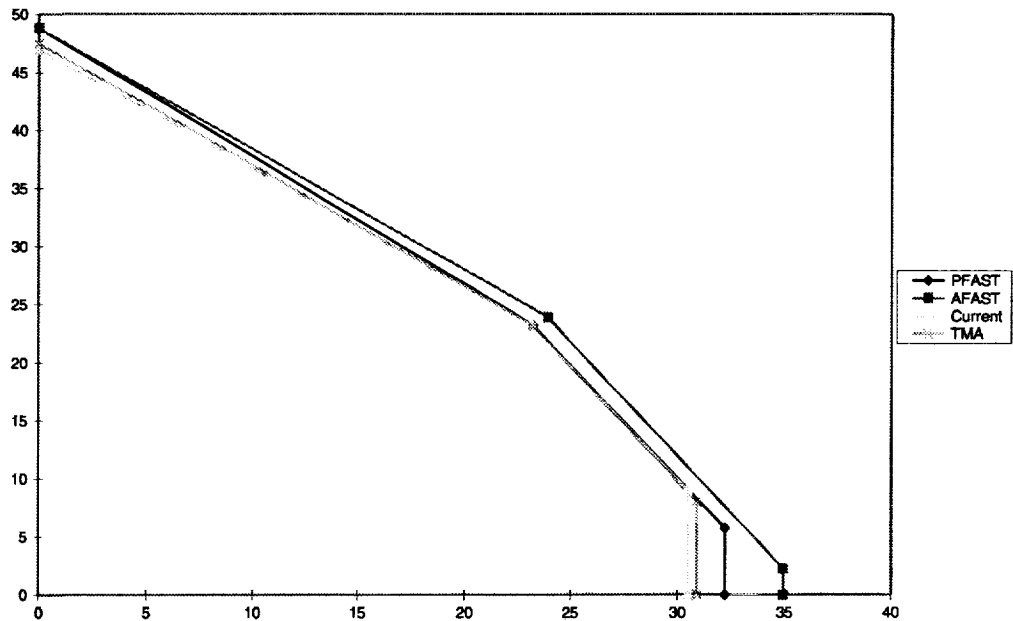
En Route and Descent Advisor

We understand that this DST embraces technologies previously covered by the Conflict Prediction and Trial Planning (CPTP), Airspace Tool and Sector Tool (AT/ST), and Advanced En Route Ground Automation (AERGA). Our specific

information about the En Route and Descent Advisor (EDA) comes from discussions of CPTP, AT/ST, and AERGA in the AATT Program's ATM concept definition. [13] Accordingly, we will discuss modeling EDA in terms of these previously named elements.

CONFLICT PREDICTION AND TRIAL PLANNING TOOL

The CPTP tool will help en route sector controllers identify and resolve potential conflicts. Intended as a precursor of the AT/ST DSTs described in the next subsection, CPTP will serve as a research tool for developing those DSTs while assisting controllers.

CPTP will receive radar track and flight plan information from the host system and winds aloft from the National Weather Service's Rapid Update Cycle predictions. These data, with extensions of CTAS trajectory synthesis algorithms, will provide predictions of potential conflicts considerably in advance of those developed now by individual controllers.

CPTP will send warnings of identified potential conflicts to the displays of the controllers whose sectors are affected. Controllers may then use the "trial planning" feature of CPTP to test resolution strategies before issuing clearances to the aircraft involved. For controllers directing aircraft in transition between en route and terminal airspace, CPTP's trial planning functions have the ability to respect any imposed miles-in-trail restrictions.

Models of CPTP must capture the tool's effects on individual sector operations and on the NAS as a whole. The latter task can be done by a queuing network model such as LMINET. Such models characterize sector performance by only a few parameters: LMINET uses just three, namely, the maximum number of aircraft that a controller team can handle at one time in a given sector; the index, k, of the E_k distribution of times-in-sector, which characterizes the degree to which times-in-sector are concentrated about their mean; and the mean time-in-sector.

Detailed analyses of sector operations are required to generate numerical values that characterize the changes CPTP may be expected to make in the sector model's parameters. In the present work, we used FAM, which is capable of modeling sector operations in considerable detail.

We set up FAM to model one sector in the Denver ARTCC (ZDV), together with the Denver TRACON and the Denver and Colorado Springs airports. For each of the parts modeled, FAM monitors the utilization of the controllers and operators. We took the basic demand event file that FAM uses for this task directly from actual ETMS data for flights that flew through the sector that we considered. To increase demand in the sector, we modified the original event file. The model simulates a 4-hour period of operations.

We derived the initial conflict resolution time of 50 seconds used in the model from an average of the 40 and 60 seconds that Grossberg, Richards, and Robertson report it takes to resolve "crossing conflicts and overtaking conflicts, respectively." [14] This is a fixed conflict resolution time for the purposes of this model. In our simulation, conflicts are generated by a random event generator that produces events based on the number of aircraft in the sector.

We ran simulations for a set of event files covering a range of values of the maximum number of aircraft in the sector. This established the variation of controller utilizations with the maximum number of aircraft. We repeated the simulations, using varying conflict resolution times of 5 seconds, 25 seconds, and 50 seconds per conflict. We adjusted the conflict generator so that the number of conflicts generated in a 4-hour period agreed with reported observations. [14] Figure 4-2 shows the results from runs of the simulations. We smoothed the curves by fitting a quadratic function to them:

$$\text{max} = c_0 + c_1\,(util) + c_2\,(util)^2$$

A decrease in conflict resolution time from 50 seconds to 25 seconds is plausible for CPTP. When we reduced the time to resolve conflicts using a maximum number of aircraft of 17, the maximum number of aircraft able to be handled increased to 18. As the controller utilization increased, the difference between the 50- and 25-second conflict resolution times caused a larger increase in maximum number of aircraft able to be controlled.

To conform with FAA standards, we use 18 as the standard maximum number of aircraft in an ARTCC or TRACON sector. [15] While the results of Figure 4-2 might be used to justify a larger increase, to be conservative we chose to reflect CPTP's effect as increasing the maximum number by 1, to 19.

AIRSPACE TOOL AND SECTOR TOOL

The AT will help controllers manage traffic that passes through sectors without making transitions to or from terminal airspace. It is intended to support a new controller position, the "airspace coordinator." The airspace coordinator will have cognizance over the airspace of more than one sector, perhaps over all the sectors in a center. Using accurate forecasts of aircraft's future positions, current flight plan information, and, possibly, trial planning features of the AT, the airspace coordinator will develop proposals for clearances that make efficient resolutions of conflicts and conform closely to users' wishes. The airspace coordinator will then interact with sector controllers to implement and deliver these clearances.

The AT may be modeled with an extension of the CPTP model. The AT's principal benefits for airspace users will be in more efficient conflict resolutions and in clearances closer to the users' desired routes than the CPTP results.

*Figure 4-2. Variation of Controller Utilization with Maximum
Number of Aircraft in Sector*
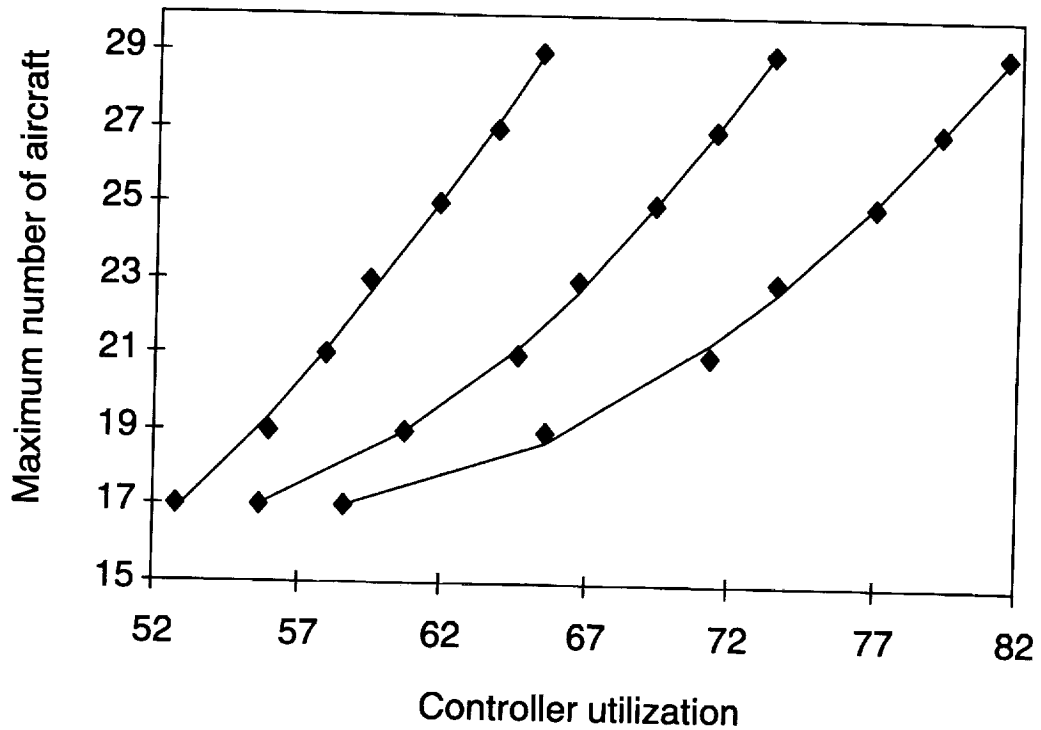
The AT's benefits to the sector controllers should exceed those of the CPTP because the airspace coordinator will develop even more efficient conflict resolutions than the CPTP and will deliver them even more efficiently to controllers. Simulation modeling, like that of the FAM modeling reported here, may be used to develop quantitative measures of the AT's benefits to sector controllers.

The ST will assist controllers managing transition airspace by developing proposals for efficient clearances. This tool will directly attack the inefficient descent profiles that are all too common at busy terminals. Eliminating them may have substantial payoffs in fuel, time, and schedule integrity.

ST's benefits to airspace users may be modeled by comparing the fuel burns and times of actual descent profiles with those of optimal descent profiles, using a tool such as the Base of Aircraft Data (BADA) model or Flight Segment Cost Model (FSCM). ST's benefits to air traffic managers may be modeled by simulations, for example, with FAM.

ADVANCED EN ROUTE GROUND AUTOMATION

This tool is intended to extend the efficiency and flexibility of ATM in en route and transitional airspace beyond the levels provided by AT/ST. It will provide such advanced features as automatic conflict resolution, coordination among

adjacent ARTCCs, and automated negotiation among ATM functions, airline aircraft operational control centers (AOCs), and aircrew.

Modeling AERGA will require extending the FAM models of ARTCC and TRACON sectors to include AOCs. FAM presently models aircrew workloads and functions, although we did not require this feature for the tools analyzed in this report.

Expedite Departure Path

EDP's performance has been characterized as "decrease time-to-cruise-altitude by 15 percent." Our work on NASA Task 97-10 suggests that bringing times-to-climb for departures from busy airports to values characteristic of less-busy airports could reduce this time (specifically, the time-to-climb averaged over a day) by 3 minutes from a base of 22 minutes at certain busy terminals, a decrease of 14 percent. [3] In view of this, the 15 percent goal seems reasonable, if it is interpreted as applying only to busy airports.

EDP is to achieve its results by giving controllers suggested clearances that balance flows to departure fixes and allow efficient climb-out paths whenever they are possible with the existing mix of arrivals and departures. Presenting controllers with suggested clearances changes their cognitive processes from doing all the work of analyzing the traffic picture and determining appropriate clearances, to reviewing the suggested clearances. This change could reduce the thinking time required for each flight. If this happens, EDP could also increase the maximum number of aircraft that a controller can handle at one time. If so—and if the controller's utilization is the binding constraint on the maximum number of aircraft in a particular departure TRACON—then EDP would increase the maximum number of aircraft in the departure TRACON.

Standard instrument departures (SIDs) from busy airports often do not have a fixed route but, rather, instruct crews to expect vectors to one of several fixes or navigation aids. (There is just one SID for ORD, for instance, and it is of this kind.) Consequently, it seems likely that for many busy airports the controllers' utilization, rather than airspace limitations, will in fact govern the maximum number of aircraft that can be accommodated in the departure TRACON at one time.

An interview with a controller who had experience in the NYC TRACON raised a note of caution, however, about the chances for EDP to increase the number of aircraft handled at one time. The controller told us that controller teams generally develop standard operating procedures that they carry out largely mechanically, particularly during busy periods. The controller believed that this often resulted in conservative clearances. EDP operations might require controllers to do more complex tasks to issue less-conservative clearances for departures. In this case it is not clear that the maximum number of aircraft handled could increase, even with the help provided by EDP.

A solid assessment of EDP's effects on the maximum number of aircraft simultaneously in a departure TRACON must wait until the tool is more fully defined. Therefore, we model EDP by reducing the mean time in certain departure TRACONs by 3 minutes, leaving the maximum number in the sector unchanged.

National Surface Movement Tool

This class of decision support tools will expedite aircraft movements on airport groundsides. It is the current global name for DSTs formerly known as SMA-1 (Passive Surface Movement Advisor), SMA-2 (Enhanced Surface Movement Advisor), and SMA-3 (Active Surface Movement Advisor). Because our information on surface movement tools is keyed to these older names, we will discuss our National Surface Movement Tool (NSMT) model with reference to them.

PASSIVE SURFACE MOVEMENT ADVISOR

SMA-1 also known as Passive Surface Movement Advisor, extracts data relevant to surface movements from several sources and distributes them to operational users. A proof-of-concept prototype has been implemented at ATL. Early results indicate that the tool reduces average taxi times by about 1 minute. [16]

ENHANCED SURFACE MOVEMENT ADVISOR

SMA-2 (Enhanced Surface Movement Advisor) will provide information from many sources—such as Automated Radar Terminal System (ARTS) data, airline schedule and gate data, flight plans, Aeronautical Radio Incorporated (ARINC) Communications Address and Reporting System (ACARS) data on flight status, runway status data—to optimize the use of surface movement resources, probably by means of collaborative decision-making among surface traffic managers and airlines. Specific benefits are to include runway load balancing and managed competition for a taxiway resource.

Modeling SMA-2's benefits from runway load balancing would begin with determining how runways are assigned now. Presumably, each runway's load and mix are presently dictated by airlines' specific gates, OAG departure schedules, and a choice of taxiways made by ground controllers. With SMA-2, the runways' loads and mixes would be determined by well-informed, collaborative decisions, minimizing total time from gate to wheels-up in general and giving due consideration to promoting certain flights when it is to a carrier's overall advantage.

Simulation modeling probably will be necessary to determine the changes in runway loading and mixes that SMA-2 would be likely to realize. With this information, LMI's runway model would capture the effects of better mixes on capacity. LMI's airport models would then determine the effects on capacity, and LMINET would capture the consequent effects on delays throughout the NAS.

Another interesting option would be to integrate a simulation model of a specific airport or set of airports directly into LMINET.

This modeling is quite likely to be airport specific. It should be validated by reviews with FAA controllers at each airport treated and by reviews with airline ground operations managers.

Modeling management of a scarce taxiway resource would also begin by determining how traffic reaches the resource in present operations. Presumably, each concourse's pushback schedule is now dictated by individual airline's gates and schedules, together with decisions by the ground controller. With SMA-2, pushback schedules could be determined collaboratively to minimize the effects of congestion at the scarce resource.

SMA-3 (ACTIVE SURFACE MOVEMENT ADVISOR)

Our only information about SMA-3 is from two sentences in sections on "Expected Course of Development" in write-ups on SMA-1 and SMA-2. [13] These sentences suggest that SMA-3 will augment capabilities developed in SMA-1 and SMA-2 by tracking the ground movements of individual aircraft with interfaces with the Airport Movement Area Safety System (AMASS) and Airport Surface Detection Equipment (ASDE-3).

MODELING EFFECTS OF SURFACE-MOVEMENT ADVISORS

In light of the three preceding sections, we modeled the effects of NSMT by adjusting the basic taxi-in service rates, μ_{ta}, as follows:

◆ At all airports where 1995 mean taxi-in delays exceeded 2 minutes, we increased μ_{ta} to reduce the mean delay to 1 minute.

◆ At airports where mean taxi delays were between 1 and 2 minutes, we increased μ_{ta} to reduce the mean delay to 1 minute.

◆ At airports where mean taxi-in delays were less than 1 minute, we left μ_{ta} unchanged.

We chose this procedure in view of the sample probability distribution function of mean delays at the LMINET airports, shown in Figure 4-3.

The delay-time distribution shows a group of airports with mean delays clustered around a value slightly less than 1 minute and another group of airports where larger mean delays generate a "fat tail" stretching out to more than 2 minutes. Some exceptional airports have significantly larger mean taxi-in delays. For example, DFW's mean delay is over 4 minutes (4.6 minutes).

It seems that a reasonable goal of the fully functioning NSMT program would be to move airports out of the "tail" of the distribution of Figure 4-3. A test of surface movement advisors at ATL indicates a reduction of mean taxi-in delays from about 2 minutes to about 1 minute. [16] To move all airports—even those which, like DFW, show mean taxi-in delays substantially greater than 2 minutes—out of the "tail" may be optimistic. These considerations led to our choice of the 1-minute reduction for airports with mean delays larger than 2 minutes.

Surface-movement tools may not be able to affect the delays that produce the cluster at around 1 minute in Figure 4-3. For this reason, we did not adjust μ_{ta} at those airports.

Figure 4-3. Smoothed Sample PDF of Mean Taxi-in Delay Times
at the 64 LMINET Airports
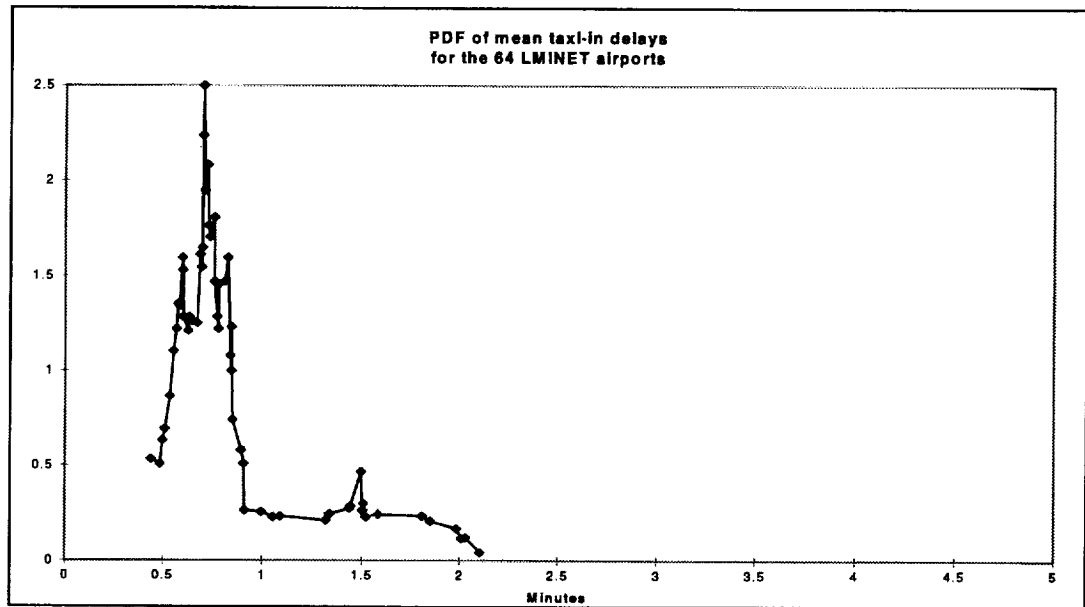
Since part of the taxi-in delays are waits for arrival gates, reducing mean taxi-in delays amounts to assuming that the fully functioning NSMT reduces such waits. This is possible, given the intention of NSMT to facilitate coordination among ground controllers and airlines.

E-CDTI and APATH

These tools are intended to enable flight crews to perform some conflict-avoidance and route planning tasks. This may reduce controllers' workloads, but, according to one source "this is not a foregone conclusion and much research is needed to support this assumption." [12]

The purpose of the Enhanced Cockpit Display of Traffic Information (E-CDTI) is to give flight crews minimum capabilities needed for airborne conflict avoidance

4-13

in en route sectors. The Airborne Planner to Avoid Traffic and Hazards (APATH) is designed to add substantially to the E-CDTI data and provide flight crews with weather, traffic, and aircraft performance information that will allow strategic flight planning and replanning. It is quite possible that APATH would result in reduced controller workloads when crews self-select away from heavy-traffic sectors. Crews provided with winds-aloft and turbulence indicators might well make fewer requests for ride information from controllers.

Moreover, APATH may provide functionality for implementing the A-FAST/FMS data links of ATM-1 and ATM-2. We note this aspect of APATH in Chapter 5, Table 5-3. We do not model other APATH effects in this report.

Chapter 5
ATM Impacts on Network Parameters

This chapter summarizes the models of TAP and AATT tools. It includes a section reviewing the Institute's levels of confidence in the models of the several tools.

TOOLS MODELED AND NOT MODELED

We considered developing models of the 17 tools whose research and development schedules are given in Appendix B of Volume 2 of *ATM Concept Definition*, Version 1.0, prepared by NASA's AATT Program Office. Those tools are

◆ Traffic Management Advisor (TMA),

◆ Complex Airspace Adaptation Planner (CA-AP),

◆ Passive Final Approach Spacing Tool (P-FAST),

◆ Passive Surface Movement Advisor (SMA-1),

◆ Conflict Prediction and Trial Planner (CPTP),

◆ Enhanced Surface Movement Advisor (SMA-2),

◆ Airspace Tool (AT),

◆ Sector Tool (ST),

◆ Expedite Departure Path (EDP),

◆ Collaborative Departure Scheduling (CDS),

◆ Advanced En Route Ground Automation (AERGA),

◆ Active FAST (A-FAST),

◆ Collaborative Arrival Planning (CAP),

◆ Active Surface Movement Advisor (SMA-3),

◆ Low/Zero Visibility Tower Tools (LZVTT),

◆ Enhanced Cockpit Display of Traffic Information (E-CDTI), and

◆ Airborne Planner to Avoid Traffic and Hazards (APATH).

On March 24, 1998, a NASA official gave the following new list of DST names:

◆ Surface movement

    ➤ National Surface Movement Tool (NSMT), which combines P-SMT (SMA-1), E-SMT (SMA-2), and A-SMT (SMA-3)

    ➤ Collaborative Departure Scheduling (CDS)

    ➤ Low/Zero Visibility Tower Tools (L/ZVTT)

◆ Terminal area

    ➤ Traffic Management Advisor (TMA)

    ➤ Passive Final Approach Spacing Tool (P-FAST)

    ➤ Active Final Approach Spacing Tool (A-FAST)

    ➤ Collaborative Arrival Planning (CAP)

    ➤ Multi-Center TMA

    ➤ Expedite Departure Path (EDP)

    ➤ Complex Airspace Adaptation Planner (CA-AP)

◆ En route

    ➤ En Route and Descent Advisor (EDA), a subset of AERGA

◆ Airborne

    ➤ Airborne Planner to Avoid Traffic Hazards (APATH).

We found sufficient information to at least consider modeling 14 of the 17 "old name" tools. Those for which we presently have no information are CA-AP, CDS, and L/ZVTT. With our present understanding of the names given to us on March 24, 1998, our information allows us to model six of the newly named tools, i.e., NSMT, TMA, P-FAST, A-FAST, EDP, and EDA. We consider APATH a potential provider of A-FAST/FMS data links for ATM-1 and ATM-2.

LEVELS OF CONFIDENCE IN THE PARAMETRIC MODELS

Our models of the several TAP and AATT tools, and combinations of tools, are made with values of LMINET parameters. Our confidence in these values varies from case to case. Overall, we see three levels of confidence:

◆ At best, our parameter values rest on data concerning actual performance of prototypes of the tools or technologies.

◆ With less confidence, we have inferred some values from descriptions of tools or technologies given in NASA publications (Reference [12], for example) and/or discussions with people closely involved with the tools' or technologies' development.

◆ With least confidence, lacking quantitative information about a tool's effects, we have simply guessed.

Here is a breakout of our models, by confidence level. Again, since our detailed information is keyed to the older DST names, the lists are organized by those names. [13] We have, however, also shown in parentheses the newer DST names to which the listed names pertain.

Confidence level 1—Values inferred at least in part from data

◆ 1996 Reference

◆ TMA

◆ P-FAST.

Confidence level 2—Values inferred from quantitative information in descriptive publications and/or discussions with those knowledgeable about the tools' or technologies' development

◆ 2007 Reference

◆ DROM

◆ ROTO

◆ A-FAST

◆ AVOSS

◆ Ultimate TAP

◆ CPTP (EDA)

◆ EDP

◆ APATH.

Confidence level 3—Values inferred from qualitative discussions

◆ AT (EDA)

◆ ST (EDA)

◆ AERGA (EDA)

◆ P-SMA (NSMT)

◆ E-SMA (NSMT)

◆ A-SMA (NSMT)

◆ T-NASA.

TABLE OF MODELING PARAMETERS

All of our modeling parameters are shown in Table 5-2 at the end of this chapter. The following subsections contain definitions of the column headings and entries of that table.

Airport Parameters

VARIABLES

The following variables are used in the table:

◆ D_a: Length of common approach path

◆ D_d: Minimum distance to turn on departure

◆ σ_x: Standard deviation of position uncertainty

◆ σ_v: Standard deviation of approach speed

◆ σ_w: Standard deviation of wind.

ROT MULTIPLIER

The standard arrival ROTs in our model are 42 seconds for small aircraft, 47 seconds for large and Boeing 757 aircraft, and 53 seconds for heavy aircraft. These are increased by multiplication by the ROT multiplier in certain cases.

SEPARATION MATRIX

We consider several sets of miles-in-trail minima, (Table 5-1).

SEQUENCE

This parameter refers to the sequence in which aircraft of the mix arrive at a runway. "Random" means that aircraft arrive at random, in accordance with the probabilities determined by the mix. "Optimal" means that aircraft arrive in an optimal sequence, in which such time-absorbing cases as small behind heavy are eliminated.

TAXI CAPACITY

Taxi-queue capacities are either those which give mean taxi-in delays equal to the PMAC values for 1995 (indicated by "1995 obs") or those which reduce the maximum mean taxi-in delay to 1 minute at all network airports (indicated by "1' max").

TAXI CAPACITY REDUCED IN LOW VISIBILITY

This parameter shows whether or not the 25 percent reduction of taxi-queue capacity is imposed when visibility is less than 1 mile.

TRACON Parameters

The following are definitions of TRACON parameters:

- ◆ $1/\lambda$ equivalent distance—The distance traveled at the weighted average approach speed of the aircraft using a runway, during time $1/\lambda$, i.e., during the mean delay due to input-stream errors.

- ◆ μ—The mean of the Erlang-k distribution of service times, i.e., of the times aircraft spend in the TRACON.

- ◆ k—The shape parameter of the Erlang-k distribution of service times.

- ◆ N—The maximum number of aircraft that the TRACON controller can accommodate at a given time.

Table 5-1. Miles-in-Trail Minima

FAA 3.0			
	Leader →		
Follower ↓	**Small**	**Large**	**B-757**	**Heavy**
Small	3	4	5	6
Large	3	3	4	5
B-757	3	3	4	5
Heavy	3	3	4	4
FAA 2.5			
Small	2.5	4	5	6
Large	2.5	2.5	4	5
B-757	2.5	2.5	4	5
Heavy	2.5	2.5	4	4
VMC			
Small	1.9	2.7	3.5	4.5
Large	1.9	1.9	3	3.6
B-757	1.9	1.9	3	3.6
Heavy	1.9	1.9	2.7	2.7
LaRC 3.0			
Small	3	3.5	4.5	5.5
Large	3	3	3.5	4.5
B-757	3	3	3.5	4.5
Heavy	3	3	3.5	3.5
LaRC 2.5			
Small	2.5	3.5	4	5.5
Large	2.5	2.5	3.5	4.5
B-757	2.5	2.5	3.5	4.5
Heavy	2.5	2.5	3.5	3.5
LaRC 2.3			
Small	2.3	3	4	4
Large	2.3	2.3	3.5	3.5
B-757	2.3	2.3	3.5	3.5
Heavy	2.3	2.3	3	3.5

ARTCC Parameters

The following are definitions of ARTCC parameters:

◆ μ—The mean of the Erlang-k distribution of service times, i.e., of the times aircraft spend in an ARTCC sector.

◆ k—The shape parameter of the Erlang-k distribution of service times.

◆ N—The maximum number of aircraft that an ARTCC sector controller can accommodate at a given time.

FOUR SPECIFIC CASES

In this report, we considered four specific cases. This section summarizes the LMINET parameters that we used to model them.

Table 5-2 gives the specific LMINET parameters used for each case. The following paragraphs explain our choices.

2007 Reference

The LMINET parameters for this case are those for the row, "2007 Reference," in Table 5-2.

All TAP and AATT

The airport parameters for this case are those of the row "Ultimate TAP" in Table 5-2, except that the miles-in-trail matrix is LaRC 2.5 instead of LaRC 2.3 for VMC-2 and for the IMC cases. The reason for this change is that AVOSS is not usable under all wind conditions. We are unable to model this accurately with the presently available link between our capacity models and LMINET because the link does not permit epoch-by-epoch changes in runway capacity. Replacing LaRC 2.3 with LaRC 2.5 gives an approximation to the capacity reductions stemming from periods in which AVOSS is not available. These airport parameters model effects of ATM-2 (which includes TMA and A-FAST), ROTO, DROM, and AVOSS build 2.

We modeled the effects of T-NASA by eliminating the reduction in taxiway capacity associated with visibilities less than or equal to 1 mile.

The TRACON parameters of this case are $1/\lambda = 0$, service time = 16 minutes, shape parameter = 3, and maximum aircraft-in-sector = 19. These parameters model effects of TMA, A-FAST, and EDP on TRACON operations. The ARTCC parameters are service time = 24 minutes, shape parameter $k = 3$, and maximum aircraft-in-sector = 21. These last three parameters model effects of EDA.

TAP Only

We modeled TAP only by keeping the airport parameters the same as for "everything," with the exception of the taxiway capacities. Even though A-FAST is an AATT program, it is such an integral part of the TAP technologies that we maintained its presence for the "TAP only" case. APATH also should be considered a part of this case, since it may provide A-FAST/FMS data links.

We maintained taxiway capacities at the baseline level, since NSMT, an AATT program, would not be present. We eliminated the reductions in taxiway capacity associated with visibilities less than 1 mile, and with darkness, since that is how we model the effects of T-NASA, a TAP program.

We kept TRACON and ARTCC parameters at baseline values, except for $1/\lambda$. We set this parameter to zero, since this reflects the effect of TMA, which we assume to be implemented with A-FAST.

To summarize, the "TAP Only" case considers effects of ATM-2 (which includes TMA and A-FAST), ROTO, DROM, and AVOSS build 2.

AATT Only

We modeled AATT Only by removing our models of the benefits of the TAP technologies, while retaining benefits of AATT technologies. Thus, this case models effects of TMA, A-FAST, EDP, EDA, and NSMT

Table 5-2. LMINET Parameters Modeling TAP and DST Tools and Combinations of Tools

Case	Da nmi	Dd nmi	σx nmi	σv kt	σw kt	IMC-2 ROT M'pl	IMC-2 Sep. Mat.	IMC-1 ROT M'pl	IMC-1 Sep. Mat.	VMC-2 ROT M'pl	VMC-2 Sep. Mat.	VMC-1 ROT M'pl	VMC-1 Sep. Mat.	Sequence	Taxi capacity	Taxi capacity red. for lo viz?	TRACON Eq. dist. nmi	TRACON μ min	TRACON k	N	ARTCC μ min	ARTCC k
1996 Reference	7	3.5	0.25	5	7.5	1.2	FAA 3.0	1	FAA 3.0	1	FAA 3.0	1	FAA 2.5	Random	1995 obs	Yes	0.25	19/22*	3	18	24	3
2007 Reference	7	3.5	0.25	5	7.5	1.2	FAA 3.0	1	FAA 3.0	1	FAA 3.0	1	FAA 2.5	Random	1995 obs	Yes	0.25	19/22*	3	18	24	3
TMA	7	3.5	0.25	5	7.5	1.2	FAA 3.0	1	FAA 3.0	1	FAA 2.5	1	FAA 2.5	Random			0.2	19/22*	3	18	24	3
P-FAST	7	3.5	0.25	5	7.5	1.2	FAA 3.0	1	FAA 2.5	1	FAA 2.5	1	FAA 2.5	Optimal			0.1	19/22*	3	18		
A-FAST***	7	3.5	0.02	2	7.5	1.2	FAA 3.0	1	FAA 3.0	1	FAA 2.5	1	FAA 2.5	Optimal			0.05	19/22*	3	18		
DROM***	7	3.5	0.25	5	7.5	1.2	FAA 2.5	1	FAA 3.0	1	FAA 2.5	1	FAA 2.5	Optimal			0.1	19/22*	3	18		
ROTO + DROM***	7	3.5	0.25	5	7.5	1.0	FAA 2.5	1	FAA 2.5	1	FAA 2.5	1	FAA 2.5	Optimal			0.1	19/22*	3	18		
DROM**	7	3.5	0.02	2	7.5	1.2	FAA 3.0	1	FAA 3.0	1	FAA 2.5	1	FAA 2.5	Optimal			0.05	19/22*	3	18		
ROTO + DROM **	7	3.5	0.02	2	7.5	1.0	FAA 2.5	1	FAA 2.5	1	FAA 2.5	1	FAA 2.5	Optimal			0.05	19/22*	3	18		
AVOSS																						
Build 1* (B1)	7	3.5	0.25	5	7.5	1.2	LaRC 3.0	1	LaRC 3.0	1	LaRC 3.0	1	LaRC 2.5	Optimal			0.1	19/22*	3	18		
ROTO+DROM+B1***	7	3.5	0.25	5	7.5	1	FAA 2.5	1	FAA 2.5	1	FAA 2.5	1	FAA 2.5	Optimal			0.1	19/22*	3	18		
Build 1**	7	3.5	0.02	2	7.5	1.2	LaRC 3.0	1	LaRC 3.0	1	LaRC 3.0	1	LaRC 2.5	Optimal			0.05	19/22*	3	18		
ROTO+DROM+B1***	7	3.5	0.02	2	7.5	1	LaRC 2.5	1	LaRC 2.5	1	LaRC 2.5	1	LaRC 2.5	Optimal			0.05	19/22*	3	18		

5-9

Table 5-2. LMINET Parameters Modeling TAP and DST Tools and Combinations of Tools (Continued)

Case	Airport parameters												
ATM-1#	7	3.5	0.02	2	5	1.2	FAA 3.0 1	FAA 3.0 1	FAA 2.5 1	VMC Optimal	0.05	19/22* 3	18
ATM 1+ROTO+DROM	7	3.5	0.02	2	5	1	FAA 2.5 1	FAA 2.5 1	FAA 2.5 1	VMC Optimal	0.05	19/22* 3	18
ATM 1+ROTO+DROM +AVOSS Build 2	7	3.5	0.02	2	5	1	LaRC 2.3 1	LaRC 2.3 1	LaRC 2.3 1	VMC Optimal	0.05	19/22* 3	18
ATM-2#	7	3.5	0.02	1.2	2	1.2	FAA 3.0 1	LaRC 2.3 1	FAA 2.5 1	VMC Optimal	0	19/22* 3	18
T-NASA										No			
Ultimate TAP	7	3.5	0.02	1.2	2	1	LaRC 2.3 1	LaRC 2.3 1	LaRC 2.3 1	VMC Optimal No	0	19/22* 3	18
CAAP	We have no information about this tool.												

***With P-FAST

** With A-FAST

+ Includes ADS-B Data Link

*May include APATH

*19 minutes in all arrival TRACONs, and in all departure TRACONs EXCEPT those for LGA, JFK, EWR, PHL, DCA, CLT, ATL, MCO, MIA, CVG, ORD, MDW, STL, IAH, DFW, MSP, PHX, LAX, SFO, and SEA

5-10

Table 5-3. Parameters For Cases in Preliminary Report

Case	Da nmi	Dd nmi	σx nmi	σv kt	σw kt	IMC-2 ROT M/pl	IMC-2 Sep. Mat.	IMC-1 ROT M/pl	IMC-1 Sep. Mat.	VMC-2 ROT M/pl	VMC-2 Sep. Mat.	VMC-1 ROT M/pl	Se-quence	Taxi capacity	Taxi capacity red. for lo viz?	TRACON 1/λ Eq. dist. nmi	TRACON μ min	TRACON k	TRACON N	ARTCC μ min	ARTCC k	ARTCC N
1996 Reference	7	3.5	0.25	5	7.5	1.2	FAA 3.0	1	FAA 3.0	1	FAA 2.5	1	Random	1995 obs	Yes	0.25	19/22*	3	18	24	3	18
2007 Reference	7	3.5	0.25	5	7.5	1.2	FAA 3.0	1	FAA 3.0	1	FAA 2.5	1	Random	1995 obs	Yes	0.25	19/22*	3	18	24	3	18
Everything	7	3.5	0.02	1.2	2	1	LaRC 2.5	1	LaRC 2.5	1	LaRC 2.5	1	Optimal	1' max	No	0	18	3	18	24	3	21
All TAP	7	3.5	0.02	1.2	2	1	LaRC 2.5	1	LaRC 2.5	1	LaRC 2.5	1	Optimal	1995 obs	No	0	19/22*	3	18	24	3	18
All AATT	7	3.5	0.02	2	7.5	1.2	FAA 3.0	1	FAA 3.0	1	FAA 2.5	1	Optimal	1' max	Yes	0.05	18	3	18	24	3	21

Chapter 6
Impacts of ATM Technologies on NAS Operations

In this chapter, we show some of the LMINET outputs that characterize operations of the NAS with the 1996, 2007, and 2017 baselines and the effects of the NASA technologies in 2007 and 2017. Let us look first at the total annual delays, which are shown in Figure 6-1.

Figure 6-1. Total Annual Delays in Aircraft-Minutes
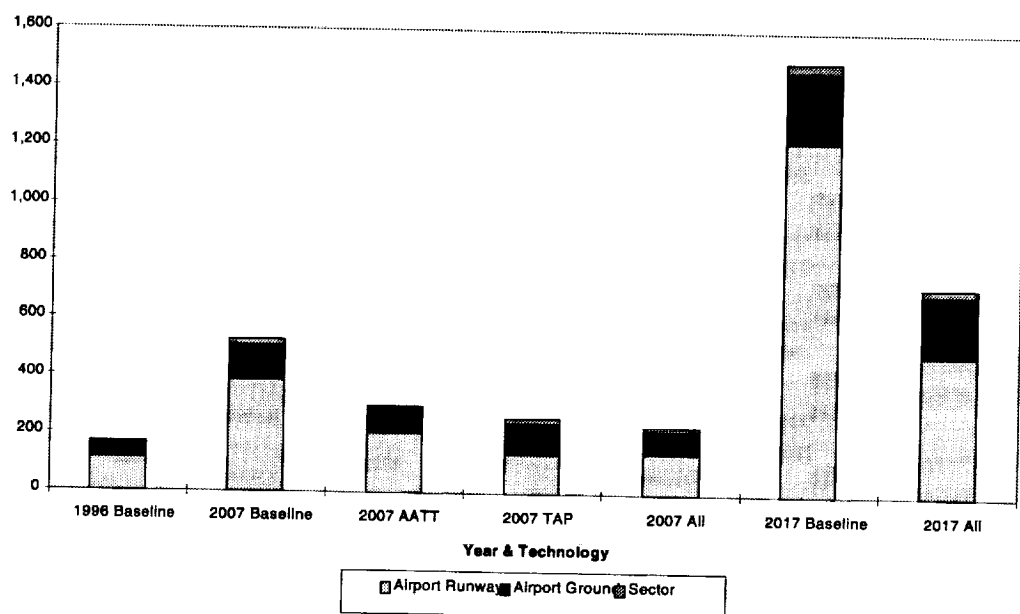
In the 1996 baseline, the bulk of delays, 67 percent of the total, are due to runway capacity limits. Surface-movement delays amount to 30 percent of the total delay. This significant amount follows fairly directly from calibrating the surface-delay models with FAA PMAC data. Sector delays contribute roughly 3 percent of the total.

We estimate that operating the NAS in 2007 in the same way it was used in 1996, with demand increased by the FAA's forecast amounts for each network airport, would cause nearly a fourfold increase in total delays (314 percent.) Effects of runway capacity limits continue to dominate, with 72 percent of the total. Surface-movement delays decrease in relative importance to 24 percent. Sector delays continue to contribute about 3 percent of the total delay.

Since our surface-movement delay model is a new one, we should comment that its relative importance is not unexpected. Some important airports experience noticeable surface-movement problems. Peak arrival capacity at LAX is limited by taxiway capacity. Taxiways at DFW are sufficiently heavily used that ground controllers manage queues for taxiways during peak periods.

Let us turn now to the effects of the NASA technologies. Applying the AATT tools TMA, A-FAST, EDP, EDA, and NSMT alone would, we estimate, reduce total delays by 43 percent. Our model of NSMT indicates that this tool would reduce surface-movement delays to 68 percent of their 2007 baseline values. The AATT tools cause a 47 percent reduction in delays from airport airside capacity limits and a 32 percent reduction in en route delays.

Applying just the TAP technologies ATM-2, ROTO, DROM, T-NASA, and AVOSS build 2—which includes A-FAST and, potentially, A-FAST/FMS data links from APATH—would cause a 50 percent reduction in total delays by our present estimate. The TAP tools are quite effective against airport runway capacity constraints, reducing delays from this cause by 65 percent. Since our assumed benefit of T-NASA is active only in low visibility conditions (a horizontal visibility of 1 nautical mile or less, or darkness), which are relatively infrequent, by our present estimate T-NASA reduces surface delays by 15 percent.

Applying all the TAP and AATT technologies would, by our present estimates, reduce total delays by 56 percent. Delays from airport runway capacity limits would be reduced by 63 percent, to just 26 percent above their values in the 1996 baseline. Surface movement delays would be reduced by 36 percent. Sector delays would be reduced by 55 percent.

The changes in delays between the "TAP only" and "All AATT and TAP" cases give an interesting illustration of the interactions of DSTs' effects. In comparison with the "All TAP" case, the "All AATT and TAP" tools reduce ground and sector delays significantly, by 25 percent and 56 percent, respectively. These improvements stress airport runways, resulting in a slight increase in airside delays of just under 5 percent. Total delays are still reduced by 12 percent.

We doubt that the airlines would continue 1996 patterns of operation in the face of delays as large as the 2007 baseline. If all AATT and TAP tools were used, our estimate of the increase in total delay is 37 percent. That level of increase may be close to what the carriers would tolerate. Viewed in this way, our results suggest that applying all AATT and TAP tools would allow the NAS to accommodate 2007 demands with 1996 patterns of operation, with somewhat increased but perhaps still acceptable delays.

Continuing to operate the NAS with 1996 methods and the demands forecast for 2017 would, in our models, increase total delays by almost an order of magnitude

(by a multiple of 8.9). Applying all AATT and TAP tools would reduce these de-lays by 52 percent.

These results push our models far from the data on which they were calibrated. Moreover, we doubt that the airlines would accept delays as large as those pre-dicted when all AATT and TAP tools are applied. Thus, the results for 2017 are useful chiefly for theoretical discussions.

Returning to the 2007 cases, we note that the overall delay statistics are reflected in time histories of queues at individual airports and sectors. For example, Fig-ures 6-2 and 6-3 show the arrival and ground-hold queues at ATL for the weather date of June 12, 1996.

Figure 6-2. Arrival Queues at ATL

Figure 6-3. Ground-Hold Queues at ATL
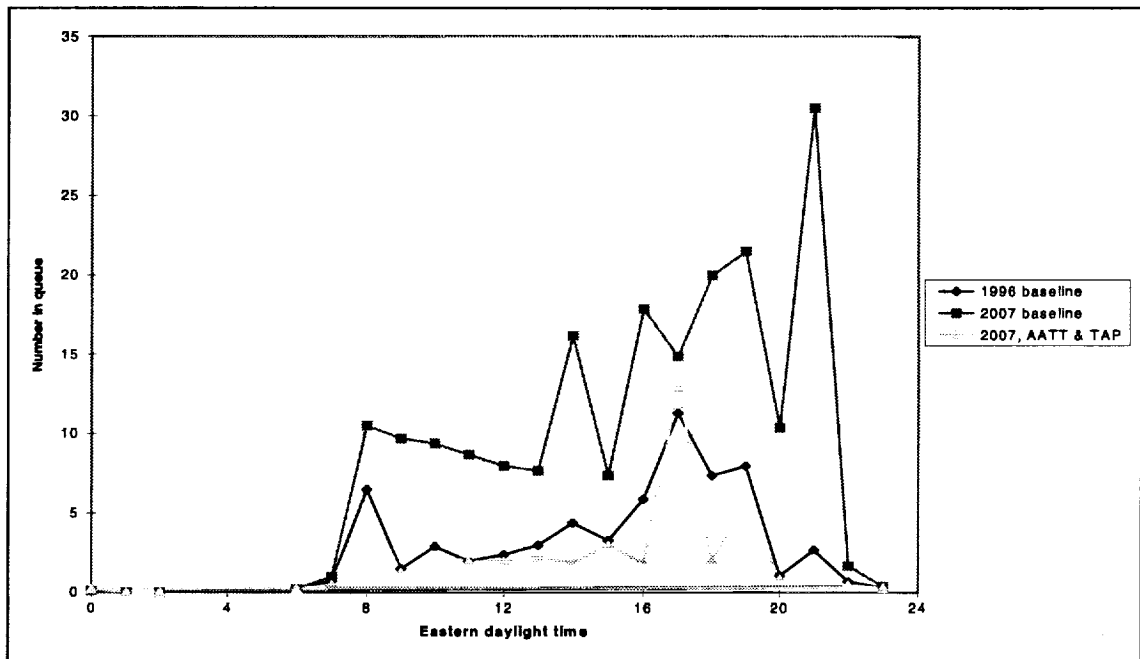
Figure 6-3. Ground-Hold Queues at ATL
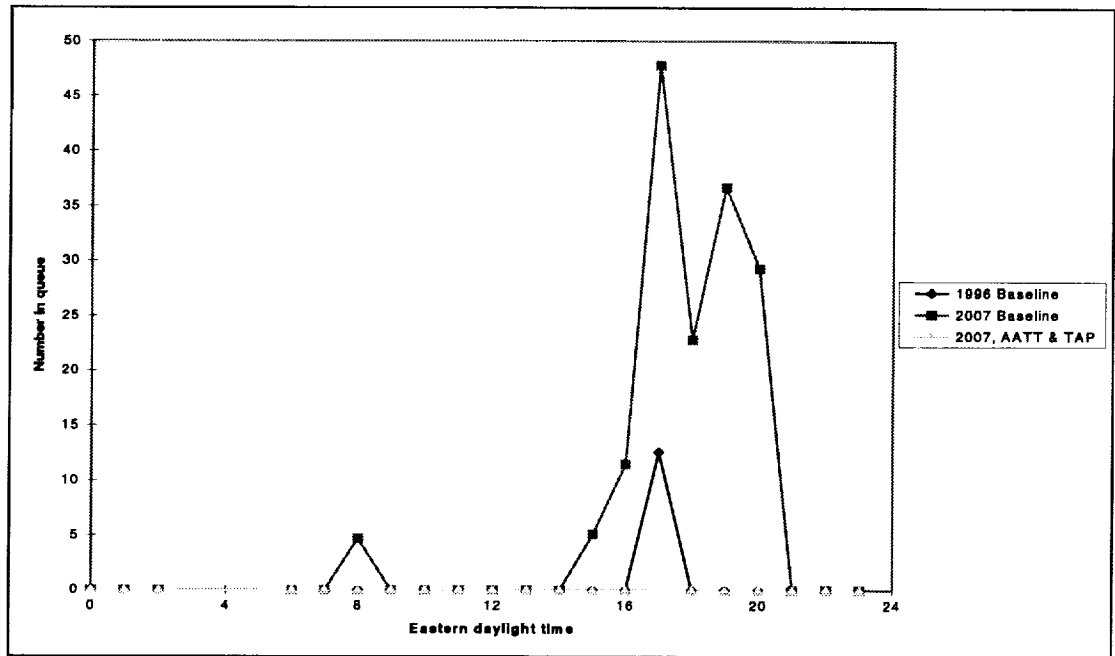
June 12 was a good-weather day at ATL, and with 1996 traffic there were only insignificant delays. But with that same weather, the 2007 demands would have caused significant arrival and ground-hold queues over much of the day. ATL's arrival capacity usually does not exceed 110, so the queues imply 10-minute delays for much of the day and 20- to 25-minute delays in the evening rush periods.

Queues at other major airports behaved in similar ways. For example, Figures 6-4 and 6-5 show arrival and ground-hold queues, respectively, at ORD.

Figure 6-4. Arrival Queues at ORD
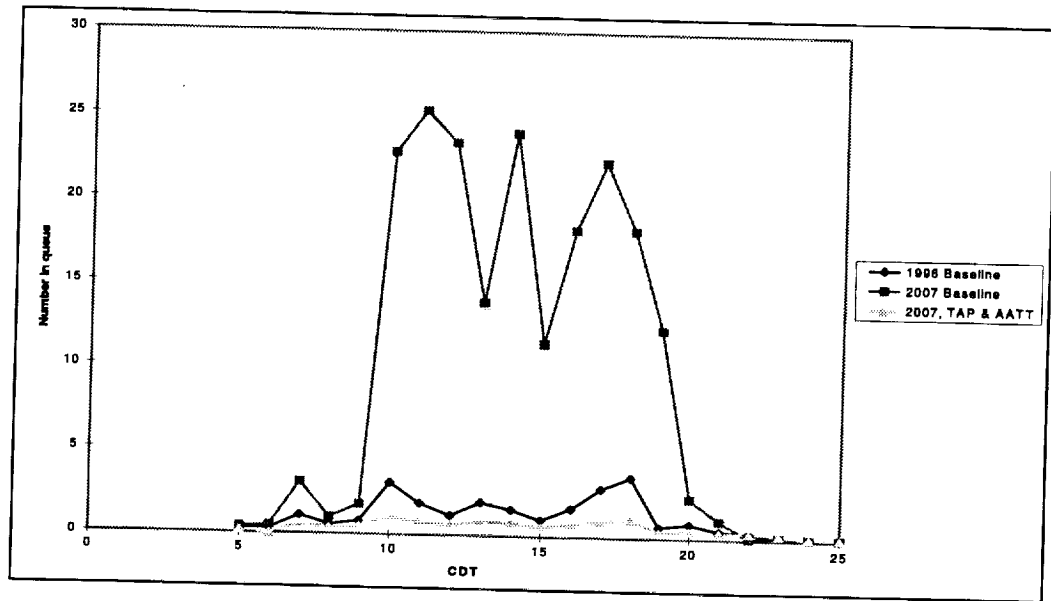
Figure 6-5. Ground-Hold Queues At ORD
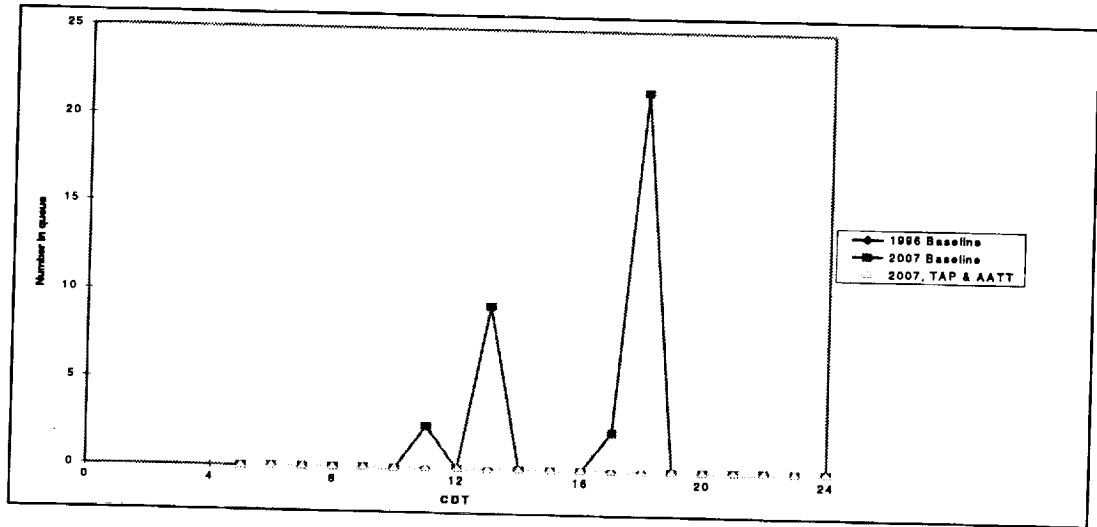
Certainly, the NASA technologies are very helpful, but they are by no means panaceas. To see this, we may consider tables analogous to Table 6-1, showing events at BOS with the weather of April 8, 1996.

Table 6-1. LMINET Output for BOS, 2007 Baseline

EDT	λ_A	μ_A	Arrivals	q_A	q_{ta}	Reservoir	q_p	q_{td}	λ_D	μ_D	Departures	q_D	Ground hold
6	6.6	7.1	4.6	2	0.1	94.3	0	1	37.2	39.7	31.9	4.3	0
7	32.2	17.9	16.4	17.5	0.4	49.3	0	1.9	49.5	28.7	27.4	25.5	0
8	7.6	10.9	10.8	14.6	0.2	10.6	0	2.6	55.1	35.8	35.3	44.7	17.2
9	0.1	6.3	6.2	8.6	0.1	0	25.4	0.2	46.8	40.5	40	28.5	37.5
10	14.0	15.7	14.5	7.9	0.3	0	59.8	0.1	40.6	30.9	29.8	5	49.7
11	16.4	20.1	18.5	5.6	0.5	0	90.5	0.2	45.2	26.3	18.6	0.7	61.3
12	25.8	22.5	21	10.3	0.6	0	109.8	0.3	37.9	23.9	17.4	1.8	72.3
13	68.1	62.3	57.1	18.3	3.5	0	130.3	0.4	41.4	50.7	22.3	0.4	58.9
14	51.4	61.9	59.7	10.1	3.5	0	113.6	3.3	40.4	53.1	45.2	9.3	56.2
15	77.7	62.2	60	27.5	3.8	0	94.3	3.5	40.3	51.4	49.5	19.3	39.7
16	47.8	60.7	59.6	16.1	3.5	0	87.3	3.7	53.1	60.9	59.3	19.8	43
17	65.8	61.1	59.4	22.5	3.6	0	80.1	3.5	52.4	58.9	57.5	22.1	36
18	57.5	60.4	59.1	21.1	3.4	0	77.2	3.5	56.4	61.1	59.7	21.8	36.2
19	56.9	60.9	59.3	18.6	3.5	0	67.8	3.4	49.7	59.8	58.4	22.5	33.4
20	74.3	62.7	60.8	31.5	4	0	37.6	3.5	29.1	47.9	47	34.7	21.1
21	66.0	69.3	65.9	29.4	6.3	0	5	3.9	28.2	53.4	52.6	42.5	4.5
22	50.3	70.4	67.6	11.2	7.2	49.5	0	0.2	11.1	52	51	11.4	0
23	17.8	73.6	35.7	0.2	0.3	112.6	0	0.1	4.5	40.7	15.9	0.1	0
0	7.5	73.6	7.8	0.1	0.1	146.6	0	0	1.7	17.9	1.8	0.1	0
1	9.5	67	9.5	0.1	0.1	154.4	0	0	0	0.6	0	0	0
2	2.0	67	2.2	0	0	163.9	0	0	0	1	0	0	0

BOS is an airport with a relatively small traffic increase: the FAA forecasts a 7.8 percent increase there, in contrast to increases of 16.9 percent at ATL and 16.6 percent at ORD. Accordingly, delays are worse at BOS, but not dramatically so. Table 6-2 shows events as we forecast them, with TAP and AATT technologies in place.

There is a marked improvement, to be sure, but this bad-weather day at BOS is still a day of significant delay.

Table 6-2. LMINET Output For BOS, TAP and AATT Technologies In Place

EDT	λ_A	μ_A	Arrivals	q_A	q_{ta}	Reservoir	q_p	q_{td}	λ_D	μ_D	Departures	q_D	Ground hold
6	6.6	8.3	5.1	1.5	0.1	94.3	0	0.6	37.2	46.7	34.6	2	0
7	32.5	20.4	18.6	15.1	0.2	47.9	0	1	51.5	32.5	30.6	22.5	0
8	7.6	12.4	12.1	10.8	0.1	13.4	0	1.1	53.1	41.9	41.1	34.5	17.2
9	3.7	8.2	7.8	6.7	0.1	0	21	0.1	46.9	46.8	46	15.4	35.7
10	24.6	21	19.7	11.5	0.2	0	56	0	42.8	31.8	23	0.2	42.7
11	14.6	23.7	22	4	0.3	0	79.2	0.2	42.9	28.6	18.5	1.2	55.1
12	34.3	25.8	24.2	14.1	0.3	0	95.5	0.3	38.4	26.1	20.8	2.4	61.8
13	84.1	80.3	75.1	20.3	3.1	0	114.8	0.3	43.4	58.7	26.2	0.4	40.3
14	98.1	82.1	80.1	37.8	3.6	0	78.4	3	38.8	54.3	49.3	23.5	14.4
15	67.5	78.6	77.9	27.9	3	0	40.6	3.5	42.2	63	61.9	41.1	3.7
16	62	71.3	70.7	20.1	2.1	0	15.9	3.1	53.2	75.7	74.8	44.8	0
17	53.3	61.5	60.3	13.8	1.4	1.1	0	1.5	53.7	80.8	79.8	36.1	0
18	57.4	61.1	58.8	12.4	1.3	4.7	0	1.2	56.7	81	79.2	13.8	0
19	51.5	73.2	62.9	1.3	1	13.4	0	1	50.2	74.7	63.2	1.1	0
20	50	83.4	50.5	0.8	0.9	47.1	0	0.4	29.1	50.8	30.1	0.7	0
21	33.3	77.9	34.1	0.4	0.5	69.6	0	0.4	28.1	66.8	28.4	0.4	0
22	39.5	98.1	39.4	0.4	0.6	93.5	0	0.1	10.1	26.7	10.5	0.3	0
23	18.3	104	19	0.3	0	130.7	0	0	2.2	14.9	2.6	0.1	0
0	7.4	108.1	7.6	0.1	0	149.7	0	0	0	1.6	0.1	0	0
1	8.9	98.8	8.9	0.1	0	157.3	0	0	0	0.1	0	0	0
2	2	98.8	2.1	0	0	166.1	0	0	0	0.2	0	0	0

Chapter 7
Economic Impacts of ATM Technologies

In the previous chapters, we analyzed the quantitative effects of these technologies. This chapter describes our analyses of their economic impacts.

The costs associated with air travel delay are borne by the flying public and/or the air carriers. For this study, we will only examine the air travel delay costs that accrue to the carriers. These delay costs have two effects. The first is to increase the costs of service on a particular flight, while the second is to increase the costs on future flights that may use the same aircraft, personnel, or gates. These costs are particularly important because efficient use of the aircraft is a key component of every carrier's profitability.

MODEL STRUCTURE

In this section, we examine the individual daily-delay costs used to calculate the annual delay costs. A total of 21 cases were examined. Each technology, consisting of various combinations of DSTs, was analyzed, as were the three baseline cases (with 1996 representing the present baseline, 2007 representing the near future baseline, and 2017 representing the far future baseline) for each of three representative weather days. The benefits are defined as the cost savings of delays of the DSTs over the future baseline cases.

The cost is made up of two components: the sector delay costs and the airport queue costs. We also tracked the cost and amount of the fuel embedded in those two costs separately.[1]

The sector delay costs can be further divided into airport delay and en route delay. The airport delay can be yet further divided into arrival TRACON delay and departure TRACON delay. Finally, all sector delay components are composed of time and fuel.

Airport queue costs comprise the costs of six queues: departure, taxi-in, taxi-out, arrival, airplane, and ground hold. The costs of the first four queues are those for

---

[1] This is a subtle but important breakout. The fuel costs represents direct and noticeable savings to the airlines. In the short run, these are the only savings that the airlines capture. The other costs are accrued to the airlines but on a much more incremental basis because they represent changes to a set of costs that are fixed in the short run. For example, pilots typically are paid on the basis of a maximum time of actual flight time and/or expected block flight time. In order for the airlines to realize savings in pilot wages consistent with savings in either flight time or block time, either the wage rules or the scheduled travel times will have to be changed.

time and fuel, while the costs of the last two are for time only. We show a schematic diagram of the overall cost structure in Figure 7-1.

Figure 7-1. Schematic Diagram of Overall Cost Structure
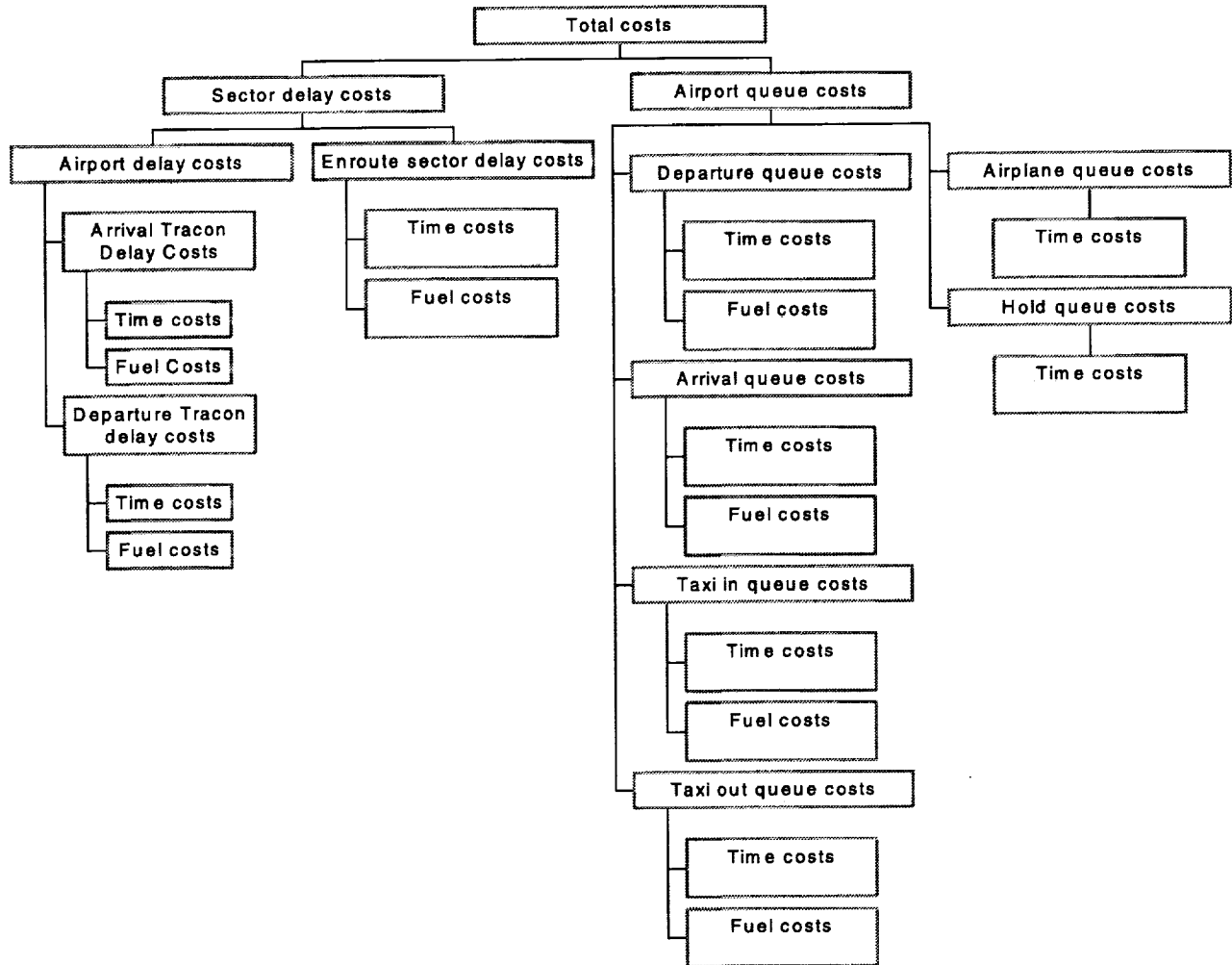
VOC VERSUS DOC

The derivation of the delay costs starts with the concept of operating costs. The delay costs must be equal to some value that represents either the additional costs directly attributable to the delay and/or revenues lost due to the delay. There are two methods that can be used to calculate the cost of delay. Each produces a different type of aircraft operating cost, which will define the cost of delay. In fact, these two methods will define a lower and upper bound of the delay cost.

The first method is based on the direct operating cost (DOC). Here the delay cost is based on the DOC divided by the block hours flown. Since this measure

includes capital costs, it produces a relatively high estimate of delay cost. This calculation results in a relatively large delay costs, which then creates very favorable economics for any new delay-reducing technology. In addition, the analytical models developed in this analysis are sophisticated enough to analyze delay by phase of flight. This DOC-based calculation averages costs, which include the fuel cost, across all phases of flight. Therefore, using this calculation will not produce accurate costs by phase of flight, but it is useful because it provides an approximate upper bound of the delay costs incurred by the carriers.

The DOC per block is published in *The Aviation & Aerospace Almanac*. [17] For 1996, this block weighted cost is $2,591 per block hour or almost $44 per block minute. This cost should be considered as an upper limit since this calculation is based solely on the jet aircraft of the carriers recording the Form 41 DOT data filings.[2]

The second method is based on the variable operating cost (VOC). Here the costs are those strictly attributable to moving the passengers from origin to destination. This cost includes no capital costs. This number is also calculated from the DOT's Form 41 data filings. Because of the additional complexity of the models, the fuel costs have been removed from this calculation. The resulting average VOC was $21.51 per block minute in 1996. Furthermore, this VOC can be decomposed into its component costs of jets ($23.40 per block minute), turboprops ($6.15 per block minute), piston-engined aircraft ($2.85 per block minute), or the combination of jets and turboprops ($21.58). The complete data used in the calculation are shown in Appendix A. Using the VOC as the delay cost will produce relatively much smaller total delay costs. This makes the economic case for new delay-reducing technology much harder to meet.

CALCULATION OF DELAY COSTS

The VOC calculation represents the costs associated with aircraft flown by carriers sufficiently large enough to file the Form 41 data. These aircraft are actually a subset of all the aircraft included in this study. Missing are the aircraft which perform the GA role, including air taxis. These aircraft include some of the piston-powered aircraft as well as a few of the smaller jets, but the primary aircraft fulfilling this role is the turboprop.

An adjustment is made to extend the basic VOC calculation to all aircraft included in the study. The operations are split into GA and non-GA. The delay cost for the non-GA operations is set equal to the VOC of the combined jet and turboprop aircraft. The delay cost for the GA operations are set equal to the VOC of the turboprop aircraft. The total delay cost is then found as the operations-weighted

---

[2] The DOT Form 41 schedule data are composed of a series of federally mandated reports that document the financial and operational status of the individual carriers. These data are publicly available and can be analyzed for a variety trends at both the carrier and industry levels.

average of these two VOCs. These results, for each test year, are shown in Table 7-1.

Table 7-1. GA and Non-GA Combined Variable Operating Cost Calculation

Year	GA operations (%)	Non-GA operations (%)	VOC jet and turboprops	VOC turboprops	Combined VOC
1996	18.00	82.00	$21.580	$6.150	$18.803
2007	14.80	85.20	$26.832	$7.647	$23.993
2017	14.06	85.94	$32.708	$9.321	$29.420

The extension of the delay cost calculation to the future is predicated on a specific set of assumptions. These assumptions lead to the future delay costs shown in Table 7-2. These data represent the assumptions of

♦ 0.10 percent yearly increase in the cost of fuel,

♦ yearly nominal interest rate of 2.0 percent,

♦ yearly real increase in aircraft operating costs of 1 percent, and

♦ gallon-to-kilogram conversion factor of 0.33125.

Table 7-2. Total Delay Cost Drivers in 1996 Dollars

Parameter	1996	2007	2017
Average price of a gallon of airplane fuel	$0.650	$0.657	$0.664
DOC-based delay cost per block minute	$43.181	$53.691	$65.449
VOC-based delay cost per block minute	$21.580	$26.832	$32.708

The most important of these variables is the VOC-based delay cost per block minute. This parameter, when combined with the fuel costs, forms the basis of all of the block minute delay costs per flight phase, except for the case of ground hold.

The costs of delay per block minute are shown in Table 7-3 by model and mode of flight. The case where the cost is based on the variable operating costs is used so these delay costs represent the minimum delay costs. The delay costs are also calculated based on the expected operating costs in 2007 and 2017 but deflated back to 1996 dollars. We then added the cost of the fuel used, by flight phase or sector mode, to the VOC cost per block minute to arrive at the final delay cost per flight phase or flight mode.

Table 7-3. Yearly Block Minute Delay Costs in 1996 Dollars

Cost item	1996	2007	2017
Base delay costs	$18.803	$23.993	$29.420
Ground idle	$21.175	$26.391	$31.843
Taxi out	$22.434	$27.664	$33.128
Climb	$40.724	$46.156	$51.806
Vector out	$29.503	$34.811	$40.347
Cruise	$29.200	$34.505	$40.038
Vector in	$26.012	$31.282	$36.783
Descent	$21.195	$26.411	$31.863
Taxi in	$22.071	$27.297	$32.757
Ground hold	$18.803	$23.993	$29.420
In arrival TRACON	$27.606	$32.893	$38.410
In departure TRACON	$21.175	$26.391	$31.843
In en route sector	$29.200	$34.505	$40.038

The first observation is that the bulk of the delay costs (more than 91 percent in all 21 cases) is composed of airport queue costs. This suggests that the major reductions in delay costs are to be found in those technologies that primarily affect the airport queues. Some of these technologies are also intrinsically linked to the operations of the carriers themselves. This then adds another layer of difficulty in reaching the optimal effectiveness of the DSTs.

The comparative analysis results are shown in Table 7-5. One approach to looking at the effectiveness of the DSTs is to gauge their results relative to the expected future state of NAS. The expected increase of 22 percent in operations translate to an average increase of 313 percent (unweighted) in delay costs in 2007. On that basis, the AATT-based DSTs produce savings of an average of 40 percent across all three weather scenarios, while the TAP-based DSTs produce an average savings of 45 percent. A savings of an average of 53 percent is obtained when both sets of technologies are implemented.

The year 2017 cases include only the baseline and the complete set of all tools. Here, the increase in operations drive the delay costs (unweighted) up almost 1200 percent over the 1996 baseline and almost 250 percent over the 2007 baseline. The use of both sets of technologies results in an average decrease of 54 percent.

Table 7-4. Case Summary

Case	Name	Year	Date	Total Delay Costs	Sector Delay Costs	Airport Queue Costs
1	Baseline	1996	8 Apr	$9,484,782	$334,176	$9,150,606
2	Baseline	1996	12 Jun	$8,893,514	$392,161	$8,501,353
3	Baseline	1996	29 Nov	$17,430,792	$298,158	$17,132,634
4	Baseline	2007	8 Apr	$35,407,029	$1,544,367	$33,862,662
5	Baseline	2007	12 Jun	$36,482,529	$1,711,977	$44,770,552
6	Baseline	2007	29 Nov	$49,890,013	$1,061,172	$48,828,841
7	AATT	2007	8 Apr	$20,242,958	$680,506	$19,562,452
8	AATT	2007	12 Jun	$20,043,438	$774,028	$19,269,410
9	AATT	2007	29 Nov	$35,711,042	$576,917	$35,134,125
10	TAP	2007	8 Apr	$19,646,026	$1,372,078	$18,273,948
11	TAP	2007	12 Jun	$17,144,070	$1,511,152	$15,632,917
12	TAP	2007	29 Nov	$37,283,714	$1,158,316	$36,125,398
13	ALL	2007	8 Apr	$15,640,208	$690,807	$14,949,402
14	ALL	2007	12 Jun	$15,757,001	$782,411	$14,974,590
15	ALL	2007	29 Nov	$29,504,870	$591,184	$28,913,686
16	Baseline	2017	8 Apr	$119,357,203	$3,431,476	$115,925,727
17	Baseline	2017	12 Jun	$131,563,892	$3,725,638	$127,838,254
18	Baseline	2017	29 Nov	$136,259,976	$2,751,336	$133,508,640
19	ALL	2017	8 Apr	$58,985,858	$2,142,109	$56,843,749
20	ALL	2017	12 Jun	$59,789,121	$544,237	$59,244,884
21	ALL	2017	29 Nov	$81,658,706	$1,800,026	$79,858,681

COMPOSITE ANALYSIS

The previous analysis treats the technologies on a specific weather day basis. This section extends the analysis to an annual composite basis. The first step is to extend the three weather days into a representative day. Then the representative day delays can be multiplied by 365.25 for a representative year. A composite day is found by calculating the data from weather days 4/8, 6/12, and 11/29 by 0.13, 0.80, and 0.07, respectively. This assumption states that for 80 percent of the year, the weather patterns will produce delay results consistent with 6/12 weather, and similarly for 13 percent of the year with 4/8 weather, and finally 7 percent of the year with 11/29 weather.

The airport queue delays can be divided into airport ground delay and airport runway delay. The airport ground delay is the sum of the delay attributable to the taxi-in and the taxi-out queues. The airport runway delay is the sum of the other four airport queues, departure, arrival, airplane, and hold.

Table 7-5. Comparative Analysis

Case	Name	Year	Date	Increase over 1996 Baseline	Increase (%)	Increase over 2007 Baseline	Increase (%)	Increase over 2017 Baseline	Increase (%)
1	Baseline	1996	8 Apr						
2	Baseline	1996	12 Jun						
3	Baseline	1996	29 Nov						
4	Baseline	2007	8 Apr	$25,922,246	273.30				
5	Baseline	2007	12 Jun	$27,589,015	310.22				
6	Baseline	2007	29 Nov	$32,459,221	186.22				
7	AATT	2007	8 Apr	$10,758,176	113.43	($15,164,071)	−42.83		
8	AATT	2007	12 Jun	$11,149,925	125.37	($16,439,091)	−45.06		
9	AATT	2007	29 Nov	$18,280,250	104.87	($14,178,971)	−28.42		
10	TAP	2007	8 Apr	$10,161,244	107.13	($15,761,002)	−44.51		
11	TAP	2007	12 Jun	$8,250,556	92.77	($19,338,459)	−53.01		
12	TAP	2007	29 Nov	$19,852,922	113.90	($12,606,299)	−25.27		
13	ALL	2007	8 Apr	$6,155,426	64.90	($19,766,820)	−55.83		
14	ALL	2007	12 Jun	$6,863,488	77.17	($20,725,528)	−56.81		
15	ALL	2007	29 Nov	$12,074,078	69.27	($20,385,143)	−40.86		
16	Baseline	2017	8 Apr	$109,872,421	1158.41	$83,950,175	237.10		
17	Baseline	2017	12 Jun	$122,670,378	1379.32	$95,081,363	260.62		
18	Baseline	2017	29 Nov	$118,829,184	681.72	$86,369,963	173.12		
19	ALL	2017	8 Apr	$49,501,076	521.90	$23,578,830	66.59	($1,289,367)	−37.57
20	ALL	2017	12 Jun	$50,895,607	572.28	$23,306,592	63.88	($3,181,401)	−85.39
21	ALL	2017	29 Nov	$64,227,914	368.47	$31,768,693	63.68	($951,311)	−34.58

The results for a composite day, for each of the seven cases, are shown in Table 7-6. The net effect is that unabated growth more than triples the delay costs in 2007. This implies an explicit nonlinearity in delay costs because the total operations over the same time period will increase by only 22 percent. The implementation of the TAP technology reduces the 2007 yearly costs by approximately $6.9 billion. The AATT technology also produces benefits, but of a slightly lower magnitude than the TAP technology. Here the yearly costs are reduced by approximately $5.9 billion from the 2007 baseline. The most dramatic results occur when both technologies are used. Here, there is a $8 billion decrease from the 2007 baseline delay costs, which represents a 60 percent increase over the 1996 yearly costs.

The results of the 2017 case are even more profound. Unabated growth leads to a 1300 percent increase in total delay cost over the 1996 baseline, or a 283 percent delay over the 2007 baseline. The implementation of both sets of technologies results in a decrease of $34 billion, or 43 percent. These data are also shown graphically in Figure 7-2.

Table 7-6. Yearly Delay ($ billion) in 1996 Dollars

	Airport runway	Airport ground	Sector	Total
1996 Baseline	$2.3	$1.1	$0.1	$3.6
2007 Baseline	$9.7	$3.5	$0.6	$13.8
2007 AATT	$5.2	$2.4	$0.3	$7.9
2007 TAP	$3.4	$3.0	$0.5	$6.9
2007 All	$3.3	$2.2	$0.3	$5.8
2017 Baseline	$38.4	$8.1	$1.4	$47.9
2017 All	$15.1	$7.0	$0.3	$22.4

Figure 7-2. Annual Cross Comparable Benefits
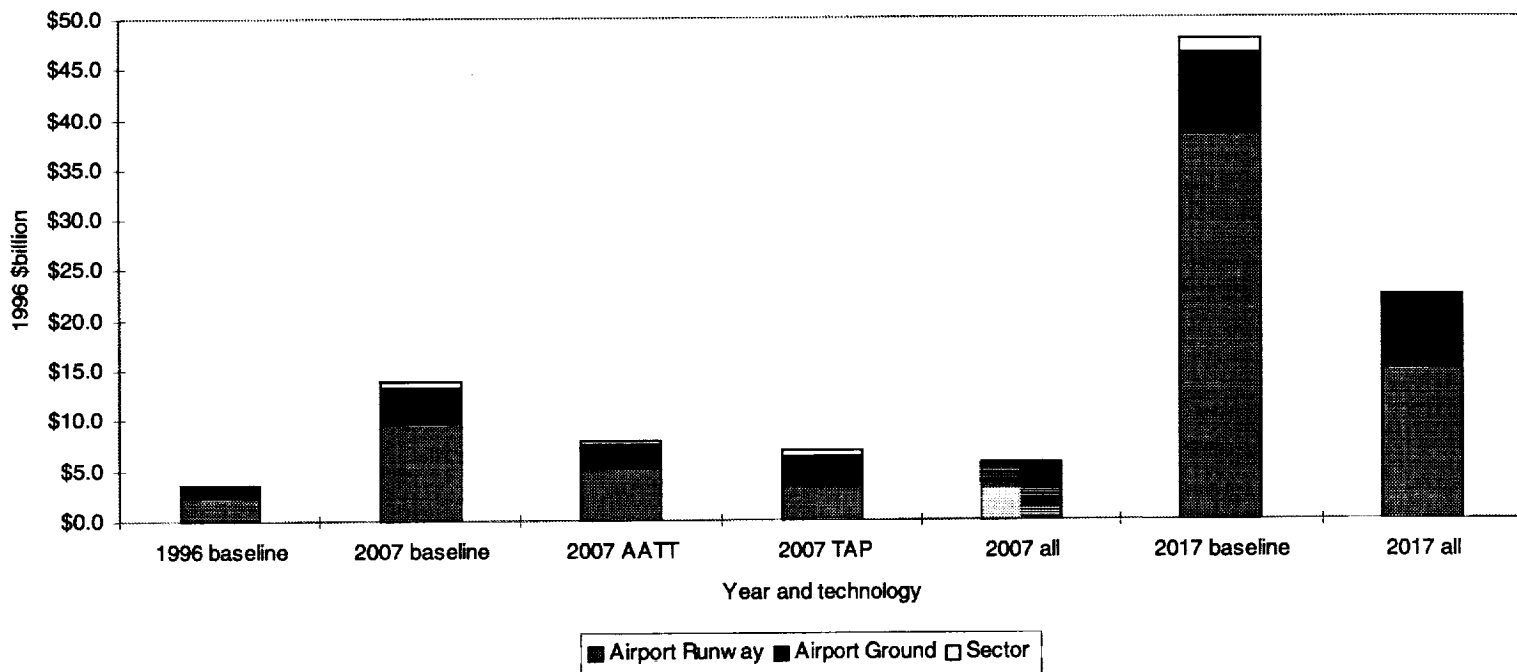
Of interest is that neither set of technologies, nor their combination, reduces the delays on a proportional basis. The net effect is that the technologies reduce delays in the portions of the NAS—most notable, the airport ground system—that are most critical to increasing throughput.

It is quite important, when considering Table 7-5 and Figure 6-1, that the AATT and TAP results have different degrees of uncertainty. We have not developed quantitative indicators of uncertainty, but, nevertheless, our models of the TAP technologies presently rest on firmer bases than do our models of the AATT technologies. This is indicated by our assessments in Chapter 5.

7-8

Consequently, it would be wrong to use the results of Table 7-5 and Figure 6-1 to say that either TAP or AATT is "better." Indeed, since the TAP technologies include A-FAST, such a comparison would be meaningless.

Further work is required to quantify the uncertainties in the results and develop meaningful comparisons of the benefits of specific groups of technologies.

SUMMARY

The benefits from the DSTs are real. They contribute directly to the bottom line of the air carriers and the airport owners/operators, while affecting the flying and the nonflying public indirectly.

At the individual trip level, some of the DSTs that result in shorter travel times generate two distinct benefits. The first is that the cost of that specific flight is decreased. Shorter travel times result in less fuel usage, less aircraft wear and tear, and, after flight schedule reoptimization, lower labor costs. The second is that shorter flight times allow additional flights to be added after schedule reoptimization. Individually, these savings are minute. Because of the high capital and fixed costs, the air passenger transportation business is essentially a transaction-based business. The carriers can increase revenues and profits with little addition to the fixed costs, by better utilization of the current aircraft. But because there are a relatively large number of flights, the minute savings begin to add up.

Another set of DSTs will not affect travel times, but will lower the cost of a specific flight. The efficient use of this set of DSTs results in holds occurring at trip or carrier optimal flight segments, which results in significant fuel savings.

An additional set of DSTs serve a primary function of increasing throughput or capacity of the airspace, rather than affecting individual flights. The effects are not in the operation of the aircraft but in that their usage allows more aircraft to be flown.

The AATT technologies are composed of six DSTs: TMA, AFAST, APATH (considered as a source of A-FAST/FMS links), EDP, EDA, and NSMT. The TAP technologies consists of ATM-2, ROTO, DROM, and AVOSS build 2. These results show that the both sets offer reductions in delay costs over all weather scenarios. What is not known is the relative contribution of each of these DSTs to the total delay reduction. This analysis would need to be done for any true measure of cost-effectiveness as well as weather sensitivities.

The TAP technologies produce greater reductions in delay time under all three weather scenarios. Since we have not examined the costs of these technologies, we cannot make any statements about their cost-effectiveness. Also, since the TAP technologies use some AATT technologies, our present results are not directly useful for comparing the effectiveness of the two groups of technologies.

The case in which both sets of technologies are implemented deserves special attention. This combined set offers superior reductions over either technologies used singly. As before, without knowing the costs of the technologies, no more can be said. But the relative effectiveness can be calculated. The sums of the average delay reductions for each of the technologies in 2007 is $6.9 billion for TAP and $5.9 billion for AATT, while for the combined technology it is $8.0 billion. This ratio is 64 percent, meaning that some combination of the component DSTs add capacity or throughput in one portion of the NAS without another subset adding equivalent capacity or throughput at portion. Therefore a portion of the capacity increase is wasted. A more in-depth analysis need to be performed to see if this ratio could be raised above 64 percent. It would entail analysis of various sets of DSTs rather than the two macro sets under study here.

Chapter 8
Delay Impact on System Throughput

This chapter describes our methods and results for estimating the impact of delay-reducing technologies on system throughput. It might seem that this could be done simply in light of the physical capacity measures of the NAS components. However, system throughput is *not* determined exclusively by the physical constraints of the airspace.

To understand this, consider arrival demands at a busy, slot-controlled airport such as DCA. Figure 8-1 shows the actual arrival traffic for DCA on April 8, 1996, along with the hourly capacity limitations.

Figure 8-1. Arrival Demand and Capacity at DCA
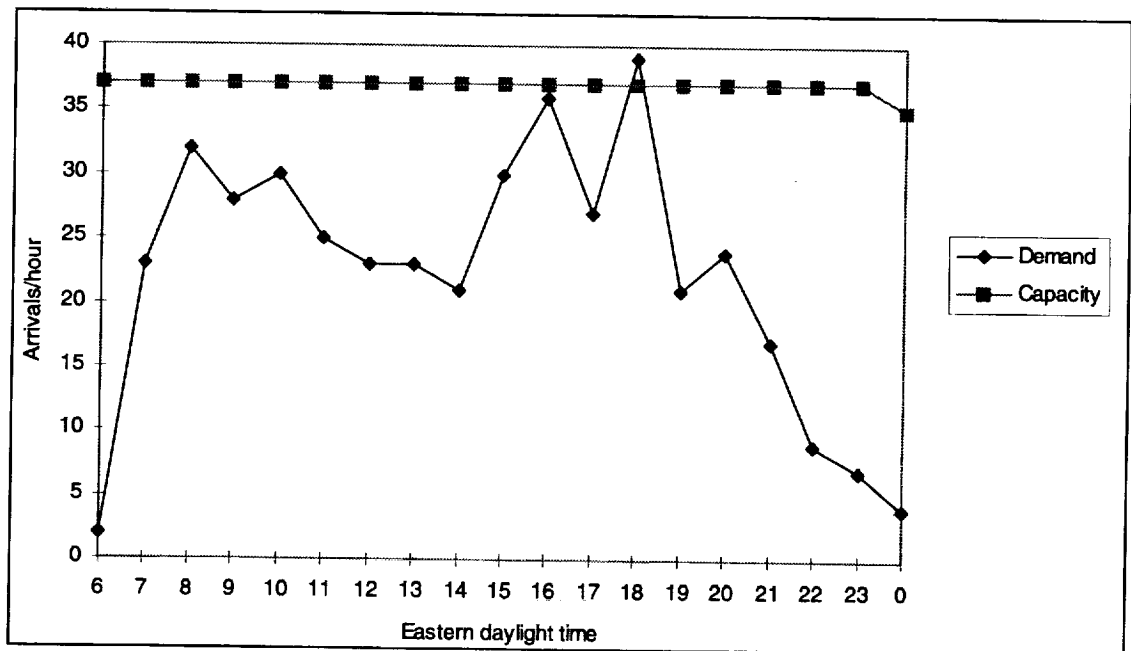
While demand exceeds capacity for one epoch, it is less than capacity in every other epoch and much less than capacity in most epochs. If they chose, airlines could operate many more flights into DCA. The airport's physical capacity is *not* a binding constraint.

Consequently, any methodology that links changes in delay to changes in throughput must incorporate the strategic response of the airspace user community

to delay. That is, any methodology must recognize that system throughput is determined by the interaction of airspace supply, measured by the physical capacity of the airspace and airspace demand. The methodology we developed utilizes the Aviation System Analysis Capability (ASAC) Air Carrier Investment Model (ACIM) to link changes in delay to changes in air carrier operating costs and air travel demand. [18] Our estimates of system throughput are, therefore, a function of both airspace capacity and air travel demand. The remainder of this chapter provides a brief introduction to the ACIM, discusses our methodology to evaluate changes in throughput, and presents our results.

AIR CARRIER INVESTMENT MODEL

To link the technology of flight with the economics of flight, ASAC requires a parametric model of airline costs and air travel demand. As such, the ACIM incorporates air travel demand, airline productivity, input prices, and profit considerations into the airline investment decision. The result is a forecast for air travel throughput, fares, airline employment, and aircraft fleet requirements for a given technology scenario. Therefore, by comparing the results from a technology scenario with those from a baseline scenario, we obtain estimates of throughput benefits.

The ACIM consists of four core modules: the U.S. Econometric Module, the U.S. Functional Cost Module (FCM), the Asian Econometric Module, and the European Econometric Module. In addition, there are extension modules that map the aggregate fleet requirements into seat-size categories and estimate the impact of changes in technology on U.S. aircraft manufacturing and related employment. The distinction between the U.S. Econometric Module and the FCM is the approach by which airline operating costs are estimated. The econometric module uses an econometric approach to estimate air carrier costs, while the FCM uses an activity-based costing approach. For this study, we employed the FCM exclusively.

In the FCM, total costs are calculated for six functional cost categories as a function of input prices, factor productivities, and total output. As shown in Figure 8-2, the cost categories consist of fuel, flight personnel labor, maintenance, aircraft capital, ground property and equipment capital, and a residual category termed other indirect. The measure of output that drives the cost calculations is available seat miles (ASM). The FCM solves for industry equilibrium by iterating fare yields until the profit constraints are satisfied. Thus, any changes in airline operating costs are passed on to the traveling public in the form of changes in fares. Implicitly, such analysis assumes that the commercial air travel industry will remain price competitive.

The model is based upon U.S. DOT Form 41 reports for 26 of the largest U.S. air carriers. The FCM represents approximately 91 percent of the 1995 U.S. flag

scheduled traffic. The default assumptions of the model determine an unconstrained forecast, which compares quite favorably with other published forecasts by Boeing and the FAA. [19,20] However, these unconstrained forecasts are predominately driven by demand and have little or no consideration of possible capacity shortfalls. The following section discusses our modifications to the unconstrained forecast in order to measure the impact of delay. Scenarios for delay-reducing technologies are subsequently compared with this baseline forecast.

Figure 8-2. FCM Schematic
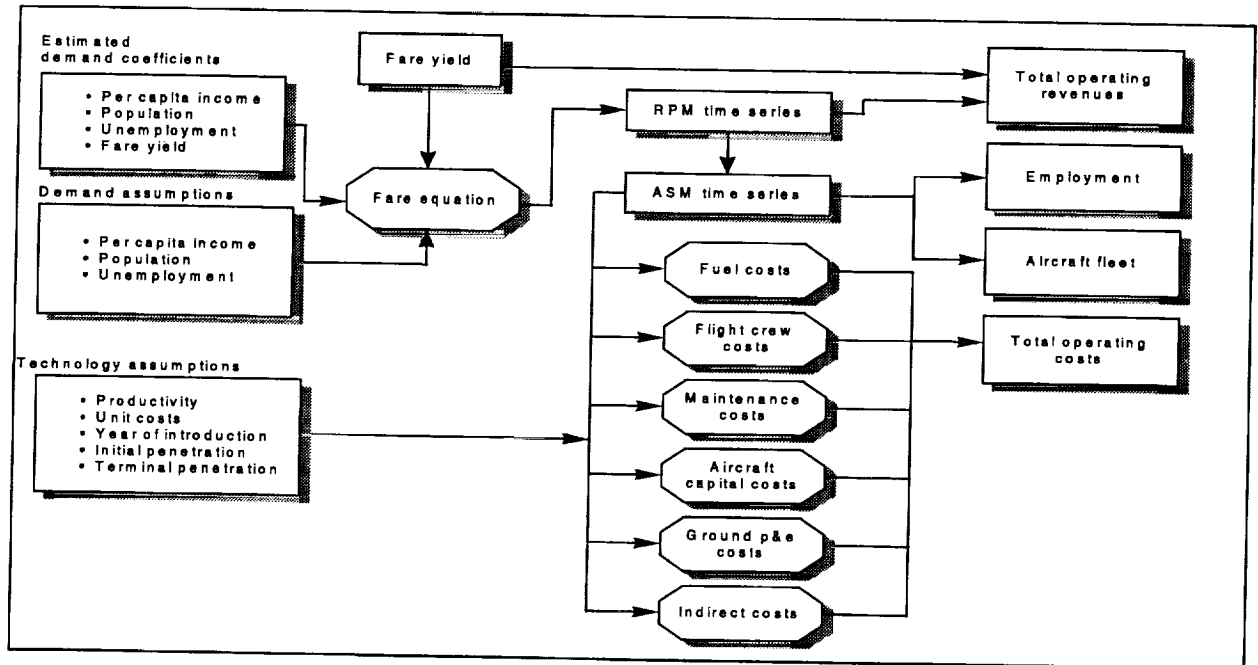
USING THE ACIM TO EVALUATE CHANGES IN SYSTEM THROUGHPUT

The basic premise of using the ACIM to evaluate the impact of delay on throughput is that delay imposes additional costs on air carriers, drives up fare yields, and depresses air travel demand growth. The result is a revised forecast for throughput, as measured by RPMs, which takes into account the impact of delay. We then convert RPMs to both operations and enplanements to get a more complete picture of the impact of delay and delay-reducing technologies. Figure 8-3 illustrates a schematic of this approach.

As shown in 8-3, the primary linkage between the NAS model and the FCM is the projected delays per flight. The block time required to complete a flight segment of a given length is a measure of the aircraft productivity employed by the FCM. Generally, when stage length is held constant, shorter block times imply more productive aircraft and consequently more departures per aircraft per day. The

FCM accepts changes in aircraft productivity as changes in aircraft block speed, which, by definition, is inversely proportional to changes in block time. Aircraft block speed, in conjunction with the number of seats per aircraft, therefore determines the number of ASM that can be flown by a given aircraft. Since ASM drive costs, the changes in aircraft productivity implied by changes in delay are central to the model's calculations.

Figure 8-3: Schematic of ACIM Approach
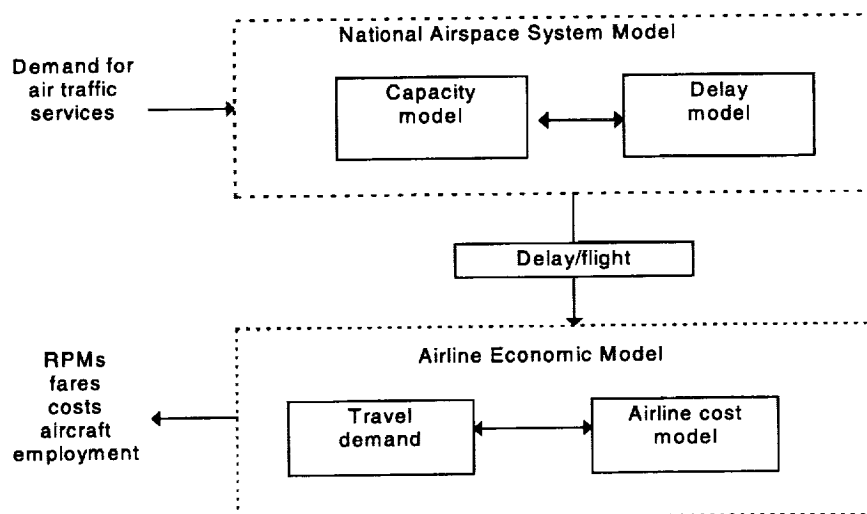
As shown in Table 8-1, we begin with the total delay minutes from the NAS model for each scenario. Since the FCM has no representation from GA and air taxi, and only limited representation from commuter carriers, we deduct the proportion of operations and delays attributed to these groups. The remainder is denoted as delays attributed to commercial carriers. The next column contains the number of commercial operations with which we calculate the average delay per flight for each scenario.

Table 8-1. FCM Delay Inputs

Scenario	Total delay minutes (millions)	Total commercial delay minutes (millions)	Commercial operations (millions)	Average delay minutes per flight
1996 baseline	167.7	94.3	11.9	15.90
2007 baseline	525.5	312.8	15.4	40.72
2017 baseline	1,521.0	940.4	18.3	102.69
2007 AATT	299.1	179.1	15.4	23.11
2007 TAP	300.9	178.0	15.4	23.25
2007 all	229.5	136.6	15.4	17.71
2017 all	726.6	449.3	18.9	47.60

One issue that arises in modeling aircraft productivity in this way is that in order to fly the same schedule in the face of rising delays, the airline would have to purchase additional aircraft. This may be unreasonable since airline financial departments would resist additional investments for increasingly less productive aircraft. We developed an alternate approach that assumes that airlines would stretch their schedules out during the day while simultaneously increasing the number of daily aircraft block hours. Operationally, this appears as an increase in aircraft utilization (more aircraft hours per day), although the total output as measured by miles flown or RPMs remains constant because of the delay.

As outlined previously, the key variables that we modify to estimate the impact of delay on throughput are aircraft block speed (inversely proportional to block time) and aircraft utilization. Since the FCM accepts input in the form of annual percentage changes, we converted the gross changes in delay from Table 8-1 to compound annual rates of change. These compound annual rates of change are then input to the ACIM separately for each scenario.

An additional issue that arises in modeling system throughput in this way is that the revised forecast generated by the ACIM may have considerably less traffic than was assumed by the NAS model in generating the initial delay estimates. In this case, the initial delay estimates may be overstated given the corresponding reduction in traffic. Thus, the need arises for a feedback loop between the revised traffic forecasts and the estimated delay. The most accurate method to implement this feedback effect would be to pass revised traffic forecasts from the ACIM to the NAS model and recompute the delay estimates. This process could then be repeated until the difference between subsequent revisions converged to zero. Unfortunately, the NAS model requires more detailed input than the ACIM can provide. Specifically, LMINET requires a flight schedule with highly detailed information on individual flights and airport operations, while the ACIM functions at the aggregate level only. Thus, to implement a feedback loop involving LMINET would require a complex algorithm to distribute changes in the aggregate traffic forecast to the underlying schedule. At this time, no such algorithm exists.

In light of the difficulties in disaggregating the revised traffic forecast for input to LMINET, we developed an alternate implementation for the feedback effect. The approach is based upon a piecewise log-linear approximation of the delay model applied to the aggregate traffic forecasts from the ACIM. To see the logic of this approach, consider that the core function of the delay model is to calculate delay as a function of traffic throughput and system capacity (as determined by the technology scenario assumptions). Thus, for any fixed capacity, the delay model represents a nonlinear mapping from throughput to delay.

Our approach is to use the actual output from the LMINET delay model to estimate this nonlinear relationship for each technology scenario. A good approximation of the delay model was achieved using a piecewise log-linear specification for

each scenario. Thus, the results from the initial run of the ACIM are fed to the approximated delay model to produce revised delay estimates. The revised delay estimates subsequently provide new inputs for an additional run of the ACIM. This process is repeated until the change in system throughput for subsequent runs of the ACIM converges to less than one-half of one percent.

Incorporating these increased costs into the airline economic model requires several assumptions about the likely airline response to the increase in congestion. We assume that fuel and labor costs increase proportionally with the increase in delay as scheduled block times get longer and less predictable. However, since the airlines operate a highly coordinated schedule of aircraft and crew movement, delay in one portion of the system can have repercussions system wide. For this reason, the cost of delay can be significantly larger than variable operating costs indicate. To address this issue we have employed a set of cost multipliers that were derived from a study by American Airlines. [21] The value of the cost multiplier is a nonlinear function of the duration of the delay and the time of day.

ACIM THROUGHPUT RESULTS

Implementing the ACIM under the methodology discussed yields a time series of system throughput, as measured by RPMs, for each scenario. To convert RPMs to operations and enplanements, we use the projected ratio of RPMs to operations and RPMs to enplanements from the 1998 FAA forecast. [20] Implicit in the FAA forecast projections are assumptions about increasing average stage length and increasing average seat size, which cause RPMs to grow considerably faster than enplanements and operations.

Additionally, there are discrepancies between the absolute operations numbers reported in Table 8-4 and those presented in previous chapters. These discrepancies are expected and are explained by differences in the size of the air system considered by LMINET and the ACIM. Specifically, LMINET only measures operations for the 64 airports identified in a previous chapter. The ACIM, however, measures operations system wide for the largest 26 passenger air carriers. Casual inspection indicates that the ACIM measures approximately 200 airports. Thus, the absolute ACIM unconstrained operations are larger than the LMINET operations, as expected.

Comparing estimates from each technology scenario with the baseline forecast provides estimates of the benefits of the technologies in terms of system throughput. Tables 8-2, 8-3, and 8-4 present our results.

Table 8-2. Commercial RPM Results (billions)

Year	Unconstrained	Baseline	AATT	TAP	All
1996	563.2	563.2	563.2	563.2	563.2
1997	593.7	589.1	591.6	592.4	593.4
1998	625.8	616.2	621.6	623.1	625.3
1999	659.7	644.5	653.0	655.4	659.0
2000	695.4	674.1	686.0	689.3	694.4
2001	733.0	705.2	720.7	725.1	731.7
2002	765.1	729.8	749.6	755.1	763.5
2003	798.6	755.2	779.6	786.4	796.6
2004	833.6	781.6	810.8	818.9	831.2
2005	870.1	808.8	843.3	852.8	867.3
2006	908.2	837.1	877.0	888.2	905.0
2007	947.9	865.1	912.2	924.9	937.8
2008	989.2	894.1			971.9
2009	1,032.3	924.1			1,007.2
2010	1,077.3	955.1			1,043.8
2011	1,124.3	987.1			1,081.7
2012	1,173.1	1,019.1			1,118.1
2013	1,224.0	1,052.1			1,155.8
2014	1,277.1	1,086.1			1,194.7
2015	1,332.6	1,121.3			1,234.9
2016	1,390.4	1,157.6			1,276.4
2017	1,450.8	1,195.1			1,319.4

Table 8-3. Commercial Enplanement Results (millions)

Year	Unconstrained	Baseline	AATT	TAP	All
1996	593.1	593.1	593.1	593.1	593.1
1997	625.2	620.4	623.1	623.8	625.0
1998	659.0	648.9	654.6	656.2	658.6
1999	694.7	678.8	687.7	690.2	694.0
2000	732.3	710.0	722.5	726.0	731.3
2001	772.0	742.6	759.0	763.6	770.6
2002	805.8	768.5	789.4	795.2	804.1
2003	841.1	795.4	821.0	828.2	839.0
2004	877.9	823.1	853.9	862.4	875.4
2005	916.4	851.8	888.1	898.2	913.4
2006	956.5	881.6	923.6	935.3	953.1

Table 8-3. Commercial Enplanement Results (millions)
(Continued)

Year	Unconstrained	Baseline	AATT	TAP	All
2007	998.2	911.1	960.6	974.1	987.7
2008	1,041.8	941.7			1,023.6
2009	1,087.2	973.2			1,060.8
2010	1,134.6	1,005.9			1,099.3
2011	1,184.1	1,039.6			1,139.2
2012	1,235.5	1,073.2			1,177.6
2013	1,289.1	1,108.0			1,217.2
2014	1,345.0	1,143.8			1,258.1
2015	1,403.4	1,180.9			1,300.5
2016	1,464.3	1,219.1			1,344.2
2017	1,527.9	1,258.6			1,389.5

Table 8-4. Commercial Operation Results (millions)

Year	Unconstrained	Baseline	AATT	TAP	All
1996	13.54	13.54	13.54	13.54	13.54
1997	13.89	13.78	13.84	13.86	13.89
1998	14.28	14.06	14.19	14.22	14.27
1999	14.69	14.35	14.54	14.60	14.68
2000	15.09	14.62	14.88	14.95	15.06
2001	15.61	15.02	15.35	15.44	15.58
2002	15.99	15.25	15.66	15.78	15.95
2003	16.27	15.38	15.88	16.02	16.23
2004	16.58	15.54	16.12	16.28	16.53
2005	16.89	15.70	16.36	16.55	16.83
2006	17.22	15.87	16.63	16.84	17.15
2007	17.55	16.02	16.89	17.13	17.37
2008	17.92	16.20			17.61
2009	18.29	16.37			17.84
2010	18.67	16.55			18.09
2011	19.05	16.73			18.33
2012	19.45	16.89			18.53
2013	19.85	17.06			18.74
2014	20.25	17.22			18.94
2015	20.67	17.39			19.15
2016	21.09	17.56			19.36
2017	21.53	17.73			19.58

Figure 8-4 depicts the results for commercial operations graphically. As shown, the scenario for all technologies closely approaches the unconstrained forecast through 2007 but diverges shortly after. Basically, the combined technologies allow the projected traffic growth between 1996 and 2007 to occur without increasing delay. However, beyond 2007 the combined technologies are unable to further restrain delay. Interestingly, the TAP technology and AATT technology scenarios are nearly identical in their ability to restrain delay for the projected traffic growth. Finally, the baseline projections show that growth in operations will be considerably restrained by delay in the absence of any new technologies.

Figure 8-4: Commercial Operations
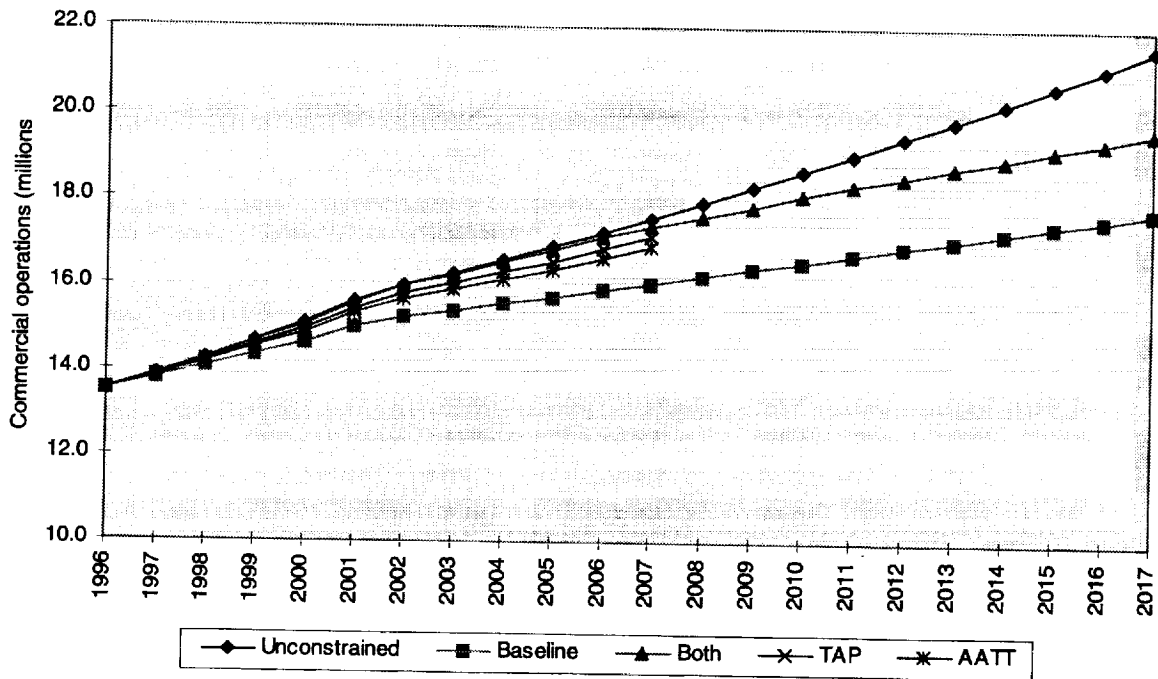
EXTENDING THE RESULTS TO COMMUTER AND GA TRAFFIC

An obvious omission from the described analysis is the impact of delay on commuter, air taxi, and GA operations. Since we lacked any full-scale economic model of these industries, however, we fell back on an assumption that operations would be reduced in proportion to the reductions in commercial air traffic operations. While this assumption is most likely a good approximation for the impact of delay on commuter and air taxi operations, its suitability for GA remains an open question. Because the proportion of total operations attributed to commuter, air taxi, and GA is projected to decline over the forecast period, the total operations grow less rapidly than the commercial operations. Table 8-5 presents the operations results as extended for all types of operations.

Table 8-5. Total Operation Results (millions)

Year	Unconstrained	Baseline	AATT	TAP	All
1996	24.07	24.07	24.07	24.07	24.07
1997	24.57	24.38	24.48	24.51	24.56
1998	25.13	24.74	24.96	25.02	25.11
1999	25.71	25.12	25.45	25.55	25.69
2000	26.27	25.47	25.92	26.04	26.23
2001	27.04	26.01	26.59	26.75	26.99
2002	27.56	26.28	27.00	27.19	27.50
2003	27.90	26.38	27.23	27.47	27.83
2004	28.28	26.51	27.50	27.78	28.20
2005	28.66	26.64	27.77	28.09	28.56
2006	29.07	26.79	28.07	28.43	28.97
2007	29.48	26.91	28.37	28.77	29.17
2008	29.99	27.11			29.47
2009	30.49	27.29			29.75
2010	31.00	27.49			30.04
2011	31.53	27.68			30.33
2012	32.05	27.84			30.55
2013	32.59	28.01			30.77
2014	33.13	28.17			30.99
2015	33.68	28.34			31.21
2016	34.24	28.51			31.44
2017	34.81	28.68			31.66

Chapter 9
Summary and Conclusions

We find that current delay costs to the airlines are about $3.6 billion annually, about 4 percent of the total domestic air carriers' annual revenue. This total delay cost figure is slightly larger than what the air carriers themselves estimate.[1] The difference is due to the method of measurement: we measure delay against ideal, undelayed flight times, while the carriers measure delay against their schedules, which already include substantial "padding" for expected delays. (One major carrier's operations center told us that they base their schedules on block times that their experience indicates can be met with at least 80 percent confidence.)

Under the assumptions that air carriers

1. keep their present hub-and-spoke operations,

2. grow traffic to the levels predicted by the FAA, and

3. keep the present daily operations peaks,

delay costs to air carriers and GA will increase from about $3.6 billion in 1996 to about $13.6 billion in 2007, and to about $47.9 billion in 2017. The average delay per flight would increase from 16 minutes in 1996 to 41 minutes in 2007, and to 103 minutes in 2017, while delay as a percentage of block time would increase from 11 percent in 1996, to 23 percent in 2007, and to 38 percent in 2017. The reason that the delay times and percentages of delay times grow at different rates is because of the forecast lengthening of stages.

With about 2 percent annual growth in operations, we see a greater than threefold increase of delays in a decade. The message from this analysis is quite clear: the NAS, a nonlinear queueing network, is operating close to its present capacity, so even modest increases in traffic will result in substantially increased delays. It is imperative, therefore, to augment NAS capacity—either through the deployment of new technologies or the construction of new air traffic facilities—if the NAS is not to become a limit on achievable air traffic growth.

---

[1] The amount also exceeds our earlier estimates (for example, see Reference [3]). This difference comes chiefly from our use of the $M/E_k/1$ queues for airport arrivals and departures in place of the fluid model for queues that we used in earlier LMINET studies. Introduction of surface delays also contributes to the difference, as does including GA operations in our demand schedules. The fluid queue model assigns no delay unless demand actually exceeds capacity. The new model correctly shows that, as demand/capacity ratios approach 1 from below, some delays occur. Generally, the old and new models agree fairly well during periods of substantial delay. The new model also accumulates many instances of relatively small delays.

One characterization of the technologies' benefits is the set of differences of delay costs with the technologies and the baseline, as computed in Chapter 7. In dollar terms, these benefits are huge: they amount, annually, to about $8 billion in 2007 and $25 billion in 2017 (for the deployment of both TAP and AATT). The benefits of deploying either TAP or AATT are equally impressive: they are $6–7 billion annually in 2007.

These measures of the benefits of the technologies, albeit impressive, are nevertheless unrealizable, because the airlines and traveling public would not tolerate the exorbitant delays predicted by the models. This simple comparison method does, however, provide a means of measuring the technologies' *potential* benefits.

A better method to measure the technologies' benefits, delineated in Chapter 8, is to calculate the improvements in system throughput that they would make. This is a more realistic method, since the airlines can be relied upon to raise fares to dampen demand if their usual fares would result in demands that cannot be met without excessive delays.

Without improvements, we estimate that the NAS can only accommodate about 53 percent of the FAA's forecast traffic operation growth from 1996 to 2007, and only about 42 percent of their forecast operation growth from 1996 to 2017. With the deployment of TAP or AATT, about 80 or 87 percent of operation growth from 1996 to 2007 could be accommodated, respectively. With both TAP and AATT phased in through 2007, our models predict that the NAS can sustain 94 percent of the potential air traffic growth from 1996 to 2007. Even with both TAP and AATT implemented, we estimate that the NAS could sustain only about 71 percent of forecast operation growth from 2007 to 2017.

The basic thrust of our predictions is that phasing in both TAP and AATT technologies through 2007 is likely to allow the NAS to sustain nearly the full demand growth forecast by the FAA, while air carriers continue to operate as described by previous assumptions 1–3. Crudely stated, we predict that the NASA technologies would allow users and operators of the NAS to operate with little change through the next decade. The models also suggest, however, that the NAS will become a bottleneck to potential air traffic growth after about 10 years, even with the NASA technologies deployed.

Without knowing the costs of the technologies, we cannot discuss their cost-effectiveness. In the present work, we applied the tools at all airports and at all sectors, but it may well be that the cost-effective implementation would be for a smaller set. Nor can we say at present if the tools integrate efficiently, that is, if capacity gains from one set of tools are vitiated by NAS inefficiencies that other tools do not address adequately. More in-depth analyses could clarify these issues.

Based on the current delay figures and model predictions, the overwhelming bulk of the delays are airport related, more than 90 percent according to our models.

Many tools are designed with multifaceted purposes, and enhancing capacities may just be one of them, but any tools that will enlarge the runway or taxiway capacities should be particularly effective in reducing congestion.

No technology assessment is complete without a sensitivity analysis or derived confidence level, and this one is no exception. In this report we have expressed various degrees of confidence in constructing the present models, some of them quantifiable and many of them unquantifiable. The uncertainties in our models are due in some cases to the lack of detailed operating characteristics and field tests of the tools, in others to the elusive nature of air carriers' responses to the excessive delay.

Nevertheless, we are confident that our basic methods are solid: we have a sound queueing network model of NAS and have used

◆ validated airport and sector capacity models developed under previous NASA-sponsored tasks,

◆ the official terminal area forecasts from FAA,

◆ real airline and GA cost figures, and

◆ measures of system throughput that are based on the economic principles that airlines have to make a profit and that their industry is competitive.

Details of the numbers may change when new data are incorporated. We are confident, however, of our conclusions that the NAS needs immediate capacity improvement if it is not to restrain air travel and that, with both TAP and AATT technologies implemented, the NAS could support the FAA's forecast demand increases for about a decade.

References

[1] Logistics Management Institute, *Technical and Economic Analysis of Air Transportation Management Issues Related to Free Flight*, NS501T1, David A. Lee, Peter F. Kostiuk, Bruce J. Kaplan, Marcos Escobar, Amedeo Odoni, and Brett Malone, February 1997.

[2] National Aeronautics and Space Administration, *Estimating the Effects of the Terminal Area Productivity Program*, NASA Contractor Report 201682, David A. Lee, Peter F. Kostiuk, Robert V. Hemm, Earl R. Wingrove III, and Gerald Shapiro, Langley Research Center, April 1997.

[3] Logistics Management Institute, *A Method for Making Cross-Comparable Estimates of the Benefits of Decision Support Technologies for Air Traffic Management*, NS710S1, David A. Lee, Dou Long, Melvin R. Etheridge, Joana R. Plugge, Jesse P. Johnson, and Peter F. Kostiuk, March 1998.

[4] Logistics Management Institute, "Capacity/Delay Modeling Parameters for TAP Technologies," White Paper, Robert V. Hemm and David A. Lee, March 1997.

[5] Michael H. Rothkopf and Shmuel S. Oren, "A Closure Approximation for the Nonstationary $M/M/s$ Queue," *Management Science*, Vol. 25, No. 6, June 1979.

[6] Logistics Management Institute, "$M/E_3/N/N+Q$ and $M/E_k/N/N+Q$," Internal Paper, David A. Lee, January 1997.

[7] NASA, *An Analysis of Landing Rates and Separations at the Dallas-Fort Worth International Airport*, NASA Technical Memorandum 110397, Mark G. Ballin and Heinz Erzberger, NASA Ames Research Center, Moffett Field, CA, 1996.

[8] NASA, *Final-Approach Spacing Aids (FASA) Evaluation for Terminal-Area, Time-Based Air Traffic Control*, NASA Technical Paper 3399, Leonard Credeur, William R. Capron, Gary W. Lohr, Daniel J. Crawford, Dershuen A. Tang, and William G. Rodgers Jr., December 1993.

[9] Department of Transportation, *1996 Aviation Capacity Enhancement (ACE) Plan*, Report DOT/FAA/ASC-96-1, Federal Aviation Administration Office of System Capacity, Washington, DC, December 1996.

[10] Department of Transportation, *National Airspace System Architecture,* Version 2.0, Federal Aviation Administration Office of System Architecture and Program Evaluation, Washington, DC, October 1996.

[11] T.J. Davis, D.R. Isaacson, J.E. Robinson III, W. den Braven, K.K. Lee, and B. Sanford, "Operational Test Results of the Passive Final Approach Spacing Tool," 8th IFAC Symposium on Transportation Systems, Chania, Greece, June 1997.

[12] NASA, *Summary Overview and Status of AATT Program Development Activities,* Draft NASA Internal Report, M.G. Ballin, R.A. Coppenbarger, D.R. Schleicher, and S.C. Johnson, May 29, 1997.

[13] NASA, *ATM Concept Definition,* Volume 2, "Coverage of Future National Airspace System Operational Requirements," NASA Ames Research Center, AATT Program Office, October 21, 1997.

[14] Department of Transportation, *Validation of Air Traffic Controller Workload Models,* Report FAA-RD-79-83, M. Grossberg, J. Richards, and A. Robertson, Federal Aviation Administration, Washington, DC, September 1979.

[15] Department of Transportation, FAA Order 7210.3M, Change 1, Federal Aviation Administration, Washington, DC, May 13, 1996.

[16] MCA Research Corporation, Wilma Rada, *Surface Movement Advisor (SMA) Benefit Analysis,* Arlington, VA, October 1977.

[17] R. Lampl (Ed.), *The Aviation & Aerospace Almanac,* Aviation Week Group, McGraw-Hill, New York, 1998.

[18] NASA, *The ASAC Air Carrier Investment Model (Third Generation),* NASA Contractor Report 207656, Earl R. Wingrove III, Eric M. Gaier, and Tara E. Santmire, 1998.

[19] Boeing, *1998 Current Market Outlook,* Boeing Commercial Airplane Group Marketing, P.O. Box 3707, Seattle, WA 98124-2207.

[20] Department of Transportation, *FAA Aviation Forecast—Fiscal Years 1998–2009,* Report No. FAA APO-98-1, Federal Aviation Administration, Office of Aviation Policy and Plans, Statistics and Forecast Branch, Washington, DC, March 1998.

[21] American Airlines, *Preliminary Evaluation of Flight Delay Propagation Through an Airline Schedule,* Roger Beatty et al., 1998.

Appendix A
1996 Variable Operating Costs For the U.S. Fleet

The following is the Form 41 data used to calculate the 1996 variable operating costs for the U.S. fleet.

Table A-1. 1996 Variable Operating Costs for the U.S. Fleet

Equipment	Type	VOC	Fuel	Block hours	VOC-Fuel per block hour	VOC-Fuel per block minute
Form 41—U.S. Domestic Fleetwide		$32,924,714,441	$11,727,624,898	16,427,986	$1,290.30	$21.51
Jets only		$32,078,774,657	$11,531,056,681	$14,632,047	$1,404.30	$23.40
Turboprop only		$825,129,300	$188,191,406	$1,726,173	$368.99	$6.15
Piston Only		$20,179,380	$8,348,254	$69,109	$171.20	$2.85
Jets & Turboprops		$32,903,903,957	$11,719,248,087	$16,358,220	$1,295.05	$21.58
<Boeing 777> <627>	Jet	$184,290,000	$80,362,000	58,298	$1,782.70	$29.71
<Boeing B-707-300C> <49>	Jet	$27,241,949	$9,931,543	9,315	$1,858.34	$30.97
<Boeing B-727-100> <710>	Jet	$477,012,049	$79,978,811	108,240	$3,668.08	$61.13
<Boeing B-727-100C/QC> <711>	Jet	$48,637,727	$4,760,890	27,950	$1,569.83	$26.16
<Boeing B-727-200/231A> <715>	Jet	$3,896,306,472	$1,381,260,892	1,644,279	$1,529.57	$25.49
<Boeing B-737-100/200> <620>	Jet	$1,537,573,780	$498,435,018	954,174	$1,089.05	$18.15
<Boeing B-737-200C> <621>	Jet	$191,946,615	$57,034,477	98,762	$1,366.03	$22.77
<Boeing B-737-300> <619>	Jet	$2,654,196,569	$938,408,362	1,858,836	$923.04	$15.38
<Boeing B-737-400> <617>	Jet	$451,360,825	$164,919,157	310,134	$923.61	$15.39
<Boeing B-737-500> <616>	Jet	$568,123,724	$210,638,953	448,452	$797.15	$13.29
<Boeing B-747-100> <536>	Jet	$1,742,736,499	$759,133,033	301,397	$3,263.48	$54.39
<Boeing B-747-200/300> <537>	Jet	$495,655,522	$186,277,401	80,029	$3,865.83	$64.43
<Boeing B-747-400> <539>	Jet	$899,565,000	$432,213,000	175,486	$2,663.19	$44.39
<Boeing B-747F> <820>	Jet	$330,563,449	$95,494,132	36,170	$6,499.01	$108.32
<Boeing B-757-200> <622>	Jet	$3,165,320,714	$1,129,559,624	1,648,105	$1,235.21	$20.59
<Boeing B-767-200/ER> <625>	Jet	$942,944,260	$345,847,732	368,093	$1,622.13	$27.04
<Boeing B-767-300/ER> <626>	Jet	$1,407,934,726	$571,830,278	545,046	$1,534.01	$25.57
<British Aero. BAE-146-100/RJ7> <866>	Jet	$1,396,977	$652,015	1,174	$634.55	$10.58
<British Aero. BAE-146-200> <867>	Jet	$7,535,212	$4,652,643	12,547	$229.74	$3.83
<British Aero. BAE-146-300> <868>	Jet	$57,453,090	$18,790,410	37,210	$1,039.04	$17.32
<Douglas DC-10-10> <730>	Jet	$963,525,378	$322,854,089	219,887	$2,913.64	$48.56
<Douglas DC-10-30> <732>	Jet	$1,056,525,190	$390,938,468	227,571	$2,924.74	$48.75
<Douglas DC-10-40> <733>	Jet	$369,502,000	$139,896,000	53,057	$4,327.53	$72.13
<Douglas DC-8-50> <848>	Jet	$7,793,859	$6,056,372	6	$289,581.17	$4,826.35
<Douglas DC-8-50F> <850>	Jet	$97,459,966	$32,049,982	30,686	$2,131.59	$35.53
<Douglas DC-8-61> <851>	Jet	$49,742,293	$17,448,897	9,086	$3,554.19	$59.24
<Douglas DC-8-62> <854>	Jet	$87,868,113	$26,285,077	33,309	$1,848.84	$30.81
<Douglas DC-8-63> <880>	Jet	$23,815,335	$7,122,929	9,878	$1,689.86	$28.16
<Douglas DC-8-63F> <852>	Jet	$89,827,801	$19,671,801	31,761	$2,208.87	$36.81

Equipment	Type	VOC	Fuel	Block hHours	VOC-Fuel per block hour	VOC-Fuel per block minute
<Douglas DC-8-71> <860>	Jet	$204,824,599	$46,520,348	73,343	$2,158.41	$35.97
<Douglas DC-8-73> <864>	Jet	$226,093,578	$72,389,531	64,565	$2,380.61	$39.68
<Douglas DC-8-73F> <865>	Jet	$61,091,697	$6,192,415	30,805	$1,782.15	$29.70
<Douglas DC-9-10> <630>	Jet	$152,708,546	$47,321,548	100,289	$1,050.83	$17.51
<Douglas DC-9-15/15F> <635>	Jet	$24,343,542	$8,187,443	19,150	$843.66	$14.06
<Douglas DC-9-30> <640>	Jet	$1,277,998,591	$438,508,128	815,059	$1,029.98	$17.17
<Douglas DC-9-40> <645>	Jet	$68,017,962	$24,259,072	45,592	$959.79	$16.00
<Douglas DC-9-50> <650>	Jet	$319,985,731	$110,279,662	188,154	$1,114.54	$18.58
<Douglas MD-11> <740>	Jet	$953,691,000	$357,404,000	211,802	$2,815.30	$46.92
<Euro Airbus A-300-600/R/CF/RCF> <691>	Jet	$475,149,000	$157,735,000	142,746	$2,223.63	$37.06
<Euro Airbus A-300 B4/C/F-100/2><690>	Jet	$57,841,075	$20,000,678	18,382	$2,058.56	$34.31
<Euro Airbus A310-200 C/F> <692>	Jet	$161,363,000	$32,016,000	32,074	$4,032.77	$67.21
<Euro Airbus A320-100/200> <694>	Jet	$663,990,524	$235,733,330	442,582	$967.63	$16.13
<Fokker 70> <604>	Jet	$9,674,149	$4,543,445	7,387	$694.56	$11.58
<Fokker 100> <603>	Jet	$556,311,000	$163,274,000	400,855	$980.50	$16.34
<Fokker F-28-4000/6000> <602>	Jet	$120,263,000	$27,535,000	61,244	$1,514.07	$25.23
<Lear Jet 35> <663>	Jet	$119	$114	12	$0.42	$0.01
<Lockheed L-801-1/100/200> <760>	Jet	$906,993,505	$349,477,962	218,603	$2,550.36	$42.51
<Lockheed L-801-500Tristar> <765>	Jet	$397,755,000	$138,503,000	80,966	$3,201.99	$53.37
<MD-80 & DC-9-4 All> <655>	Jet	$3,539,915,441	$1,327,763,271	2,279,138	$970.61	$16.18
<MD-87> <654>	Jet	$4,232,518	$2,899,739	8,010	$166.39	$2.77
<MD-90-30/50> <680>	Jet	$62,675,986	$28,009,009	52,351	$662.20	$11.04
<ATR-42 Aerospatial> <441>	Turboprop	$135,180,492	$26,808,488	238,969	$453.50	$7.56
<ATR-72 Aerospatial> <442>	Turboprop	$78,423,443	$18,480,064	118,076	$507.67	$8.46
<Beech-18> <402>	Turboprop	$33,797	$23,361	480	$21.74	$0.36
<Beech-99> <403>	Turboprop	$923	$770	16	$9.56	$0.16
<Beech-C99> <404>	Turboprop	$96,910	$79,537	1,339	$12.97	$0.22
<Beech B-1900> <405>	Turboprop	$103,745,101	$34,996,413	375,509	$183.08	$3.05
<British Aero. BAE-ATP> <408>	Turboprop	$20,384,710	$4,419,043	21,466	$743.77	$12.40
<British Aero. BAE Jetstream 31> <469>	Turboprop	$31,034,752	$6,219,826	79,253	$313.11	$5.22
<British Aero. BAE Jetstream 41> <471>	Turboprop	$19,597,299	$5,836,788	58,612	$234.77	$3.91
<Cessna 208> <416>	Turboprop	$2,337,511	$436,207	127,347	$14.93	$0.25
<Convair CV-580> <430>	Turboprop	$700,355	$581,230	2,459	$48.44	$0.81
<Convair CV-600> <435>	Turboprop	$5,452,166	$617,401	8,034	$601.79	$10.03
<Convair CV-640> <440>	Turboprop	$3,272,868	$739,970	2,356	$1,075.08	$17.92
<Dassault Falcon> <653>	Turboprop	$99,714	$84,613	350	$43.15	$0.72
<De Havilland DHC 8-100> <483>	Turboprop	$50,700,000	$8,029,000	66,395	$642.68	$10.71
<De Havilland DHC 8-300> <484>	Turboprop	$5,460,943	$2,631,776	17,669	$160.12	$2.67
<Dornier 328> <449>	Turboprop	$18,448,000	$3,316,000	29,983	$504.69	$8.41
<Embraer EMB-120 Brasilia> <461>	Turboprop	$170,204,207	$39,158,199	345,838	$378.92	$6.32
<Lockheed L-188A-08/188C> <550>	Turboprop	$35,252,549	$6,507,384	11,738	$2,448.90	$40.81
<Lockheed L-382E L-100-30> <580>	Turboprop	$39,819,621	$9,217,380	17,857	$1,713.74	$28.56
<SAAB-Fairchild 340/B> <480>	Turboprop	$58,025,173	$12,088,371	114,491	$401.23	$6.69

Table A-1. 1996 Variable Operating Costs for the U.S. Fleet (Continued)

Equipment	Type	VOC	Fuel	Block hHours	VOC-Fuel per block hour	VOC-Fuel per block minute
<Shorts 360> <489>	Turboprop	$20,782,865	$3,584,364	31,780	$541.17	$9.02
<Shorts SD330> <487>	Turboprop	$112,885	$91,658	1,004	$21.14	$0.35
<Swearingen Metro II SA-226> <466>	Turboprop	$23,103	$17,975	272	$18.85	$0.31
<Swearingen Metro III SA-227> <467>	Turboprop	$25,939,913	$4,225,588	54,880	$395.67	$6.59
<Beech 18 C-185> <110>	Piston	$54,200		51,554	$1.05	$0.02
<Cessna-206/207> <035>	Piston	$516		730	$0.71	$0.01
<Cessna 404 C-4-4, Titan> <128>	Piston	$96	$87	8	$1.13	$0.02
<Cessna C402/402-A> <125>	Piston	$1,128	$905	754	$0.30	$0.00
<Convair CV-240> <140>	Piston	$202	$137	13	$5.00	$0.08
<Dornier DO-28> <161>	Piston	$164,019	$124,636	2,262	$17.41	$0.29
<Douglas DC-6> <216>	Piston	$19,959,219	$8,222,489	13,788	$851.23	$14.19
<Bell-206A> <315>	Helicoptor	$631,104	$28,557	657	$917.12	$15.29
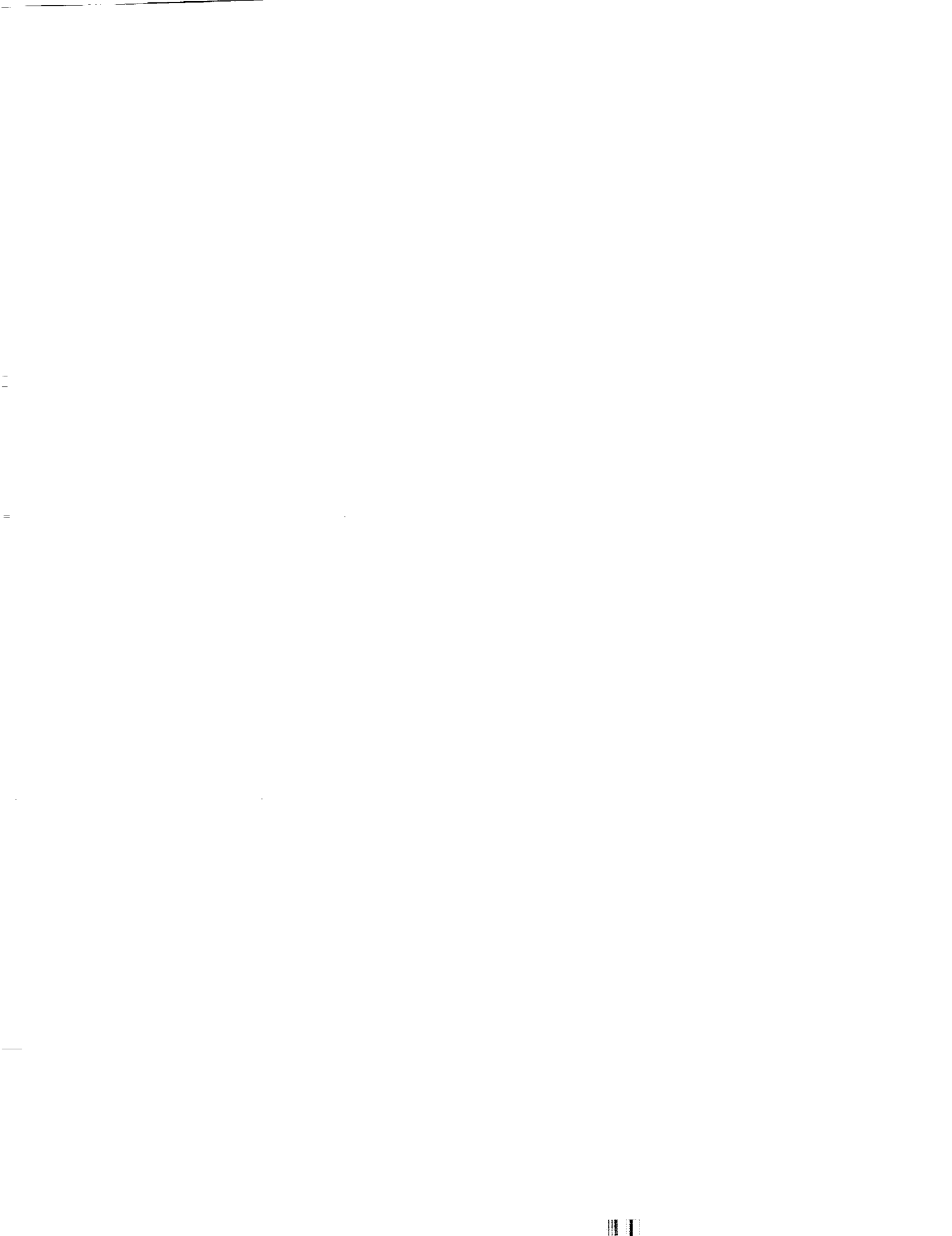
Appendix B
A First-Moment Closure Hypothesis for $M/E_k/1$ Queues

In *Elements of Queuing Theory with Applications*, published by McGraw-Hill in 1961, Thomas L. Saaty gives the evolution equations for the $M/Ek/1$ queue (Section 6-3, "Poisson Input, Erlangian Service Times"). From Saaty's equations 6-56 there follow two equations describing the time evolution of the mean number in the system, $<n>$, and the variance of that number, σ^2. These are

$$\frac{d}{dt} < n >= k(\lambda - \mu) + k\mu P_0 \qquad \text{[Eq. B-1]}$$

and

$$\frac{d}{dt}(\sigma^2) = k^2\lambda + k\mu[1 - (2 < n > +1)P_0] \qquad \text{[Eq. B-2]}$$

In steady state, B-1 and B-2 lead to the conclusion that

$$P_0 = 1 - \lambda / \mu; \quad < n > = \frac{1}{2}\frac{(k+1)\lambda / \mu}{1 - \lambda / \mu} \qquad \text{[Eq. B-3]}$$

These two equations allow one to express the steady-state P_0 in terms of the steady-state $<n>$ as

$$P_0 = \frac{k+1}{2 < n > +k + 1} \qquad \text{[Eq. B-4]}$$

Our first-moment closure hypothesis is to use the expression B-4 for P_0 in the full evolution equation for $<n>$, thus taking as a single evolution equation for $<n>$

$$\frac{d}{dt} < n > = k\left[\lambda - \mu + \mu\frac{k+1}{k+1+2 < n >}\right] \qquad \text{[Eq. B-5]}$$

While this approximation is undoubtedly a rough one, its results seem reasonably good, as illustrated by the figure.

Figure B-1. Comparison of Exact and Closure-Hypothesis Results for <n>

B-2
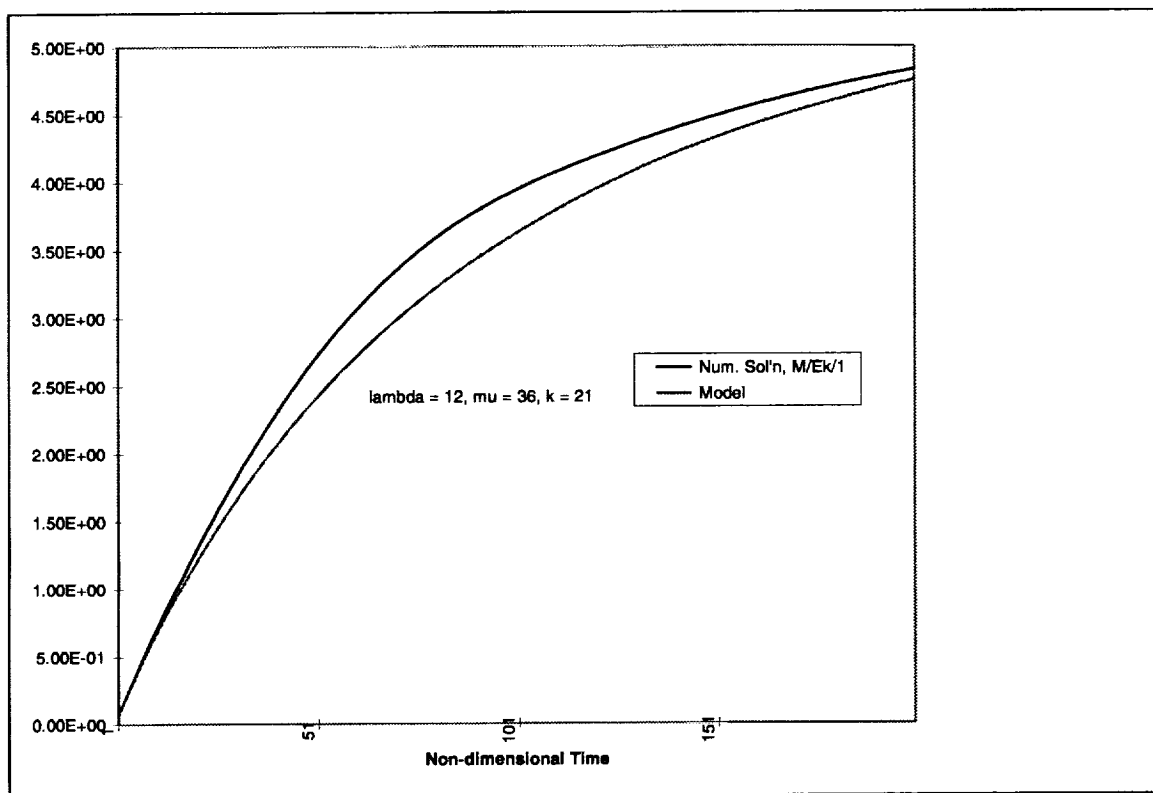
Appendix C
Glossary of Airport Identifiers

ATL   The William B. Hartsfield Atlanta International Airport, Atlanta, Georgia

BNA   Nashville, Tennessee Airport

BOS   General Edward Lawrence Logan International Airport, Boston, Massachusetts

BUR   Burbank, California Airport

BWI   Baltimore-Washington International Airport

CLE   Hopkins International Airport, Cleveland, Ohio

CLT   Douglas Airport, Charlotte, North Carolina

CMH   Columbus International Airport, Columbus, Ohio

CVG   Cincinnati-Northern Kentucky Airport, Cincinnati, Ohio

DAL   Love Field, Dallas/Fort Worth, Texas

DAY   Dayton International Airport, Dayton, Ohio

DCA   Washington National Airport, Washington, D. C.

DEN   Denver International Airport, Denver, Colorado

DFW   Dallas-Fort Worth International Airport, Dallas/Fort Worth, Texas

DTW   Detroit Metropolitan Wayne County Airport, Detroit, Michigan

EWR   Newark International Airport, Newark, Ohio

HOU   William P. Hobby Airport, Houston, Texas

HPN   Westchester County Airport, Westchester County, NY

IAD   Dulles International Airport, Washington, D. C.

IAH   Houston Intercontinental Airport, Houston, Texas

IND   Indianapolis International Airport, Indianapolis, Indiana

ISP	MacArthur Field, Long Island, New York
JFK	John F. Kennedy International Airport
LAS	McCarran International Airport, Las Vegas, Nevada
LAX	Los Angeles International Airport, Los Angeles, California
LGA	La Guardia Airport, New York, New York
LGB	Daugherty Field, Long Beach, California
MCI	Kansas City International Airport, Kansas City, Missouri
MCO	Orlando International Airport, Orlando, Florida
MDW	Midway Airport, Chicago, Illinois
MEM	Memphis International Airport, Memphis, Tennessee
MIA	Miami International Airport, Miami, Florida
MKE	General Mitchell Field, Milwaukee, Wisconsin
MSP	Minneapolis-Saint Paul International Airport, Minneapolis-Saint Paul, Minnesota
MSY	New Orleans International Airport, New Orleans, Louisiana
NYC	New York City (used to represent the three New York terminals considered as a group)
OAK	Oakland International Airport, Oakland, California
ONT	Ontario International Airport, Ontario, California
ORD	Chicago O' Hare International Airport
PBI	Palm Beach International Airport, Palm Beach, Florida
PDX	Portland International Airport, Portland, Oregon
PHL	Philadelphia International Airport, Philadelphia, Pennsylvania
PHX	Phoenix Sky Harbor International Airport, Phoenix, Arizona
PIT	Pittsburgh International Airport, Pittsburgh, Pennsylvania
SAN	Lindbergh Field, San Diego, California

SEA	Seattle-Tacoma International Airport, Seattle, Washington
SFO	San Francisco International Airport, San Francisco, California
STL	Lambert Field, Saint Louis, Missouri
SYR	Hancock Field, Syracuse, New York

Appendix D
Abbreviations

AATT	Advanced Air Transportation Technologies
ACARS	ARINC Communications Addressing and Reporting System
ACIM	Air Carrier Investment Model
AERGA	Advanced Enroute Ground Automation
AMASS	Airport Movement Area Safety System
AOC	aircraft operational control
APATH	Airborne Integrated Route Planner for Avoiding Traffic and Hazard
ARINC	Aeronautical Radio, Incorporated
ARTCC	Air Route Traffic Control Center
ARTS	Automated Radar Terminal System
ASAC	Aviation Systems Analysis Capability
AT	Airspace Tool
ATM	Air Traffic Management
AVOSS	Aircraft Vortex Spacing System
BADA	Base of Aircraft Data
CAP	Collaborative Arrival Planning
CBM	Cost-Benefit Model
CONUS	Contiguous United States
CP/TPT	Conflict Probe/Trial Planning Tool
CTAS	Center-TRACON Automation System
DOT	Department of Transportation
DROM	Dynamic Runway Occupancy Measurement
DST	Daylight Saving Time
EDA	En route and Descent Advisor
EDP	Expedite Departure Path
ETMS	Enhanced Traffic Management System
FAA	Federal Aviation Administration

FAM	Functional Analysis Model
FAST	Final Approach Spacing Tool
FMS	flight management system
FSCM	Flight Segment Cost Model
GA	general aviation
IFR	Instrument Flight Rules
ILS	Instrument Landing System
IMC	Instrument Meterological Conditions
LMINET	A queuing network model of the U. S. national airspace system
NAS	National Airspace System
NASA	National Aeronautics and Space Administration
NASPAC	National Airspace System Performance Analysis Capability
OAG	Official Airline Guide
OASIS	National Climatic Data Center's On-Line Access and Service Information System
PMAC	Performance Monitoring Analysis Capability
RISC	Reduced Instruction Set Computer
ROT	runway occupancy times
ROTO	roll out and turn off
RPM	revenue passenger miles
SID	Standard Instrument Departure
SMA	Surface Movement Advisor
ST	sector tool
TAF	Terminal Area Forecast
TAP	Terminal Area Productivity
TMA	Traffic Management Advisor
TRACON	Terminal Radar Approach Control
VFR	Visual Flight Rules
VMC	Visual Meteorological Conditions
VOC	Variable Operating Cost

REPORT DOCUMENTATION PAGE

Public reporting burden for this collection of information is estimated to average 1 hour per response, including the time for reviewing instructions, searching existing data sources, gathering and maintaining the data needed, and completing and reviewing the collection of information. Send comments regarding this burden estimate or any other aspect of this collection of information, including suggestions for reducing this burden, to Washington Headquarters Services, Directorate for Information Operations and Reports, 1215 Jefferson Davis Highway, Suite 1204, Arlington, VA 22202-4302, and to the Office of Management and Budget, Paperwork Reduction Project (0704-0188), Washington, DC 20503.

1. AGENCY USE ONLY *(Leave blank)*	2. REPORT DATE	3. REPORT TYPE AND DATES COVERED
	January 1999	Contractor Report

4. TITLE AND SUBTITLE	5. FUNDING NUMBERS
Modeling Air Traffic Management Technologies with a Queuing Network Model of the National Airspace System	C NAS2-14361 WU 538-16-11-01

6. AUTHOR(S)

Dou Long, David Lee, Jesse Johnson, Eric Gaier and Peter Kostiuk

7. PERFORMING ORGANIZATION NAME(S) AND ADDRESS(ES)	8. PERFORMING ORGANIZATION REPORT NUMBER
Logistics Management Institute 2000 Corporate Ridge McLean, VA 22102-7805	NS808S1

9. SPONSORING / MONITORING AGENCY NAME(S) AND ADDRESS(ES)	10. SPONSORING / MONITORING AGENCY REPORT NUMBER
National Aeronautics and Space Administration Langley Research Center Hampton, VA 23681-0001	NASA/CR-1999-208988

11. SUPPLEMENTARY NOTES

Langley Technical Monitor: Robert E. Yackovetsky
Final Report

12a. DISTRIBUTION / AVAILABILITY STATEMENT	12b. DISTRIBUTION CODE
Unclassified - Unlimited Subject Category 01 Availability: NASA CASI (301) 621-0390 Distribution: Nonstandard	

13. ABSTRACT *(Maximum 200 words)*

This report describes an integrated model of air traffic management (ATM) tools under development in two National Aeronautics and Space Administration (NASA) programs --Terminal Area Productivity (TAP) and Advanced Air Transport Technologies (AATT). The model is made by adjusting parameters of LMINET, a queuing network model of the National Airspace System (NAS), which the Logistics Management Institute (LMI) developed for NASA. Operating LMINET with models of various combinations of TAP and AATT will give quantitative information about the effects of the tools on operations of the NAS. The costs of delays under different scenarios are calculated. An extension of Air Carrier Investment Model (ACIM) under ASAC developed by the Institute for NASA maps the technologies' impacts on NASA operations into cross-comparable benefits estimates for technologies and sets of technologies.

14. SUBJECT TERMS			15. NUMBER OF PAGES
National Airspace System, Air Traffic Management, Terminal Area Productivity, Advanced Aviation Transport Technologies, Queueing Network Model, Flight Delay, System Throughput			121
			16. PRICE CODE A06

17. SECURITY CLASSIFICATION OF REPORT	18. SECURITY CLASSIFICATION OF THIS PAGE	19. SECURITY CLASSIFICATION OF ABSTRACT	20. LIMITATION OF ABSTRACT
Unclassified	Unclassified	Unclassified	Unlimited

NSN 7540-01-280-5500